

WATER AND CARBON DIOXIDE ICES-RICH AREAS ON COMET 67P/CG NUCLEUS SURFACE

Gianrico Filacchione¹, Fabrizio Capaccioni¹, Andrea Raponi¹,
Maria Cristina De Sanctis¹, Mauro Ciarniello¹, Maria Antonella Barucci², Federico Tosi¹,
Alessandra Migliorini¹, Maria Teresa Capria¹, Stephane Erard², Dominique Bockelee-Morvan²,
Cedric Leyrat², Gabriele Arnold³, David Kappel³, Thomas B. McCord⁴

1. INAF-IAPS, Istituto di Astrofisica e Planetologia Spaziali, Rome, ITALY.
2. LESIA, Laboratoire d'Études Spatiales et d'Instrumentation en Astrophysique, Observatoire de Paris, PSL Research University, CNRS - Centre National de la Recherche Scientifique, Sorbonne Universités, UPMC Univ. Paris 06, Univ. Paris Diderot, Sorbonne Paris Cité, France FRANCE.
3. Institute for Planetary Research, DLR - Deutsches Zentrum für Luft- und Raumfahrt, Berlin, GERMANY.
4. Bear Fight Institute, Winthrop, WA, USA.

ABSTRACT: So far, only two ice species have been identified by Rosetta/VIRTIS-M [1] on the surface of 67P/Churyumov-Gerasimenko during the pre-perihelion time: crystalline water and carbon dioxide ice. Water ice has been spectroscopically identified in three distinct modalities: 1) On the active areas of Hapi region where water ice changes its abundance with local time and illumination conditions, condensing during the night hours and sublimating during daytime [2]; 2) On recent debris fields collapsed from two elevated structures in the Imhotep region where more fresh and pristine material is exposed [3]; 3) On eight bright areas located in Khonsu, Imhotep, Anhur, Atum and Khepry regions [4] where single or multiple grouped icy patches with sizes ranging between few meters to about 60 m are observed. Carbon dioxide ice has been detected only in a 60×80 m area in Anhur region while it was exiting from a four year-long winter-night season [5]. This ice deposit underwent a rapid sublimation, disappearing in about one month after its initial detection. While water and carbon dioxide ice appear always mixed with the ubiquitous dark material [6,7], there are no evidences of the presence of water and carbon dioxide ices mixed together in the same area. If observed, ices always account for very small fraction (few percent) with respect to the dark material. Moreover, the surface ice deposits are preferentially located on the large lobe and the neck while they are absent on the small lobe. Apart from these differences in the spatial distribution of ices on the surface, a large variability is observed the mixing modalities and in the grain size distributions, as retrieved from spectral modeling [8]: 1) very small μm -sized water ice grains in intimate mixing with the dark terrain are detected on Hapi active regions [2]; 2) two monodispersed distributions with maxima at 56 μm and at 2 mm, corresponding to the intimate and areal mixing classes, are observed on the Imhotep debris fields ice grains [3]; 3) different combinations of water ice and dark terrain in intimate mixing with small grains (tens of microns) or in areal mixing with large grains (mm-sized) are seen on the eight bright areas discussed in [4]; 4) the CO_2 ice in the Anhur region appears grouped in areal patches made of 50 μm sized grains [5]. While the spectroscopic identification of water and carbon dioxide ices is made by means of diagnostic infrared absorption features, their presence cause significant effects also at visible wavelengths, including the increase of the albedo and the reduction of the spectral slope which results in a more blue color [9,10]. In summary, thermodynamic conditions prevailing on the 67P/CG nucleus surface allow the presence of only H_2O and CO_2 ices. Similar properties are probably common among other Jupiter family comets.

REFERENCES

- [1] Coradini, A. et al., 2007. VIRTIS: an imaging spectrometer for the Rosetta mission. *Space Sci. Rev.*, 128, 529-559.
- [2] De Sanctis, M. C. et al., 2015. The diurnal cycle of water ice on comet 67P/Churyumov-Gerasimenko. *Nature*, 525, 500-503.
- [3] Filacchione, G., et al., 2016a. Exposed water ice on the nucleus of comet 67P/Churyumov-Gerasimenko. *Nature*, 529, 368-372.
- [4] Barucci, M.A. et al., in press. Detection of exposed H_2O ice on the nucleus of comet 67P/Churyumov-Gerasimenko as observed by Rosetta OSIRIS and VIRTIS instruments. *Astron. Astrophys.*, doi:10.1051/0004-6361/201628764
- [5] Filacchione, G., et al. Seasonal exposure of carbon dioxide ice on the nucleus of comet 67P/Churyumov-Gerasimenko. *Science*, in press.
- [6] Capaccioni, F., et al., 2015. The organic-rich surface of comet 67P/Churyumov-Gerasimenko as seen by VIRTIS/Rosetta. *Science* 347.
- [7] Quirico, E., et al., 2016. Refractory and semi-volatile organics at the surface of comet 67P/Churyumov-Gerasimenko: Insights from the VIRTIS/Rosetta imaging spectrometer. *Icarus*, 272, 32-47.
- [8] Raponi, A., et al. Properties and temporal evolution of exposed water ice on the nucleus of comet 67P/Churyumov-Gerasimenko as observed by the Rosetta VIRTIS instrument: spectral analysis. *MNRAS*, submitted.
- [9] Filacchione, G., et al., 2016b. The global surface composition of 67P/CG nucleus by Rosetta/VIRTIS. I) Prelanding mission phase. *Icarus*, 274, 334-349.
- [10] Ciarniello, M., et al. The global surface composition of 67P/Churyumov-Gerasimenko nucleus by Rosetta/VIRTIS. II) Diurnal and seasonal variability. *MNRAS*, submitted.

Impact of radiogenic heating on the formation conditions of comet 67P/Churyumov-Gerasimenko

O. Mousis¹, A. Drouard¹, P. Vernazza¹, J. I. Lunine², K. Altwegg^{3,4}, H. Balsiger³, J.-J. Berthelier⁵, A. Bieler^{3,6}, P. Bochslers³, C. Briois⁷, G. Cessateur⁸, M. Combi⁶, J. De Keyser⁸, F. Dhooghe⁸, B. Fiethe⁹, S. A. Fuselier¹⁰, S. Gasc³, T. I. Gombosi⁶, K. C. Hansen⁶, M. Hässig^{3,10}, E. Kopp³, A. Korth¹¹, L. Le Roy³, R. Maggiolo⁸, U. Mall¹¹, B. Marty¹², H. Rème¹³, M. Rubin³, T. Sémon³, C.-Y. Tzou³, J. H. Waite¹⁰, P. Würz³

⁽¹⁾ Aix Marseille Université, CNRS, LAM (Laboratoire d'Astrophysique de Marseille)
UMR 7326, 13388, Marseille, France

⁽²⁾ Department of Astronomy and Carl Sagan Institute, Space Sciences Building Cornell University, Ithaca, NY 14853, USA

⁽³⁾ Physikalisches Institut, University of Bern
Sidlerstr. 5, CH-3012 Bern, Switzerland

⁽⁴⁾ Center for Space and Habitability, University of Bern
Sidlerstr. 5, CH-3012 Bern, Switzerland

⁽⁵⁾ LATMOS/IPSL-CNRS-UPMC-UVSQ
4 Avenue de Neptune F-94100, Saint-Maur, France

⁽⁶⁾ Department of Climate and Space Sciences and Engineering, University of Michigan
2455 Hayward, Ann Arbor, MI 48109, USA

⁽⁷⁾ Laboratoire de Physique et Chimie de l'Environnement et de l'Espace (LPC2E)
UMR CNRS 7328 – Université d'Orléans, France

⁽⁸⁾ Royal Belgian Institute for Space Aeronomy, BIRA-IASB
Ringlaan 3, B-1180 Brussels, Belgium

⁽⁹⁾ Institute of Computer and Network Engineering (IDA), TU Braunschweig
Hans-Sommer-Straße 66, D-38106 Braunschweig, Germany

⁽¹⁰⁾ Department of Space Science, Southwest Research Institute
6220 Culebra Rd., San Antonio, TX 78228, USA

⁽¹¹⁾ Max-Planck-Institut für Sonnensystemforschung
Justus-von-Liebig-Weg 3, 37077 Göttingen, Germany

⁽¹²⁾ Centre de Recherches Pétrographiques et Géochimiques, CRPG-CNRS, Université de Lorraine
15 rue Notre Dame des Pauvres, BP 20, 54501 Vandoeuvre lès Nancy, France

⁽¹³⁾ Université de Toulouse; UPS-OMP-CNRS; IRAP,
Toulouse, France.

ABSTRACT

Because of the high fraction of refractory material present in comets, the radiogenic decay of elements can generate enough heat to induce the loss of ultravolatile species such as N₂, Ar or CO if the nuclei accreted early in the protosolar nebula. Here we investigate the influence of this decay heat on the formation conditions of comet 67P/Churyumov-Gerasimenko as a function of its accretion epoch and size of parent body. We consider two possibilities: either, to account its bilobed shape, 67P assembled from two primordial ~1 kilometer-sized planetesimals or it results from the disruption of a bigger parent body. To match the volatile content observed in the coma, we find that 67P/Churyumov-Gerasimenko must have formed several Myr after the protosolar nebula initiation, independent of i) the size of parent body and ii) the composition of the icy material (amorphous ice, clathrates or crystalline ice). This places stringent conditions on the formation timescales of 67P/Churyumov-Gerasimenko and other comets.

ON THE SURVIVAL OF LOW VOLATILITY ICES ON THE SURFACE OF 67P/CHURYUMOV-GERASIMENKO: A THERMOPHYSICAL POINT OF VIEW

Maria Teresa Capria¹, Gianrico Filacchione¹, Fabrizio Capaccioni¹, Federico Tosi¹, Maria Cristina De Sanctis¹, Mauro Ciarniello¹, Andrea Raponi¹, Alessandro Longobardo¹, Alessandra Migliorini¹, Michelangelo Formisano¹, Dominique Bockelée-Morvan², Eric Quirico³, Gabriele Arnold⁴

- 1) INAF-IAPS, Istituto di Astrofisica e Planetologia Spaziali, Rome, Italy
- 2) LESIA, Observatoire de Paris, LESIA/CNRS, UPMC, Université Paris-Diderot, 92195 Meudon, France
- 3) Univ. Grenoble Alpes, CNRS, IPAG, Grenoble, France
- 4) Institute for Planetary Research, DLR - Deutschen Zentrums fuer Luft- und Raumfahrt, Berlin, Germany

ABSTRACT:

Carbon dioxide has been detected only once by VIRTIS-M [1] onboard Rosetta in a small area in the Anhur region [2]. At the detection time (March 2015) the region, on the Southern part of the nucleus, was exiting from a years-long night and entering a brief and very intense period of constant illumination. The CO₂ ice, apparently not mixed with other ices, was grouped in areal patches of 50 micron size grains and was no more visible when the area was imaged again by the spectrometer one month after the first detection. The presence of CO₂ ice on the surface of the comet implies low temperatures (<150 K) and requires the existence of a CO₂ ice-rich layer extremely close to the surface. While the disappearance of the CO₂ ice deposit is easily explained with the increasing exposure to solar illumination experienced by the region from December 2014, the presence, even for a short time, on the surface of the comet of an ice as transient as CO₂ can be difficult to explain. Two hypotheses can be made: recondensation on the surface of gas sublimating from the interior or exposition of a CO₂ ice rich layer due to a strong erosion of the surface shortly followed by a long period of extremely low temperatures.

We are using the Rome model for the thermal evolution and differentiation of nuclei in order to test the hypothesis that a CO₂ ice rich layer close to the surface can exist and survive long enough that some CO₂ ice patch can be occasionally exposed [3]. We are taking into account the illumination conditions of the Anhur region along the orbit, different and more extreme than in other parts of the nucleus. The region is experiencing during each perihelion a brief period of intense heating, probably able to drive a strong erosion; then, almost abruptly, an years-long period of darkness follows, during which the region experiences temperatures well below the sublimation temperature of CO₂.

From the preliminary results of this analysis we can confirm that the second hypothesis is viable and compatible with the VIRTIS observations.

REFERENCES

- [1] Coradini, A. et al., 2007, VIRTIS: an imaging spectrometer for the Rosetta mission. *Space Sci. Rev.*, 128, 529-559
- [2] Filacchione, G., et al., Seasonal exposure of carbon dioxide ice on the nucleus of comet 67P/Churyumov-Gerasimenko. *Science*, in press
- [3] Bockelée-Morvan, D. et al., Pre/post perihelion asymmetry of H₂O, CO₂, CH₄, and OCS outgassing in comet 67P from Rosetta/VIRTIS-H observations, in press

Stability of sulphur dimers (S_2) in cometary ices in connection with 67P observations

O. Ozgurel¹, F. Pauzat¹, Y. Ellinger¹, A. Markovits¹, O. Mousis²

¹ UPMC Univ. Paris 06, UMR 7616-CNRS, Laboratoire de Chimie Théorique, 75005 Paris, France

² Laboratoire d'Astrophysique de Marseille, UMR 7326-CNRS, Aix Marseille Université, 13388, Marseille, France

S_2 has been observed for decades in comets, but it arises a new interest with its observation in comet 67P/Churyumov-Gerasimenko (le Roy et al. 2015). As a matter of fact, the nature of its source is still unknown. In this study, we propose that S_2 is formed by irradiation (photolysis and/or radiolysis) of S-bearing molecules embedded in the icy grains precursors of comets, in particular H_2S which could exist scattered or as clumps in the middle of the bulk of H_2O ices. The irradiation is assumed to create simultaneously voids in ices within which the produced molecules can accumulate. We investigate the stability of S_2 molecules in such cavities, assuming that the surrounding ice is made of H_2S or H_2O . To support this scenario, we have used chemistry numerical models based on first principle periodic density functional theory (DFT). These models have shown to be well adapted to the description of compact ice and are capable to describe the trapping of volatiles in the ice matrix. We show that the stabilization energy of S_2 molecules in such voids is close to that of the H_2O ice binding energy, implying that they can only leave the icy matrix when this latter sublimates. Unlike O_2 whose abundance correlated to H_2O , no global trend should be drawn between the variation of S_2 and H_2O abundances as S_2 can accumulate in both S-bearing and H_2O ices. Our results are supported by the ROSINA data collected between May 2015 (equinox) and August 2015 (perihelion), showing that there is no clear correlation of S_2 with H_2O or H_2S in 67P/C-G (Calmonte et al. 2016).

Pluto's global surface composition and physical state from New Horizons Ralph/LEISA data.

B. Schmitt, S. Protopapa, S. Philippe, W.M. Grundy, D.C. Reuter, R. Côte, D.P. Hamilton, C.M. Dalle Ore, J.C. Cook, D.P. Cruikshank, E. Quirico, A.H. Parker, L.A. Young, R.P. Binzel, A.M. Earle, K. Ennico, C.J.A. Howett, D.E. Jennings, I.R. Linscott, A.W. Lunsford, C.B. Olkin, J.W. Parker, K.N. Singer, J.R. Spencer, J.A. Stansberry, S.A. Stern, C. Tsang, A.J. Verbiscer, H.A. Weaver and the New Horizons Science Team.

In July 2015 the New Horizons spacecraft recorded a large set of data on Pluto, in particular with the Ralph/LEISA spectro-imager (Reuter et al., 2008) dedicated to the study of the surface composition (Stern et al., 2015 and Grundy et al., 2016). In this talk we report complementary studies on the distribution and physical state of the ices and non-ice materials on Pluto's surface as well as their mode and degree of mixing. They are based on high resolution LEISA spectro-images covering the whole illuminated face of Pluto.

After extracting noise and instrumental artefacts by principal component analysis, several specific spectral indicators and correlation plots have been used to derive qualitative distribution maps of the main ices constituted by the molecules N₂, CH₄, CO, and H₂O as well as for the visible dark-red material (Schmitt et al. 2016, Icarus, submitted). These maps indicate the presence of 3 different types of ices: H₂O, CH₄-rich:N₂:CO and N₂-rich:CH₄:CO ices, with CH₄ and CO mixed in a ternary molecular mixture with N₂. In parallel, quantitative abundance and grain size maps of these three material (without CO yet) and tholins have been derived by inversion of the spectra using the Hapke radiative transfer model. This analysis was performed pixel-by-pixel over the whole surface of Pluto considering, for each pixel, a spatial distribution of these materials (Protopapa et al. 2016, Icarus, submitted).

The occurrence of a N₂-rich – CH₄-rich ices mixing line associated with a decrease of the CO/CH₄ ratio tell us that a fractionation sublimation sequence transforms N₂-rich ice into either a N₂-rich – CH₄-rich binary mixture at the surface or an upper CH₄-rich:N₂:CO ice crust that may hide the N₂-rich ice below. The CH₄-rich – H₂O mixing line witnesses the subsequent sublimation of CH₄ ice left behind by the N₂:CO sublimation (N spring-summer), or a direct condensation of CH₄ ice on cold H₂O ice (S autumn). H₂O ice appears to be the substratum on which other ices condense or non-volatile organic materials are deposited from the atmosphere.

The spatial distribution of these materials is very complex. However we identify large scale latitudinal variations of methane and nitrogen ices which can help setting constraints to volatile transport models. To the north, by about 55 deg latitude, the nitrogen abundance smoothly tapers off to an expansive polar plain of predominantly methane ice. This transition well correlates with expectations of vigorous spring sublimation after a long polar winter. Continuous illumination northward of 75 deg over the past twenty years, and northward of 55 deg over the past ten years, seems to have sublimated the most volatile nitrogen into the atmosphere, with the best chance for redeposition occurring at points southward. This loss of surface nitrogen appears to have created the polar bald spot seen in our maps and also predicted by Hansen and Paige (1996).

A few regions that stand out for composition with respect to the latitudinal pattern described above will be also discussed. In particular, informally named Sputnik Planitia displays gradients of composition that suggest the action of sublimation-redeposition processes.

Finally, we will compare these qualitative and quantitative composition and textural maps with Pluto's geologic features observed by LORRI panchromatic and MVIC multispectral imagers to better understand the geophysical processes in action at the surface of this astonishingly active frozen world.

Photometric Properties of Ices in the Pluto System

A. J. Verbiscer, M. W. Buie, M. R. Showalter, B. J. Buratti, R. Binzel, K. Ennico, W. M. Grundy, C. B. Olkin, J. R. Spencer, S. A. Stern, H. A. Weaver, L. A. Young

In July 2015, the New Horizons spacecraft acquired spatially resolved views of Pluto and its five satellites at viewing geometries unattainable from Earth. Hubble Space Telescope observations of the Pluto system acquired during the New Horizons encounter epoch (HST Program 13667, M. Buie, PI) span a smaller range in phase angle, from 0.06 to 1.7 degrees, and enable the measurement and characterization of the opposition effect and the estimation of geometric albedo for Pluto and its satellites. At these small phase angles, differences in the opposition effect width and amplitude appear. Pluto has a narrow opposition surge of relatively low amplitude while its moons exhibit a considerably broader surge with high amplitude. Microtextural surface properties derived from the shape and magnitude of the opposition surge of each surface can be related to the collisional, depositional, and thermal history of the system. Combining these small phase angle HST observations with those made at larger phase angles by the New Horizons Long Range Reconnaissance Imager (LORRI), we produce the most complete disk-integrated solar phase curves that we will have for decades to come. Modeling these disk-integrated phase curves generates sets of photometric parameters that inform spectral modeling of the satellite surfaces as well as terrains on Pluto from spatially resolved New Horizons Ralph Linear Etalon Imaging Spectral Array (LEISA) data from 1.25 to 2.5 microns. The high albedo region informally known as Sputnik Planitia dominates the disk-integrated reflectance of Pluto on the New Horizons encounter hemisphere and defines the maximum reflectance in Pluto's rotational lightcurve. These results lay the groundwork for observations at true opposition in 2018, when the Pluto system will be observable at phase angles so small that an Earth transit across the solar disk will be visible from Pluto and its satellites.

The ammonia distribution on Charon as seen by New Horizons. C. M. Dalle Ore^{1,2}, J. C. Cook³, Silvia Protopapa⁴, D. P. Cruikshank², William M. Grundy⁵, Kim Ennico², Cathy B. Olkin¹, S. Alan Stern³, Harold A. Weaver⁶, Leslie A. Young³ and the New Horizons Surface Composition Theme Team. 1 SETI Institute, 189 Bernardo Ave, Mountain View, CA 95043; 2 NASA Ames Research Center, 3 Southwest Research Institute; 4 University of Maryland; 5 Lowell Observatory; 6 John Hopkins University, Applied Physics Laboratory. (Cristina.M.DalleOre@nasa.gov)

Abstract: Spectral evidence for NH₃ and/or its hydrates on Charon, Pluto's largest moon, has been previously reported from ground-based observations (Cook et al. 2007, *Astrophys. J.* 663, 1406–1419; Merlin, et al. 2010, *Icarus*, 210, 930; Cook, et al. 2014, AAS/Division for Planetary Sciences Meeting Abstracts, 46, #401.04, DeMeo et al. 2015, *Icarus*, 246, 213) and recently from New Horizons closest approach data (Grundy et al. 2016 *Science* 351, 679 aad9189).

New Horizons observed Charon at high spatial resolution (better than 10 km/px) with the LEISA imaging spectrometer. Images from the New Horizons spacecraft reveal an icy surface with terrains of seemingly different ages and a moderate degree of localized coloration.

Our modeling results were obtained from the analysis of high spatial and moderately high spectral resolution data of Charon acquired close to the July 14th, 2015 flyby. They show a distribution of ammonia hydrated ices generally spread over the disk with areas of higher concentration corresponding to apparently fresher terrains such as craters. Based on laboratory experiments ammonia is a fragile molecule that will not survive UV or charged particle irradiation. On Charon's surface it should be completely dissipated within a few million years. We propose a scenario, based on Charon's formation model (Canup, 2011, *AJ*, 141, 35-43), in an attempt to justify the presence of ammonia products on its surface.

Overall, we find a uniform composition with amounts and grain sizes varying on fairly small scales, in agreement with the apparent homogeneity that seems to be the hallmark of Charon's surface.

Present and Past Glacial Activity on Pluto with a Volatile Transport Model

Tanguy Bertrand and François Forget

Laboratoire de Météorologie Dynamique, Université Pierre et Marie Curie, France.

Email: tanguy.bertrand@lmd.jussieu.fr

The high obliquity and eccentricity of the orbit of Pluto induce seasonal cycles of condensation and sublimation of the main volatile ices: N₂, CH₄, and CO. The New Horizons spacecraft, which flew by Pluto in July 2015, revealed a complex surface composition including a thousand-kilometre nitrogen glacier in the "Sputnik Planitia" basin near the Anti-Charon longitude, extensive methane frosts and even glaciers at mid and high latitudes, and equatorial ice-free regions. We present numerical simulations designed to model the evolution of Pluto's volatiles over thousands of years on the basis of straightforward universal physical equations.

Our results show that Pluto's surface is very active, with an evolution of its ices driven by three different timescales.

Firstly, every Pluto year, nitrogen condenses and sublimates in Sputnik Planitia, changing the surface pressure so that the maximum is obtained in 2015. In particular, the model predicts the 3-fold increase of pressure observed to occur since 1988. Frosts of methane, and sometimes nitrogen, seasonally cover the mid and high latitudes, explaining the bright northern polar cap reported in the 1990s. In 2015, the model shows a northern hemisphere covered by methane frost, consistent with the distribution observed by New Horizons. The model also predicts that most of these seasonal frosts should disappear in the next decade, and thus could be tested observationally in the near future.

Secondly, orbital parameters of Pluto such as obliquity and longitude of perihelion vary with time. Using prior orbital parameters of Pluto and a realistic glacial flow parametrization, we simulate Pluto over astronomical cycles. The results show that the cycles of glacial activity may explain the rugged eroded-mountain landscapes surrounding Sputnik Planitia as well as the smaller nitrogen glacier lying at higher altitudes. In addition, methane glaciers form during high obliquity climates, at mid northern and southern latitudes, which may be a key process to understand the formation of the "bladed" methane terrains east of "Tomabaugh Regio".

Thirdly, if we run the model with a thin veneer of all three ices uniformly distributed over the surface, the ices slowly and unavoidably accumulate in the Sputnik Planitia basin. Indeed, the peculiar insolation and atmosphere of Pluto favor the nitrogen condensation near the equator and in the lower altitude regions. This mechanism, which has no equivalence on Earth but is known on Mars, explains how Pluto got its icy heart.

MARS POLAR CAPS

François Forget

Laboratoire de Météorologie Dynamique (CNRS/UPMC/IPSL), Paris, France
(forget@lmd.jussieu.fr)

By many aspects planet Mars is a world of ices, with solid water or carbon dioxide playing a major role in many climatic and geological processes. As on Earth, this is particularly true at high latitudes, and one could state that Mars possess not one, but at least four kinds of polar caps.

First, both regions are permanently covered by layered water ice deposits which reach 2000 m in thickness. Their detailed structures have been revealed by radar sounding but the origin of these structures and the climatic processes that have formed them in the past millions years remain debated. Within the southern polar layered deposits, radar surveys have revealed the presence of an enigmatic buried CO₂ ice reservoir containing as much CO₂ as in the present gaseous atmosphere. It is covered by a layer of water ice, itself, covered by a 10 m-thick perennial CO₂ ice cap. This cap exhibit fascinating landforms. Their shapes vary from year to year. The stability of this relatively thin perennial cap is nevertheless enigmatic. It must be controlled by natural feedbacks, not yet fully understood.

Above these permanent "polar caps", and down to about 50 deg latitude, both hemispheres get covered by a seasonal layer of CO₂ ice, often mixed with and surrounded by water ice frost. The physical processes at work during the period of condensation and during the sublimation phases are exotic and often puzzling. In some locations CO₂ ice condenses directly on the surface to form a transparent slab-ice layer, while other areas are subject to atmospheric snow storms. Later, water ice or dust can locally accumulate enough to temporarily hide the CO₂ ice lying below. At the end of winter, the sun can trigger sub-surface sublimation which can induce the formation of spectacular geysers able to erode the rocky surface. It has even been suggested that subliming CO₂ ice may be able to carve the spectacular gullies observed on mid-latitudes Martian slopes and which had previously been assumed to have been carved by flowing water.

I will review our current knowledge on the different Martian polar caps, highlighting the numerous enigma and puzzle that remain to be solved by observation analysis, modeling and lab experiments.

Energetic charged particle interactions at icy satellites

T. A. Nordheim¹, K.P. Hand¹, C. Paranicas², C. J. A. Howett³, A. R. Hendrix⁴

¹Jet Propulsion Laboratory, California Institute of Technology, ²Applied Physics Laboratory, John Hopkins University, ³Southwest Research Institute, ⁴Planetary Science Institute

Satellites embedded within planetary magnetospheres are typically exposed to bombardment by charged particles, from thermal plasma to more energetic particles at radiation belt energies. At many planetary satellites, energetic charged particles are typically unimpeded by patchy atmospheres or induced satellite magnetic fields and instead are stopped in the surface itself. Most of these primaries have ranges in porous water ice that are at most centimeters, but some of their secondary photons, emitted during the deceleration process, can reach meter depths [Paranicas *et al.*, 2002, 2004; Johnson *et al.*, 2004]. Examples of radiation-induced surface alteration includes sputtering, radiolysis and grain sintering, processes that are capable of significantly altering the physical properties of surface material. Thus, accurate characterization of energetic charged particle weathering at icy satellites is crucial to a more comprehensive understanding of these bodies.

At Saturn's inner mid-size moons remote sensing observations by several instruments onboard the Cassini spacecraft have revealed distinct weathering patterns which have been attributed to energetic electron bombardment of the surface [Howett *et al.*, 2011, 2012, 2014; Schenk *et al.*, 2011; Paranicas *et al.*, 2014]. In the Jovian system, radiolytic production of oxidants has been invoked as a potential source of energy for life which may reside in the sub-surface ocean of its satellite Europa [Johnson *et al.*, 2003; Hand *et al.*, 2007; Vance *et al.*, 2016]. Here we will discuss the near-surface energetic charged particle environment of icy satellites, with particular emphasis on comparative studies between the Saturnian and Jovian systems and interpretation of remote sensing observations by instruments onboard missions such as Cassini and Galileo. In addition, we will discuss implications for surface sampling by future lander missions (e.g. the proposed Europa lander now under study).

Hand, K. P., *et al.* (2007), *Astrobiology*, 7(6), 1006–22

Howett, C. J. A., *et al.* (2011) *Icarus*, 216(1), 221–226

Howett, C. J. A., (2012) *Icarus*, 221(2), 1084–1088

Howett, C. J. A. (2014) *Icarus*, 241, 239–247

Johnson, R. E., *et al.* (2003), *Astrobiology*, 3(4), 823–850

Johnson, R. E., *et al.* (2004) in *Jupiter: The planet, satellites and magnetosphere*, pp. 483–508

Paranicas, C., *et al.* (2002), *Geophys. Res. Lett.*, 29(5), 10–13.

Paranicas, C., *et al.* (2004), in *Europa*, pp. 529–544

Paranicas, C. *et al.* (2014), *Icarus*, 234, 155–161,

Schenk, P., *et al.* (2011), *Icarus*, 211(1), 740–757

Vance, S. D., *et al.* (2016), *Geophys. Res. Lett.*, 43(10), 4871–4879

SPECTRAL ANALYSIS OF ENCELADUS, DIONE, AND RHEA' SURFACES: WATER ICE AND SUB-MICRON PARTICLES DISTRIBUTION. F. Scipioni¹, P. Schenk², F. Tosi³, E. D'Aversa³, R. Clark⁴, J.-Ph. Combe⁵, C. Dalle Ore⁶. ¹NASA Ames Research Center, Moffett Field, CA, 94035, francesca.scipioni@nasa.gov; ²Lunar and Planetary Institute; ³INAF-IAPS, Rome, Italy; ⁴PSI, Tucson, AZ; ⁵Bear Fight Institute, Winthrop, WA; ⁶Seti Institute, Mountain View, CA.

Water ice is the most abundant component of Saturn's mid-sized moons. However, these moons show an albedo asymmetry – their leading sides are bright while their trailing side exhibits dark terrains. Such differences arise from two surface alteration processes.

The first is due to bombardment of charged particles from the interplanetary medium and driven by Saturn's magnetosphere (e.g. [1]). These particles fracture the surface, forming sub-micron ice particles, and get contaminants implanted in the upper ice layer (e.g. [2]). The second process results from the impact of E-ring particles on the satellites' leading side. The E-ring is composed primarily of pure water ice grains, which originate from Enceladus' southern polar plumes. Tethys, Dione, and Rhea orbit outside the E-ring, while Mimas orbits inside. E-ring ice particles are continuously refreshing the leading hemisphere surfaces of Tethys, Dione, and Rhea, thereby making them bright (e.g. [3] [4] [5] [6] [7] [8]).

We present here results from our ongoing work mapping the variation of the main water ice absorption bands and sub-micron ice particles across Dione, Rhea, and Enceladus' surfaces using Cassini-VIMS data acquired in the IR range (0.8–5.1 μm).

The Cassini VIMS spectrometer acquires hyperspectral data in the 0.3–5.1 μm spectral range. We selected VIMS cubes of Enceladus, Dione, and Rhea in the IR range (0.8–5.1 μm), and minimized photometric effects due to different illumination conditions by normalizing all spectra at 2.23 μm .

For all pixels in the selected VIMS cubes, we measured the band depths for water-ice absorptions at 1.25, 1.5 and 2.02 μm and the height of the 3.6 μm reflection peak, whose value relates to grain size.

Moreover, we considered the main spectral indicators in the IR range for ice particles smaller than 1 μm [1]: (i) the 2 μm absorption band is asymmetric and (ii) it has the minimum shifted to longer λ ; (iii) the band depths ratio 1.5/2.0 μm decreases; (iv) the reflection peak at 2.6 μm decreases; (v) the Fresnel reflection peak is suppressed; (vi) the 5 μm reflectance is decreased relative to the 3.6 μm peak.

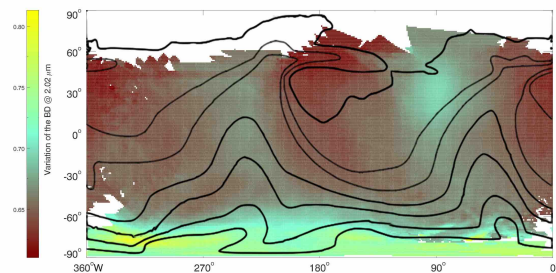
Since the first part of the VIMS-IR spectra (0.8-2.5 μm) is sometimes affected by saturation effects, for each

cube of the dataset we performed a pixel by pixel selection of spectral features to be used: for each pixel, only the absorption bands not suppressed (totally or partially) by saturation were selected.

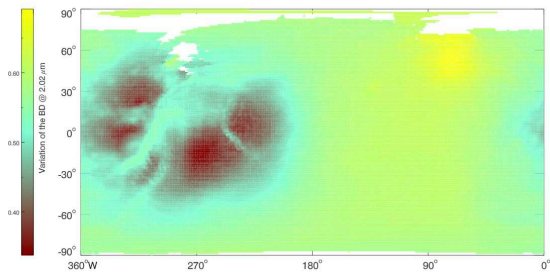
To characterize the global variation of water-ice band depths we sampled the three satellites' surface with a $1^\circ \times 1^\circ$ fixed-resolution grid and then averaged the band depths and peak values inside each square cell.

In Figure 1 we show the global variation of the water ice absorption band, centered at 2.02 μm , and in Figure 2 the variation of band depths ratio 1.5/2.0 μm , for Enceladus (panel a), Dione (panel b), and Rhea (panel c).

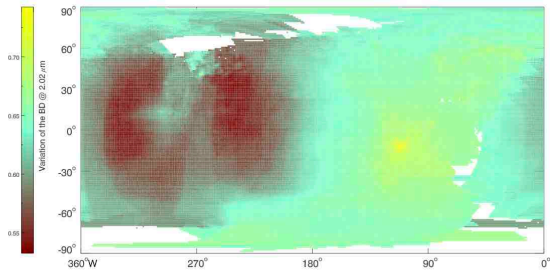
The variation of the depth of the water ice absorption bands across the surface reflects the different space weather mechanisms acting on their surface. Terrains where E-ring's ice particles deposit have in general deeper water ice absorption bands, meaning that mechanism refreshes that portion of surface. On the other hand, terrains subject just to bombardment of charged particles and micrometeorite gardening have shallower absorption bands. This can be due to an increase in contaminants abundance, and/or to a finer grain size.



(a)

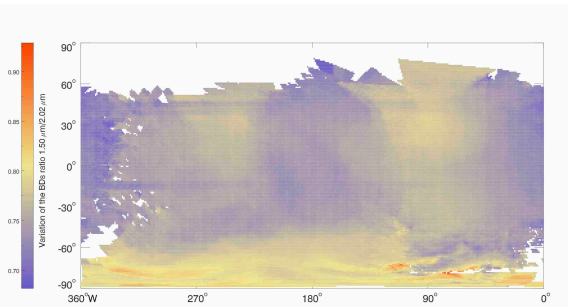


(a)

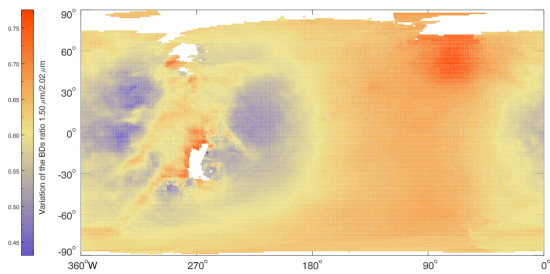


(b)

Figure 1: Variation of the water ice absorption band at 2.02 μm for Enceladus (a), Dione (b), and Rhea (c).



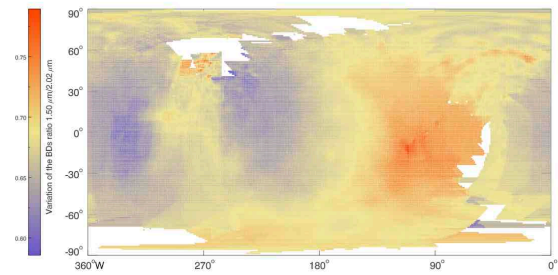
(c)



(a)



(b)



(c)

Figure 2: Variation of the band depths ratio 1.5/2.0 μm for Enceladus (a), Dione (b), and Rhea (c).

References:

- [1] Schenk, P., et al., 2011. *Icarus* 211, 740– 757. [2] Baragiola, R. A., et al., 2013. In: Gudipati, M. S., Castillo-Rogez, J. (Eds.), Vol. 356, p. 527. [3] McCord, et al., 1971. *Astrophys. J.* 165, 413–424. [4] Blair, G., Owen, F., 1974. *Icarus* 22, 224–229. [5] Buratti, et al., 1990. *Icarus* 87, 339-357. [6] Verbiscer, A.J. and Veeverka, J., 1992. *Icarus* 99, 63-69. [7] Scipioni, F., et al., 2013. *Icarus* 226, 1331-1349. [8] Scipioni, et al., 2014. *Icarus* 243, 1-16.

Physical photometric characteristics of icy and rocky bodies: a comparison

Bonnie J. Buratti, NASA Jet Propulsion Laboratory, California Institute of Technology

Physical modeling of a planetary surface by photometric theory reveals important information, including the roughness, porosity, albedo, and nature of the particles comprising the regolith, such as their sizes, shapes, and composition. In turn, these parameters reveal clues about the geophysical evolution of the surface, shedding light on the existence and nature of geological activity, exogenic alteration process, and collisional history. Over the last 3 decades, models have been fit to a wide range of both icy and rocky bodies to understand their comparative evolution.

A key physical parameter is macroscopic roughness. Two formalisms have been developed to describe rough facets, the Hapke slope model (1) and the crater roughness model (2). Hapke's model covers the surface with features characterized by a mean slope-angle, while the crater roughness model defines rough features by idealized paraboloidal craters defined by a depth-to-radius ratio. These models reveal the roughness of planetary surfaces, which yields clues to their collisional history; the infill of planetary features by either exogenously placed dust or endogenous geologic processes to create a smooth surface; and similar infilling by volcanic deposits.

The porosity of the optically active portion of a planetary regolith also offers clues to its past evolution. The porosity is defined as the fraction of space not filled by particles (3). Volcanic deposits should lead to a tenuous fluffy surface, while geologic processes such as the melting and freezing of liquids should produce smooth surfaces. Meteoritic "gardening" of a surface will produce relatively fluffy surfaces, while magnetospheric effects should anneal the surface and lessen its porosity.

Another key physical parameter is the single particle phase function (sppf), which describes the directional scattering properties of particles. It depends on the particles' size, size-distribution, real and complex indices of refraction, and shape. For example, small transparent particles tend to be forward scattering while larger opaque particles tend to be backscattering. The nature of the particles that comprise the optically active portion of a planetary surface is also a record of the surface's past evolution. The single particle phase function is often described by a Henyey-Greenstein phase function defined by g , where $g=1$ is purely forward scattering, $g=-1$ is purely backscattering, and $g=0$ is isotropic.

The table below summarizes these parameters for a select group of both icy and rocky bodies.

Object	Roughness (mean slope)	Porosity	Sppf (g)	Sources
Moon	25	90%	-0.25	Buratti, 1985
Vesta	18	0.4*	-0.27	Li et al., 2013
Comet Borrelly	20	0.008*	-0.45	Buratti et al., 2003
Enceladus	8	90%	-0.35	Buratti, 1985; Buratti et al., 2014
Europa	10	90%	-0.15	Buratti, 1985; Domingue et al. 1991
Mimas	30	95%	-0.21	Verbiscer, 1992; Buratti, 2016

Hapke's h -parameter (Hapke, 1993)

The parameters are a reflection of geophysical processes rather than icy or rocky composition. This finding is not surprising, as ice acts like a rock in the cold temperatures of the outer Solar System.

References: (1) Hapke, B. 1984. *Icarus* **59**, 41. (2) Buratti and Veverka, 1985 *Icarus* **64**, 320. (3) Irvine, W. 1966. *JGR* **71**, 2931.

Government Funding Acknowledged.

Title: Near-UV behaviour of observed TNO reflectance spectra.

Observed spectra provide the best diagnostics of the surface compositions of Trans-Neptunian Objects (TNOs). We have observed the spectra of 7 TNOs, from across almost the full range of dynamical classes, using the VLT's X-Shooter spectrograph. Compared to the 5 targets in our sample which exhibit linear spectra in the UV-optical range, two of our targets show highly unusual spectral behaviour, whereby their reflectance decreases sharply at wavelengths below 500 nm. The presence of this feature in the spectrum is accompanied in both cases by deeper characteristic absorption bands at ~ 1600 nm and ~ 2000 nm indicative of possible H₂O or methanol ices on their surfaces. This is contrary to the other 5 TNOs which have spectra exhibiting minimal distinctive NIR absorption bands. In available regions, our observed spectra of the targets are in agreement with spectra or photometry available in the literature. Using a different solar analogue to produce our reflectance spectra does not remove the UV decrease exhibited by the two targets. Further, it appears that neither reducing the spectra with different pipelines, nor using drastically different parameters in those pipelines changes this general behaviour. Based on laboratory spectra of complex hydrocarbons it is plausible that the near-UV behaviour is the result of organic substances on the surfaces of the TNOs which exhibit it. Lab spectra of organics are also consistent in having a general red slope similar to that observed in the spectra of many TNOs. While laboratory spectra of some exotic silicate substances also show a decrease in reflectance in the near-UV spectral region that is in principle consistent with our observations, those silicates do not exhibit a red slope consistent with our optical spectra. Hence, the hypothesis that silicates are present seems less likely than the hypothesis that this UV decrease is due to the presence of organics on the surfaces of these objects.

Ice on Ceres

H. G. Sizemore, T. H. Prettyman, M. C. De Sanctis, J.-P. Combe, N. Schorghofer, S. Byrne, M. E. Landis, M. T. Bland, P. M. Schenk, B. E. Schmidt, K. H. G. Hughson, J. Castillo-Rogez, R. Fu, A. Ermakov, C. A. Raymond, C. T. Russell and the Dawn Science Team

Prior to the arrival of the Dawn spacecraft at Ceres, the dwarf planet was anticipated to be an ice-rich body. Data gathered by Dawn instruments over 20 months in orbit have broadly supported the prediction of an ice-rich outer shell. We will present an overview of key results relevant to ice from the Visible and InfraRed Mapping Spectrometer (VIR-MS), the Gamma Ray and Neutron Detector (GRaND), morphological analysis of Framing Camera (FC) images, numerical modeling, and gravity data. We will also discuss an emerging consensus view of the global distribution of ice on Ceres, and key outstanding questions.

Water ice-rich areas detected on Ceres' surface from Dawn-VIR data analysis: abundance, grain size, and temperature retrieval

A. Raponi¹, M.C. De Sanctis¹, A. Frigeri¹, M. Ciarniello¹, E. Ammannito^{3,1}, F. Tosi¹, J.-Ph. Combe², F. Zambon¹, F.G. Carrozzo¹, G. Magni¹, M.T. Capria¹, M. Formisano¹, A. Longobardo¹, E. Palomba¹, C.M. Pieters⁴, C.T. Russell³, C.A. Raymond⁵, and the Dawn/VIR Team

¹ INAF-IAPS Istituto di Astrofisica e Planetologia Spaziali, Rome, Italy.

² Bear Fight Institute, Winthrop, WA, USA.

³ University of California at Los Angeles, Los Angeles, CA, USA.

⁴ Department of Earth, Environmental and Planetary Sciences, Brown University, Providence, RI, USA

⁵ NASA/Jet Propulsion Laboratory and California Institute of Technology, Pasadena, CA, USA.

Dawn spacecraft orbits around Ceres since early 2015 acquiring a huge amount of data at different spatial resolutions during the several phases of the mission. VIR, the visible and InfraRed spectrometer onboard Dawn [1], allowed to detect the principal mineralogical phases present on Ceres.

Ceres surface is mainly characterized by a large abundance of dark component, NH₄-phyllosilicates and carbonates. Other mineralogical phases, such as water ice, are also present at local scale.

Water has been detected in small areas on Ceres' surface by the Dawn-VIR instrument [1]. The most obvious finding is located in Oxo crater [2]. Further detections of water have been made during the Survey observation phase (1.1 km/pixel) and High-Altitude Mapping Orbit (400 m/px) [3]. During the LAMO phase (Low Altitude Mapping Orbit), the data with increased spatial resolution (100 m/px) coming from both regions have improved the detection of water, highlighting clear diagnostic water ice absorption features. In this study, we focused on spectral modeling of VIR spectra of Oxo and another crater (lon = 227°, lat 57°), near Messor crater.

The Hapke radiative transfer model [4] has been applied in order to retrieve the water ice properties. We consider two types of mixtures: areal and intimate mixing. In areal mixing, the surface is modelled as patches of pure water ice, with each photon scattered within one patch. In intimate mixing, the particles of water ice are in contact with particles of the dark terrain, and both are involved in the scattering of a single photon. The best fit with the measured spectra has been derived with the areal mixture. The water ice abundance obtained is up to 15-20% within the field of view, and the grain size retrieved is of the order of 100-200 μm. Phyllosilicates and carbonates, which are ubiquitous on Ceres surface [5], have been also detected and modeled in correspondence with the icy regions. The water ice is typically located near and within the shadows projected by the crater rims. Temperature of the ice is retrieved according to specific spectral parameters leading to an average temperature of 150 K. Further analysis are required to study the origin of the ice.

References

[1] De Sanctis M.C. et al., Space Sci. Rev., 2010

[2] Combe J-Ph. et al., 2016, LPI N. 1903, 1820

[3] Combe J.-Ph. et al., 2016, DPS-EPSC

[4] Hapke B., Cambridge Univ. Press., 1993, 2012

[5] De Sanctis M.C. et al., 2015. Nature 242, 528

Lifetime of Ice on Ceres

Paul O. Hayne¹, Margaret Landis², and Shane Byrne²

Dwarf planet Ceres resides in a borderland in the Main Asteroid Belt, at the edge of the icy outer solar system. Although water ice is thought to be thermodynamically unstable on Ceres' sunlit surface [1,2,3], its lifetime against sublimation is in fact finite. Furthermore, water ice is stable on billion-year timescales in the near subsurface in the mid-latitudes [4], and at the surfaces of polar cold traps created by perennial shadows [5]. Both seasonal and obliquity cycles drive variations in temperatures and ice stability. Therefore, observations of the quantity and distribution of ice among these reservoirs would provide a key indication of water activity and climatic cycles on Ceres. Age estimates can be derived for any detected ice deposits, given their thermal histories.

We investigated lifetimes for water ice on Ceres, focusing on these three regimes: 1) sunlit surfaces, 2) permanent shadows, and 3) subsurface. The model includes heat and vapor diffusion, which are calculated with a standard finite difference scheme using the instantaneous solar heating, given the most up-to-date ephemeris for Ceres. Other important quantities, such as albedo and thermal inertia are given by [3].

To estimate ice lifetimes, we first calculated the time to sublimate a pure layer of ice of thickness d , which is simply $t_{\text{sub}} \sim \rho d / \dot{m}$, with the ice density ρ , and sublimation rate \dot{m} (mass/area/time). Secondly, we calculate a “darkening timescale” for ice containing a fraction f of impurities (“dust”):

$$t_{\text{dark}} \sim \frac{4a}{3Q_{\text{ext}} f} \frac{\rho}{\langle \dot{m} \rangle} \tau_{\text{crit}},$$

where a is the radius of the dust particles, Q_{ext} is their optical extinction efficiency, and τ_{crit} is the optical depth of “lag” required to obscure the underlying ice layer.

Results are shown in the figures. We find that optical darkening is rapid at the lower latitudes (0 – 45°), with timescales $t_{\text{dark}} < 1$ yr. At higher latitudes, t_{dark} can rise to > 1 kyr, and is quite sensitive to the ice albedo and dust content; for ice albedo > 0.7 and dust content $< 20\%$, darkening timescales can be > 1 Myr at latitudes $> 75^\circ$. Thus, the fate of exposed ice depends as much on its purity as its location on Ceres.

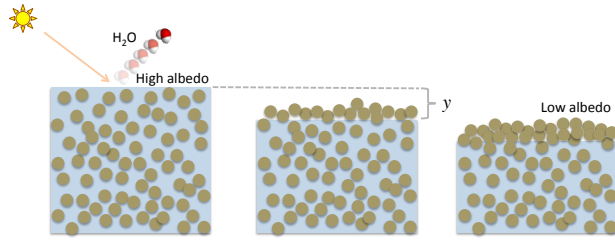
Even pure ice has a finite lifetime against sublimation (t_{sub}), which depends mostly on its latitude and porosity. The porosity affects the thermal inertia and albedo of pure ice, which can strongly reduce its sublimation rate by conducting and rejecting incident solar energy, respectively. We present a summary of our surface ice lifetime results the Table. In addition, we estimated the extent of subsurface ice and surface ice in the permanently shadowed regions (PSRs). Besides water, many other interesting volatile species may be trapped inside the PSRs [3], which could indicate the history of volatile delivery to Ceres, in addition to its own endogenic production.

¹ NASA – Jet Propulsion Laboratory, California Institute of Technology, USA

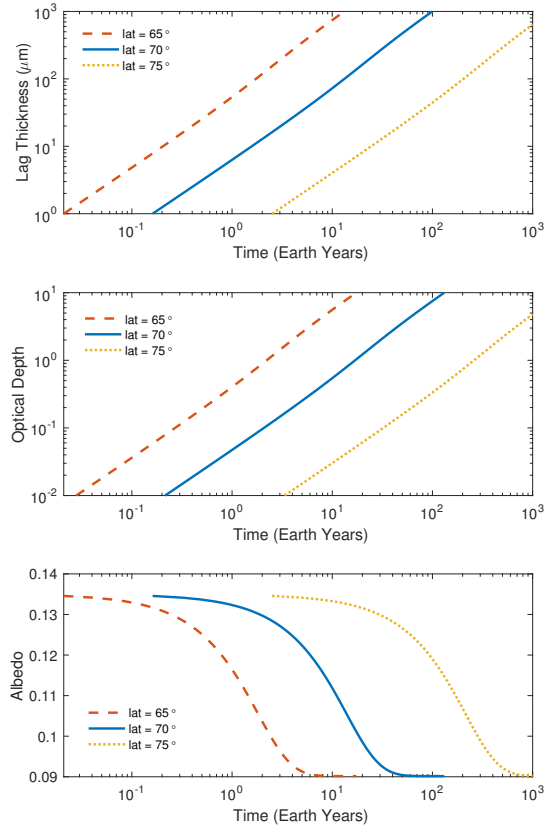
² Lunar and Planetary Laboratory, University of Arizona, USA

Part of this work was performed at the Jet Propulsion Laboratory, California Institute of Technology, under contract with the National Aeronautics and Space Administration.

We will compare our results to recent observations indicating the presence of exposed and buried ice on Ceres [6,7], and discuss the implications for its endogenic and exogenic volatile budget.



ABOVE: Schematic of the ice sublimation and dust lag model. Sunlight drives sublimation of the ice component of an ice-dust mixture, resulting in a lag deposit with thickness y and optical depth τ . Eventually, the ice is obscured when $\tau \gg 1$.



RIGHT: Example model results for 50% non-ice (dust) fraction, at three latitudes: 65° , 70° , 75° . The three panels (top-to-bottom) show dust lag thickness, optical depth, and resulting albedo of the ice-dust mixture, as a function of time.

Table: Summary of ice lifetimes undergoing sublimation and darkening. Icy crater ejecta were modeled assuming an initial radial thickness distribution $\sim 1/r^3$.

	Equator	45° Latitude	70° Latitude	PSR
Sublimation of 1 meter exposed ice	< 1 yr – 1,000 yr	1 yr – 10,000 yr	10 yr – 10 Myr	>4.5 Gyr
Sublimation of icy ejecta (1-km crater)	10 yr	100 yr	10 Myr	>4.5 Gyr
Darkening due to sublimation	~ 1 hr – 1 month	~ 1 day – 1 yr	1 – 10,000 yr	>4.5 Gyr

References:

- [1] Fanale, F. P., & Salvail, J. R. (1989), *Icarus*, 82(1), 97-110.
- [2] Titus, T. N. (2015), *GRL*, 42(7), 2130-2136.
- [3] Hayne, P. O., & Aharonson, O. (2015), *J. Geophys. Res.*, 120(9), 1567-1584.
- [4] Schorghofer, N. (2008), *Ap. J.*, 682(1), 697.
- [5] Schorghofer, N., Mazarico, E., et al. (2016), *GRL*, 43(13), 6783-6789.
- [6] Combe, J. P., McCord, T. B., et al. (2016), *Science*, 353(6303), 3010.
- [7] Prettyman, T. H., Yamashita, N., et al. (2016), *EGU General Assembly Conf. Abstr.*, 18, 10429.

Low thermal inertia of icy planetary surfaces

C. Ferrari and A. Lucas

Laboratoire IPGP/AIM - Université Paris-Diderot – 5 rue Thomas Mann 75205 Paris cedex 13

Thermal inertias of atmosphereless icy planetary bodies, such as moons of giant planets, Centaurs or TNOs happen to be very low (Figure 1). It appears to decrease with heliocentric distance and can be as low as a few in the outer solar system. To understand why it is low, we have combined available models of conductivity by contact or by radiation to understand what heat transfer process is predominant in these icy regoliths. These models relate the effective thermal conductivity and the thermal inertia of the regolith to its properties such as porosity, grain size or ice form. We were able to predict how the thermal inertia may vary with heliocentric distance depending on these properties. The magnitude of the thermal inertia of a porous icy regolith is mainly governed by the crystalline or amorphous forms of water ice, and the quality of contacts between grains, either tight or loose. Beyond the orbit of Jupiter, thermal inertias as low as a few tens $J/m^2/K/s^{1/2}$ are difficult to reproduce with plausible porosity and grains sizes made of crystalline ice unless contacts are loose (Figure 1, left). This is, on the contrary, straightforward for regoliths of sub-cm-sized grains made of amorphous water ice (Figure 1, right). The characteristic decrease of thermal inertia with heliocentric distance of icy atmosphereless surfaces and the very low thermal inertia of relevant trans-Neptunian objects are easily explained if amorphous ice is present at cm depths below a thin layer of crystalline ice, which is often detected in near-infrared spectroscopy on these bodies. This study points out the importance of including the temperature dependence of thermophysical properties of water ice forms and the radiative conduction in thermal models of these bodies, even if their temperature is low.

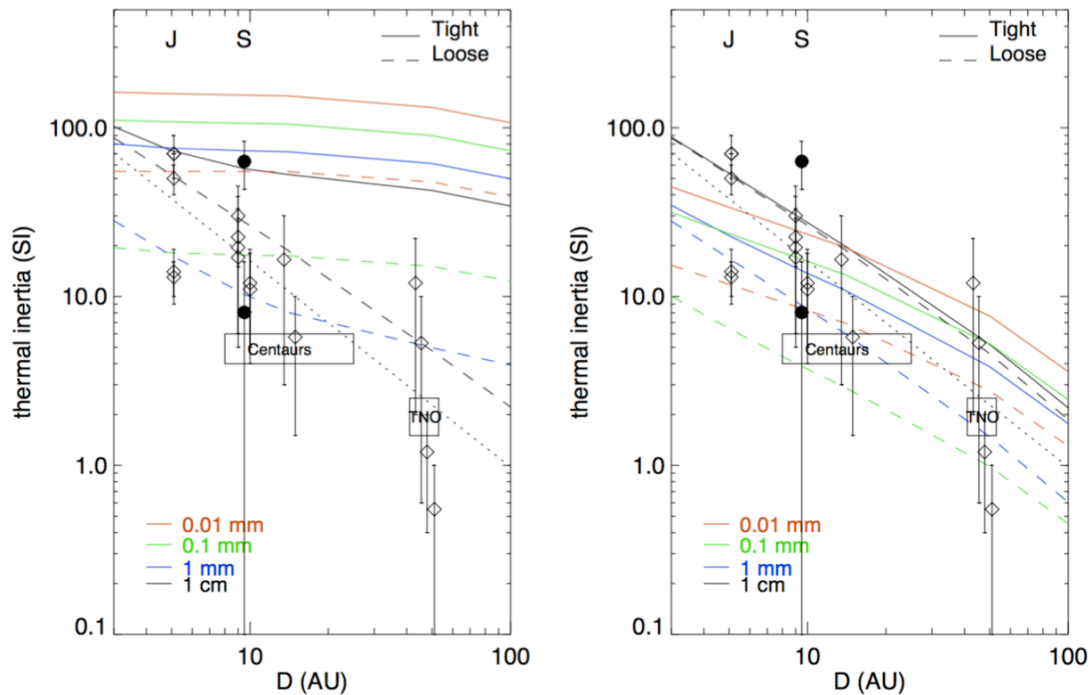


Figure 1 –Heliocentric dependence of thermal inertias of icy bodies as published by different authors (see Ferrari and Lucas, A&A 588, A133, 2016) for further references. Grain sizes range between 10 μ m and 1 cm, the contacts between grains are either tight or loose. Porosity is here of 50%. (Left) Crystalline water ice (bottom) amorphous ice

IDENTIFYING THE ACCRETION OF ICE AND HYDRATED MINERALS IN PRISTINE CARBONACEOUS CHONDRITES FROM AQUEOUS ALTERATION FEATURES FOUND IN THEIR MATRICES AT MICRO AND NANOSCALE

J.M. Trigo-Rodríguez¹, J. Alonso-Azcárate², and M. M. Abad³.
¹Institute of Space Sciences (IEEC-CSIC), Meteorites, Minor Bodies, and Planetary Sciences Group, Campus UAB Bellaterra, c/Can Magrans s/n, 08193 Cerdanyola del Vallès (Barcelona), Spain (trigo@ice.csic.es). ²Universidad de Castilla-La Mancha (UCLM), Campus Fábrica de Armas, 45071 Toledo, Spain. ³Centro de Instrumentación Científica (CIC), Universidad de Granada, 18071 Granada, Spain.

Introduction: Several groups of carbonaceous chondrites (hereafter CCs) come from hydrated parent bodies which experienced significant post-accretionary aqueous processing. The evidence indicates that they come from undifferentiated asteroids formed by chondrules, Ca- and Al-rich inclusions (CAIs), sulphides, and metal grains embedded in a nanometric matrix that preserved chemical clues on the cold forming environment. Our studies of some CCs, like e.g. Murchison CM2 chondrite, suggest the incorporation of ice-rich mantles surrounding some components of carbonaceous chondrites. Two main hypothesis have been invoked to explain the presence of hydrated minerals in CCs: one proposes parent body alteration [1-3], and other ‘preaccretionary’ hypothesis proposes the incorporation of hydrated phases from the protoplanetary disk itself [4-6]. Wet accretion can be invoked in some Murchison chondrules that exhibit mantles, and distinctive aqueous alteration features (Fig. 1). Secondary aqueous alteration minerals were formed in CCs at early times, in time scales of ~10 million of years (Ma) after CAI formation, consistent with water release due by radioactive decay heating [7]

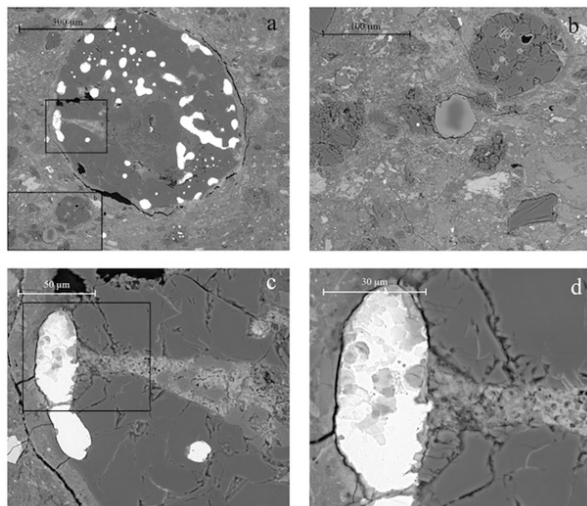


Figure 1. BSE image of a forsteritic chondrule (a) exhibiting a metal grain corroded by the action of water (c,d), and a surrounding matrix with relic grains (d). Localized dirty ice mantles, promoting parent body static alteration could explain these features.

The highly porous structure of CCs was inherited from the diverse materials present in the protoplanetary disk environment, and that porosity probably allowed them to sequester volatile compounds from the gas phase [8]. As they presumably accreted by low relative velocity encounters that led to preserve chemical and isotopic signatures of their components, cemented by a fine-grained comminuted matrix. Anhydrous carbonaceous chondrite matrices are usually represented by highly chemically unequilibrated samples that contain distinguishable stellar grains. Other chondrites have experienced hydration and chemical homogenization that reveal parent body processes. We focus here in CM chondrites because these meteorites have experienced variable hydration levels [9-10]. It is important to study the textural effects of aqueous alteration in the main minerals to decipher which steps and environments promote bulk chemistry changes, and create the distinctive alteration products. It is thought that aqueous alteration has particularly played a key role in modifying primordial bulk chemistry, and homogenizing the isotopic content of fine-grained matrix materials [7, 11, 12]. Fortunately, the mineralogy produced by parent-body and terrestrial aqueous alteration processes is distinctive [5, 11].

Experimental procedure: First of all, the meteorite sections were thinned in a ring as usually made for TEM studies using a Fischione 1050 ion mill at CIC (Granada University). The sample was bombarded with energetic ions or neutral atoms (Ar), removing sample material until the film was sufficiently thin to study by TEM. The result is a thinned ring that is cleaned to remove away the remaining amorphous materials and then analyzed by UHRTEM (ultra high resolution transmission electron microscopy). The study was performed using a FEI Titan G2 60-300 microscope available at CIC with a high brightness electron gun (X-FEG) operated at 300 kV and equipped with a Cs image corrector (CEOS) and for analytical electron microscopy (AEM) a SUPER-X silicon-drift windowless EDX detector. The AEM spectra were collected in STEM (Scanning Transmission Electron Microscopy) mode using a HAADF (High Angle Annular Dark Field) detector. Digital X-Ray maps were also collected on selected

areas of the samples. For quantitative micro-analyses, EDX data were corrected by the thin-film method [12-13]. The K-factors were determined using mineral standards. These samples were prepared as a Canada balsam-mounted thin sections, were thinned using a Fischione 1050 model ion mill, and carbon coated for TEM observation with the Titan microscope. Atomic concentration ratios were converted into formulae according to stoichiometry (number of O atoms in theoretical formulae).

Results and discussion: The complex matrix of CCs is composed by heterogeneous materials when seen at nanoscale. As an example, Fig. 2 shows a 1 μm window of the Murchison matrix where the center includes a phase with the characteristic layering of phyllosilicates oriented perpendicularly to the line of sight. The figure includes small numbered boxes where several EDX spectra were taken. Serpentine in its variety of lizardite is representative of boxes #1 and 4, but in #2 and #3 we found a mixture of serpentine with cronstedtite. Other minerals tentatively identified from their EDX spectra are: #5 and #6 pentlandite, #8 carbonate, #11 pyrrhotite, and #12 pyroxene. In general the presence of these minerals exemplify an extraordinary diversity in CM2 chondrite Murchison. We think this complexity at nanoscale might be indicative of the formation conditions of this meteorite, and the little thermal processing occurred in its parent asteroid.

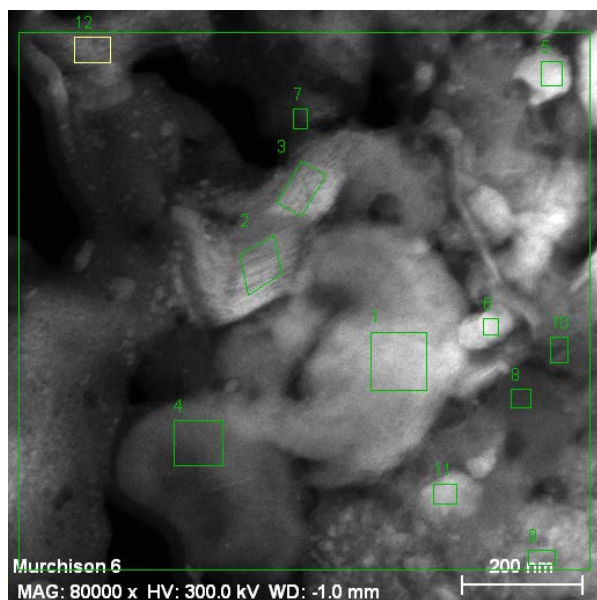


Figure 2. HAADF image showing a serpentine-cronstedtite intergrowth phase surrounded by other minerals discussed in the text.

Conclusions: Murchison matrix is exceptionally complex at the nanoscale. The existence of heavily

aqueously altered minerals in close contact with anhydrous ones is remarkable. It supports the hypothesis of a wet accretion for some CCs components. By studying hydrated minerals, and precipitates formed as consequence of aqueous-alteration we think that the CCs provide key information regarding the availability of dirty ice in the protoplanetary disk at the distances where the parent bodies of these meteorites formed [14-18]. We have found that parent body alteration of phyllosilicates in presence of water and formamide could have promoted organic complexity as consequence of catalytic processes produced by aqueous alteration [19]. Future analytical work will enable us to be more precise about the conditions in which such extensive alteration took place, and to establish constraints in the chemical composition of primordial ices.

Acknowledgements: Financial support from the Spanish MEC (research projects AYA2011-26522 and AYA2015-67175-P). Mike Zolensky kindly provided the Murchison samples here discussed.

References: [1] Bunch T.E. and Chang S. (1980) *Geochim. Cosmochim. Acta* 44, 1543. [2] Zolensky M. and McSween H.Y. (1988) In *Meteorites and the Early Solar System*, Univ. Arizona press, Tucson, p. 114. [3] Browning et al. (1996) *Geochim. Cosmochim. Acta* 60, 2621. [4] Metzler K. et al. (1992) *Geochim. Cosmochim. Acta* 56, 2873. [5] Bischoff A. (1998) *Meteorit. Planet. Sci.* 33, 1113. [6] Hanowski N.P. and Brearley A.J. (2000) *Meteorit. Planet. Sci.* 35, 1291. [7] Fujiya W. et al. (2013) *Earth Planet. Sci. Lett.* 362, 130. [8] Trigo-Rodríguez J.M. and Blum J. (2009) *Planet. Space Sci.* 57, 243. [9] Bland P. et al. (2006) in *Meteorites and the Early Solar System II*, D.S. Lauretta & H.Y. McSween Jr. (eds.), Univ. Arizona Press, Tucson, 853. [10] Zolensky M.E. et al. (1993) *Geochim. Cosmochim. Acta* 57, 3123. [11] Brearley A. and Jones R.H. (1998) In *Planetary Materials*, ed. Papike J.J., Washington, D.C.: Min. Soc. of America, 1-398. [12] Cliff G. and Lorimer G.W. (1975) *J. Microscopy* 103, 207. [13] Lorimer G.W. and Cliff G. (1976) In *Electron Microscopy in Mineralogy*, Springer-Verlag, Berlin, 506. [14] Lee M.R. (1993) *Meteoritics* 28, 53. [15] Fujimura A. et al. (1983) *Earth Planet. Sci. Lett.* 66, 25. [16] Trigo-Rodríguez J.M. et al. (2013) *MNRAS*, 437, 227-240. [17] Brearley A.J. (2006) in *Meteorites and the Early Solar System II*, D.S. Lauretta & H.Y. McSween Jr. (eds.), Univ. Arizona Press, Tucson, 587-624. [18] Trigo-Rodríguez, J.M. (2015) In: *Planetary Mineralogy*, Lee, M.R., Leroux, H. (eds.), EMU Notes in Mineralogy 15, pp.67-87. [19] Rotelli L., et al. (2017) *Nature - Scientific Reports*, in press.

Glycine formation from low energy electron irradiation of CO₂:CH₄:NH₃ ice analogs

Sasan Esmaili ¹, Andrew D. Bass, Pierre Cloutier, Leon Sanche, and Michael A. Huels

Département de médecine nucléaire et radiobiologie,
Faculté de médecine et des sciences de la santé,
Université de Sherbrooke,
Sherbrooke, QC, Canada

Low energy secondary electrons are likely produced in great numbers within astrophysical or planetary ices, by the various ionizing radiation fields encountered in space environments. They may thus play a role in the radiation processing of such ices ¹. One approach to simulate their astrochemical effect is to irradiate nanometer thick molecular solids of simple molecular constituents in ultra-high vacuum (UHV) with energy selected electron beams, and to monitor changes in film chemistry with surface analytical techniques ². Of particular interest is the formation of HCN, which is a signature of dense gases in interstellar clouds, and is ubiquitous in the interstellar medium (ISM) and Glycine which is the simplest amino acid and has been found in ISM, comets and meteorites³. Moreover, the chemistry of HCN radiolysis products such as CN⁻ may be essential to understand of the formation of amino acids ⁴ and purine DNA bases. Here we present new results on the UHV irradiation of cryogenic (22 K) multilayer films of CO₂, CH₄ and NH₃ with 70 eV electrons, leading to CN, and other new bond formations. Mass resolved electron stimulated desorption yields of anions are recorded as a function of electron fluence. Most saliently, increasing signals of new negative ion products desorbing during prolonged irradiation of CO₂/NH₃/CH₄ films included C₂⁻, C₂H⁻, as well as CN⁻ and HCN⁻. We use temperature programmed desorption (TPD) to identify the production of glycine in LEE irradiated films containing CO₂/NH₃/CH₄. (Work funded by NSERC).

REFERENCES

1. Boyera, M. C., Rivasb, N., Audrey A, T., Clarissa A, V. & Arumainayagamb, C. R. The role of low-energy (≤ 20 eV) electrons in astrochemistry. **652**, 26–32 (2016).
2. Arumainayagam, C. R., Lee, H. L., Nelson, R. B., Haines, D. R. & Gunawardane, R. P. Low-energy electron-induced reactions in condensed matter. *Surf. Sci. Rep.* **65**, 1–44 (2010).
3. Elsila, J. E. *et al.* The origin of amino acids in lunar regolith samples. *Geochim. Cosmochim. Acta* **172**, 357–369 (2016).
4. Vera, M. H., Kalugina, Y., Denis-Alpizar, O., Stoecklin, T. & Lique, F. Rotational excitation of HCN by para- and ortho-H₂. *J. Chem. Phys.* **140**, 224302 (2014).

Titan's mid-latitude regions surface composition with Cassini/VIMS

A. Solomonidou^{1,2,*}, A. Coustenis², R.M.C. Lopes¹, M. Malaska¹, S. Rodriguez³, P. Drossart², B. Schmitt⁴, M. Hirtzig⁵, R.H. Brown⁶

¹Jet Propulsion Laboratory, California Institute of Technology, California, USA; ²LESIA - Observatoire de Paris, CNRS, UPMC Univ. Paris 06, Univ. Paris-Diderot, 92190 Meudon, France; ³Laboratoire AIM, Université Paris Diderot, Paris 7/CNRS/CEA-Saclay, DSM/IRFU/Sap, Gif sur Yvette, France; ⁴Institut de Planétologie et d'Astrophysique de Grenoble, Grenoble Cedex, France; ⁵Fondation "La main à la pâte", Montrouge, France; ⁶Lunar and Planetary Laboratory, University of Arizona, Tucson, United State.

We investigate the surface of Titan by means of two Cassini instruments used in synergy. We apply a radiative transfer code to VIMS hyperspectral data to correct the strong atmospheric contribution and extract information on the surface composition [1;2;3]. We examine here the mid-latitude zones extending from 60°N to 60°S, which include key geological features identified in [4;5] and [6]: mountains, plains, labyrinths, dune fields, and possible cryovolcanic and/or evaporitic deposits. We find that many of the different units show compositional variations while units of significant geomorphological differences seem to consist of very similar material mixtures. The Huygens landing site and the candidate evaporitic regions are compositionally similar to the variable plains. We also find that temporal variations of surface albedo exist for two of the candidate cryovolcanic regions Tui Regio and Sotra Patera, possibly suggesting the presence of surface activity, while a number of other regions such as Hotei Regio and the undifferentiated plains remain unchanged [3]. The surface albedo variations, together with the presence of volcanic-like morphological features, suggest that the active regions are probably related to the deep interior, possibly via cryovolcanic processes (with important implications for the satellite's astrobiological potential) as also indicated by recent interior structure models of Titan and corresponding calculations of the spatial pattern of maximum tidal stresses [7]. Previous studies [3;5] showed that a variety of surface processes could be linked to the formation of the different geomorphological units (aeolian, fluvial, sedimentary, lacustrine) as well as of the deposition of atmospheric products through the process of photolysis and sedimentation of organics. We present here preliminary results on possible surface composition based on radiative transfer simulations of the surface albedos with various sets of ices and the inclusion of tholin and other dark material. The surface albedo differences and similarities among the various geomorphological terrains constrain the implications for the geological processes that govern Titan's surface.

References: [1] Hirtzig, M. et al: Icarus 226, 470-486, 2013; [2] Solomonidou, A. et al: JGR 119, 1729-1747, 2014; [3] Solomonidou, A. et al: Icarus 270, 85-99, 2016; [4] Lopes, R. et al: Icarus 205, 540-558, 2010; [5] Lopes, R. et al: Icarus 162-182, 2016; [6] Malaska, M. et al: Icarus 270, 130-161, 2016; [7] Sohl, F. et al: JGR, 119, 1013-1036, 2014.

Micrometer-sized water ice particles for planetary-science experiments

B. Gundlach and J. Blum

The coagulation of micrometer-sized water ice particles played an important role in planet formation as can be seen by the high water ice abundance in planetary bodies. However, the physical properties of small micrometric water ice particles are not well studied.

In our laboratory, we can produce micrometer-sized water ice particles to study their physical properties under various conditions, like the collisional behaviour, or the sinter rate at different temperatures. Furthermore, the capability to create ice aggregates composed of the micrometric particles provides the possibility to study larger water-ice samples under different astrophysical aspects.

With this presentation, we would like to give an overview of the capabilities of our laboratory work.

Reflectance and other related physical properties of icy planetary analogues

A. Pommerol, N. Thomas, B. Jost, O. Poch, A. Galli, Z. Yoldi, Y. Brouet
Physikalisches Institut, University of Bern, Switzerland and NCCR PlanetS.

Understanding the reflectivity of surfaces is key for interpreting quantitatively the data collected by passive and active remote-sensing instruments in various regions of the electromagnetic spectrum. Combining different approaches such as physical models and numerical simulations supported by laboratory measurements of carefully characterized materials has already led to significant progress in this area, in particular to decipher the respective effects of chemical composition and physical structure of the material. Icy materials and surfaces are challenging cases however due to the complexity of the possible associations between volatile and refractory material and the extreme contrast of properties between these materials. In addition, experimental research with ice necessitates specific equipment and facilities to work at low temperature and particular care to handle and characterize the icy material without modifying its properties.

In 2010, we have initiated at the University of Bern a long-term project to overcome these difficulties and produce accurate reflectance data for well characterized icy samples. The goal of this project is to help with the interpretation of past, current and future icy objects. Until now, our efforts have been focused in two directions:

- The development of original instrumentation to measure the reflectance of cm-size surfaces in the spectral range of reflected solar light. This includes measurement of the visible bidirectional reflectance over a wide range of incidence, emission and phase angle, VIS-NIR hyperspectral imaging of sample in low-temperature and pressure environments and polarization-sensitive visible reflectance measurements. [1,2]
- The development of machines and protocols to produce icy samples in a reproducible way. The setups developed are all portable. Therefore, the samples can be used for measurements not only in our own laboratory but also brought to other laboratories for complementary measurements and characterizations.

We will present at the conference an overview of results from the various measurement campaigns performed with these samples in the past six years. This includes:

- VIS-NIR spectra and low phase angle bidirectional reflectance of fine-grained ice with implications for various icy surfaces [3,4].
- The search for a plausible laboratory analogue for the surface of 67P nucleus.
- Evolution of ice/dust mixtures upon sublimation of ice in vacuum with implications for comets and larger icy objects [5,6].
- Spectro-photometric characterizations of analogues of the surface of the polar regions of Mars or permanently shadowed craters on Mercury or the Moon [7].
- Irradiation of porous ice samples by energetic ions and electrons with implications for future analyses of the surfaces of icy satellites by orbital mass spectrometers [8].
- Permittivity measurements of porous ice and ice/dust mixtures in the frequency range 50MHz-2GHz with implications for remote and in-situ radio sounding of comets nuclei [9].
- Polarization properties of reflected light from pure and dusty fine-grained ice samples as a tool to better probe the texture and composition of surfaces.

We will concentrate on describing the overall aims and general methodology of our work, discuss the main trends that appear in these results and the future necessary steps in the field. This general presentation will be complemented by focused presentations on some of these topics during the conference.

References

- [1] Pommerol, A., et al. (2011) Photometry and bulk physical properties of Solar System surfaces icy analogs: the Planetary Ice Laboratory at University of Bern, *Planet. Space Sci.*, 59, p. 1601-1612, <http://dx.doi.org/10.1016/j.pss.2011.07.009>
- [2] Pommerol, A., et al. (2015) The SCITEAS experiment: optical characterizations of sublimating icy planetary analogues, *PSS*, 109-110, p. 106-122, <http://dx.doi.org/10.1016/j.pss.2015.02.004>
- [3] Jost, B., et al. (2013) Micrometer-sized ice particles for planetary-science experiments - II. Bidirectional reflectance, *Icarus*, 225, p. 352-366, <http://dx.doi.org/10.1016/j.icarus.2013.04.007>
- [4] Jost, B., *et al.*, (2016a) Experimental characterization of the opposition surge in fine-grained water-ice and high albedo analogs, *Icarus*, 264, 109-131, <http://dx.doi.org/10.1016/j.icarus.2015.09.020>
- [5] Poch, O., *et al.* (2016b) Sublimation of ice-tholins mixtures: a morphological and spectrophotometric study, *Icarus*, 266, p. 288-305, <http://dx.doi.org/10.1016/j.icarus.2015.11.006>
- [6] Poch, O., *et al.*, (2016b), Sublimation of water ice mixed with silicates and tholins: evolution of surface texture and reflectance spectra, with implications for comets, *Icarus*, 267, 154-173, <http://dx.doi.org/10.1016/j.icarus.2015.12.017>
- [7] Yoldi, Z., *et al.*, (2015), VIS-NIR reflectance of water ice/regolith analogue mixtures and implications for the detectability of ice mixed within planetary regoliths, *Geophysical Research Letters* 42, 6205–6212, <http://dx.doi.org/10.1002/2015GL064780>
- [8] Galli, A., *et al.*, (2016) Surface charging of thick porous water ice layers relevant for ion sputtering experiments, *Planetary and Space Science*, 126, 63-71, <http://dx.doi.org/10.1016/j.pss.2016.03.016>
- [9] Brouet, Y., *et al.*, (2016), A porosity gradient in 67P/C-G nucleus suggested from CONSERT and SESAME-PP results: an interpretation based on new laboratory permittivity measurements of porous icy analogues, *Monthly Notices of the Royal Astronomical Society*, in press, <http://dx.doi.org/10.1093/mnras/stw2151>

Laboratory simulations and characterization of H₂O frost processes on Mars

Z. Yoldi (1), A. Pommerol (1), O. Poch (1), B. Jost (1) and N. Thomas (1)

(1) Physikalisches Institut and NCCR PlanetS, University of Bern, Switzerland. (zurine.yoldi@space.unibe.ch)

In addition to their widely-studied seasonal cycle, CO₂ and H₂O also experience diurnal cycles on Mars. The diurnal cycle of H₂O in particular remains poorly understood. Studies have shown a significant drop of water vapor content in the atmosphere during some nights [1, 2]. Water frost on the Martian surface has already been imaged [1] or deduced from the thermodynamical properties of the atmosphere-ground system [2, 3]. When the temperature of the ground drops below the frost point of the surrounding atmosphere, the water contained in it is likely to condensate over the surface [2]. As negative temperature gradients within the subsurface can occur, water vapour can also penetrate and condense at some depth in the porous regolith. The degree at which frost deposition is responsible for the water vapor content drop is not clear yet, since other phenomena can contribute as well such as mineral hydration. Water frost could also help explaining other intriguing observations such as the nighttime increase in regolith dielectric permittivity [1] or the variability of hydration signatures observed by OMEGA [4].

ESA's Exomars Trace Gas Orbiter (TGO) has been successfully inserted into Mars orbit and regular scientific observations will begin in late 2017 following a long aerobraking phase. The orbit of TGO will combine two properties: a low (400 km) and circular orbit, which is not Sun-synchronous. CaSSIS, the Colour and Stereo Surface Imaging System onboard TGO [5] will complement the other imagers currently observing Mars. The combination of the non-Sun-synchronous orbit of the probe and the expected high signal-to-noise ratio of the instrument will allow us to characterise given locations at different local times, thus allowing the identification of possible frost events. In order to better interpret these future data, we study the spectro-photometric signatures of simulated water frost deposits in the laboratory.

We will report on the first results from a measurement campaign recently initiated in the LOSSY Ice Laboratory (Laboratory for Outflow Studies of Sublimating materials) at the University of Bern. We simulate water frost deposition onto different analogs of the Martian regolith (JSC Mars-1 regolith simulant and darker basalts), and measure hyperspectral cubes with our SCITEAS simulation chamber [6]. Then we simulate the colours of our samples as would be seen by CaSSIS, characterising their different signatures depending on the nature of the samples and the amount of frost deposited. Several samples are being tested; different size of grains, dry samples, regolith – ice intimate mixtures, regolith covering ice layers, etc. Our aim is to study whether visible spectro-photometric signatures can help us identifying water frost from orbit or for example, distinguishing between water adsorption by the regolith and frost deposition on it. The first results will be presented at the workshop, as well as a full characterization of the icy samples created in the Laboratory.

[1] Smith, P. H. et al., 2009. H₂O at the Phoenix Landing Site. *Science* Vol 325.

[2] Martínez, G. M et al., 2016. Likely frost events at Gale crater: Analysis from MSL/REMS measurements. *Icarus* 280. 93-102 <http://dx.doi.org/10.1016/j.icarus.2015.12.004>

[3] Higuchi, K., 2001. Formation of frost layer of water ice on Mars. *Icarus* 184, 181-182. doi:10.1006/icar.2001.6697

[4] Audouard, J. et al., 2014. Water in the Martian regolith from OMEGA/Mars Express. *J. Geophys. Res.: Planets* 119 (8), 1969–1989.

[5] Thomas, N. et al., 2016. The colour and stereo surface imaging system for ESA's trace gas orbiter. *LPSC* 47.

[6] Pommerol, A. et al., 2015. The SCITEAS experiment: Optical characterizations of sublimating icy planetary analogues. *Planetary and Space Science* (2015), <http://dx.doi.org/10.1016/j.pss.2015.02.004i>

PRELIMINARY CARBON MONOXIDE-NITROGEN MIXTURES IN SIMULATED PLUTO CONDITIONS. C.J. Ahrens¹, V.F. Chevrier¹, M. Souza², Z.M. McMahon¹, ¹Arkansas Center for Space and Planetary Science, University of Arkansas, Fayetteville, AR 72701, ²Universidade Federal Da Bahia, Salvador, Brazil. (ca006@email.uark.edu).

Introduction: Laboratory simulation and analysis of solar system ices will help our understanding as to the structures of the chemistry, mineralogy, and physical processes of outer solar system bodies. After the New Horizons' 2015 flyby, the Linear Etalon Imaging Spectral Array (LEISA) data has been ideal for observing complex icy surface geology at wavelengths between 1.25 μm – 2.5 μm [1, 2].

Pluto has a varied geologic surface dominated by volatile ice-driven mechanisms. This could be due to the variety of ice-gas mixtures and the phases of those ices. Pluto's surface temperatures range from 33 K – 55 K with seasonal difference and a surface pressure of roughly 10 microbar [3,4,5]. Pluto's main gas constituent includes an abundance of nitrogen and methane with small percentages of carbon monoxide (Figure 1) [6]. These two gases are comparable in crystal lattice constants, but concentrations of the two gases at low temperatures show variability in solid-liquid phases [7].

As we begin to investigate the surface processes, we are realizing that there is a lack in literature about the physical properties of carbon monoxide and nitrogen ice mixtures at low temperatures and pressures. Here we discuss some of our current efforts to expand on previous studies and further our investigations to understanding the geologic processes on Pluto's icy surface and other icy bodies in the outer solar system.

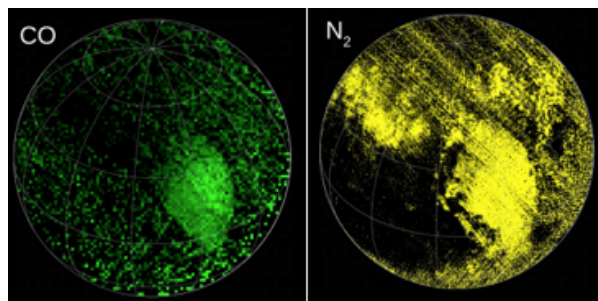


Figure 1: Concentration composition maps of carbon monoxide (CO) and Nitrogen (N₂) provided by the LEISA instrument onboard New Horizons [8].

Laboratory Simulation Setup: Our Pluto simulation chamber at the W.M. Keck Laboratory for Space Simulations at the University of Arkansas (Figure 2) is approximately 0.45 m. in diameter and

0.56 m. depth stainless steel vacuum chamber with a roughing pump, helium refrigeration system, pressure gauges, fiber optics, and several ports for observation and endoscopes for FTIR and eventually Raman spectroscopy investigations. There is also a camera for optical verification of ice growth [9]. Measurements are made by bringing the pressure down to the needed 10-microbar \pm 5-microbar through stages and cooling to the desired temperature of 44 K \pm 10 K [10].

A gas-mixing chamber is included in the design to pre-mix a percentage of carbon monoxide and nitrogen before injection into the cryo-chamber for spectral analysis for preliminary analysis. A gas chromatograph will be added for more precise concentration measurements.

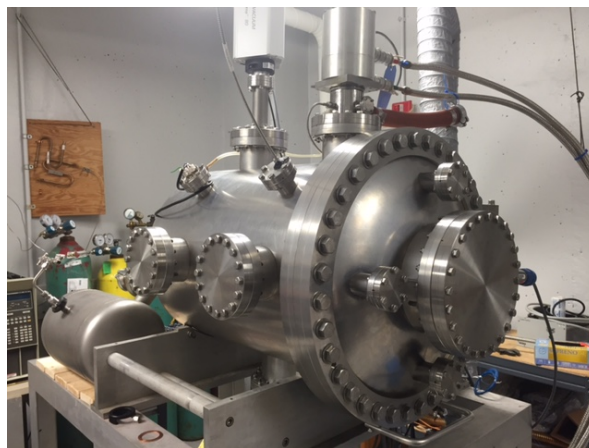


Figure 2: Pluto simulation chamber at the W.M. Keck Laboratory for Space Simulations at the University of Arkansas.

Preliminary Results: Preliminary experiments with mixing carbon monoxide and nitrogen under Pluto conditions were done with our chamber setup. Images were used as verification of potential phase changes by recording the moment of ice fracturing as we warmed the sample from 20 K to 60 K (Figure 3). We did this for a range of concentrations. We then plotted our results and compared to previous carbon monoxide-nitrogen ice studies (Figure 4). Our preliminary results show similar phase recordings to previous literature experiments between 30-80 K. However, our preliminary experiment with 10%CO-90% N₂ at 20 K has shown to be outside of the previous work region.

A study by Angwin and Wasserman (1965) showed percentage concentrations of carbon monoxide in nitrogen mixture and found that there was a lens-shaped phase region in the N₂-CO phase diagram in the 35 K to 60 K range and CO percentages from 0% to 100% known as the hcp+cubic. However, in the literature, data below 23 K were hypothetical (due to instrumentation error at lower temperatures) to assume the lens-like shape of the hcp and cubic phase region [7]. It was also noted in this study that the asymmetry found in the hcp+cubic lens-shaped region foretells the low-temperature lattice structures of nitrogen and carbon monoxide are not identical.

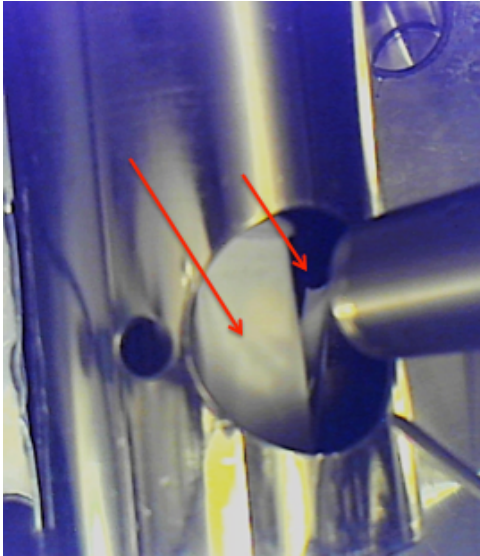


Figure 3: Optical verification of 70% CO- 30% N₂ ice mixture beginning to fracture at 50K as noted by the arrows.

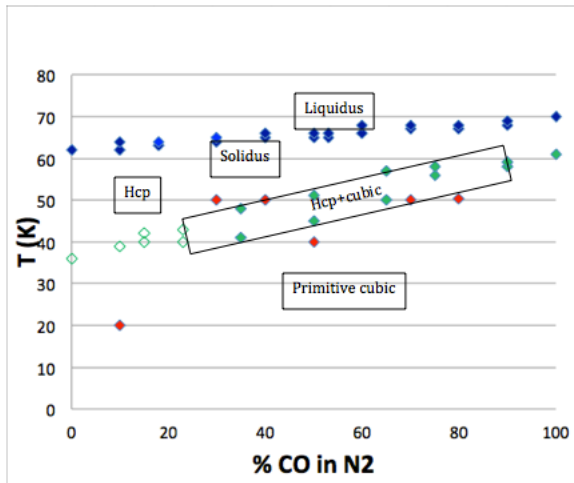


Figure 4: Preliminary collection of data of carbon monoxide and nitrogen mixtures at various percentages and temperatures. Blue indicates the liquidus (upper

points) and solidus (lower points) [7]. Solid green is the outline of the hcp+cubic lens-shaped phase region [7]. Open green points are the hypothetical points from Angwin [7]. Red points are our preliminary results for this study. The phase regions are labeled.

Discussion: Our instrumentation has provided some additional information as to this lens region at lower temperatures. During our preliminary studies with concentrations of carbon monoxide in nitrogen, we have found our data collected fits around the lens region between 30-80 K, as seen in Figure 3. Note that our preliminary studies fit the hcp+cubic lens phase region to some error.

Our preliminary studies will continue to study more mixtures of carbon monoxide and nitrogen at lower temperatures to get a better resolution of this hcp+cubic lens phase region. We hypothesize that the reason the lens region below 25 K and low percentages of carbon monoxide might be sloped more steep than the previous literature theorized is that the higher percentage of nitrogen may lower the combined freezing points of the two compounds due to nitrogen's lower melting point (63.15 K) than carbon monoxide (68.13 K) and may cause ice fracturing at lower temperatures.

Further results will measure more percentage mixtures of carbon monoxide and nitrogen in the 20 K-50 K range for better verification of phase regions with these gases. These measurements will provide a good quantitative description of ice behavior at these low temperatures and geologic evidence thereof.

References: [1] Stern, S., et al. (2015), AAS DPS meeting #47, Abstracts, #100.01. [2] Young, E., et al. (2015), AAS DPS meeting #47, Abstracts, #210.10. [3] Lorenzi, V., et al. (2015), AAS DPS meeting #47, Abstracts, #210.08. [4] Robuchon, G., Nimmo, F. (2011), *Icarus*, 216, 426-439. [5] Cruikshank, D., et al. (2015), *Icarus*, 246, 82-92. [6] Kim, Y., Kaiser, R. (2012), *The Astrophysical Journal*, 758:37, 1-6. [7] Angwin, M., Wasserman, J. (1966), *Journal Chem. Phys.* 44, 417-418. [8] Colorful Composition Maps of Pluto, NASA, JHU-APL, SWRI (2015). [9] McMahon, Z., Ahrens, C., Chevrier, V. (2016), *Lunar Planet. Sci. Conf. XLVII Abstracts*, #1728. [10] Ahrens, C., McMahon, Z., Chevrier, V., Elwood Madden, M. (2016), *Lunar Planet. Sci. Conf. XLVII Abstracts*, #1469.

Laboratory study of nitrile-containing ices of Titan's stratospheric clouds

Delphine Nna-Mvondo^{1,2}, Carrie M. Anderson¹, Jason L. McLain^{1,3}, Robert E. Samuelson^{1,3}

¹NASA GSFC, Greenbelt, MD, USA, ²Universities Space Research Association (USRA), Columbia, MD, USA, ³University of Maryland, College Park, MD, USA.

Titan's mid to lower stratosphere contains complex cloud systems of more than a dozen different organic ices involving both hydrocarbon and nitrile compounds. Most of these ice particles condense directly from their respective vapors, but for the Cassini Composite InfraRed Spectrometer CIRS-observed ice emission features, dicyanoacetylene (C_4N_2) and the 220 cm^{-1} ice feature (the "Haystack"), no associated vapor emission features can be found in Titan's atmosphere (Anderson *et al.*, 2016 a,b). Anderson *et al.* (2016 a,b) have postulated that these stratospheric ices form through solid-state chemistry, in a similar way to the formation of nitric acid trihydrate ($HNO_3 \cdot 3H_2O$) in the terrestrial polar stratosphere.

In the Spectroscopy for Planetary Ices Environments (SPICE) laboratory at NASA Goddard Space Flight Center (GSFC), our team studies the spectral, optical and chemical properties of laboratory ice analogs of the nitrogen-bearing compounds observed in Titan's stratosphere. Our aim is to identify, constrain, and explain the chemical composition of component ices of Titan's complex stratospheric clouds. We perform experiments using the SPECTroscopy of Titan-Related ice AnaLogs (SPECTRAL) high-vacuum chamber in order to measure the near to far-infrared spectroscopic properties of thin films of pure and mixed nitrile ices, and also of ice mixtures containing both nitriles and hydrocarbons. We also aim to study the effect of the adsorption of sub-saturated vapors on these ices and, finally, to investigate the chemistry induced by ultra-violet radiation of nitrile ices. Such measurements provide crucial data that are essential for the identification of Titan's observed stratospheric ice clouds by Cassini CIRS.

We will present the results obtained so far for three nitrile ices, propionitrile ($CH_3-CH_2-C\equiv N$), cyanogen ($N\equiv C-C\equiv N$) and hydrogen cyanide ($H-C\equiv N$), and their respective mixtures. Transmittance spectra of thin ice films have been acquired from 25 cm^{-1} to 11000 cm^{-1} at varying low temperatures from 14K to 150K, and we have computed their optical constants. Results from such experimental research will increase our understanding of not only Titan's stratosphere, but also of the nitrogen chemistry that may occur in the formation of additional planetary ice clouds. The SPECTRAL chamber provides, as well, a powerful laboratory tool to study more extensively the spectroscopic signatures and behavior of other pure and mixed ices of planetary icy bodies such as TNOs (Pluto), comets, and gas giants, spanning the far-IR to the near-IR spectral range.

Anderson *et al.* 2016a. *Geophys. Res. Lett.*, **43**, 3088-3094.

Anderson *et al.*, 2016b. *AAS/DPS Abstracts*, #48, #515.05.

Laboratory investigations of CO₂ ice in support of remote-sensing observations and physical modeling of planetary surfaces and atmospheres

G. Portyankina¹, J. Merrison², J. J. Iversen², Z. Yoldi³, K.-M. Aye¹, E. Carey⁴, M. Choukroun⁴, and C. J. Hansen⁵; ¹Laboratory for Atmospheric and Space Physics, CU Boulder, 3665 Discovery Drive, Boulder, CO 80303, USA (Ganna.Portyankina@lasp.colorado.edu) ²University of Aarhus, Denmark; ³University of Bern, Switzerland; ⁴Jet Propulsion Laboratory, Pasadena, USA; ⁵Planetary Science Institute, Tucson, AZ, USA

Remote sensing instruments provide wide range of observational data on present-day activity related to CO₂ ice throughout the Solar System. Martian activity related to CO₂ are the best observed to date [1, 2], however, CO₂ is also expected to play significant role in evolution of comets, icy satellites of giant planets and in the outer Solar system. For example, CO₂ ice in its slab form was detected on Pluto [3].

To advance in the analysis of remote-sensing data related to CO₂ ice, the following CO₂ ice properties are essential and still lacking either completely or partially: 1) optical properties of CO₂ ice in dependence of the grain size; 2) dependence of the grain size of forming ice on the pressure and temperature regime similar to martian conditions; 3) sublimation rates of mixes of dust and ice depending on mixture proportion; 4) mechanical properties, namely yield stress and Youngs modulus, of the slab CO₂ ice and/or granular ice after sintering.

Few experiments have been performed on CO₂ ice to measure its optical, mechanical, and thermal properties. Most experiments used millimeter-size samples. For example, visible and IR optical constants were measured on 1.6 mm thick samples [4]. Seiferlin et al. have explored the thermal properties of porous CO₂ [5]. Measurements were made at vacuum conditions and, as expected, gave very low values. Laboratory measurements of rheological properties of CO₂ ice showed that it had lowest viscosity among planetary icy analogs [6].

We will report on the ongoing laboratory investigations conducted at Environmental Wind Tunnel (WT) of Aarhus University [7] and JPL's Extraterrestrial Materials Simulations Laboratory (EMSiL) and the Ice Physics Laboratory.

We used WT to simulate CO₂ ice condensation in the conditions similar to those expected in the Martian polar areas. In this work we did the first steps towards providing experimental data for CO₂ ice properties. These results showed that CO₂ ice is created in translucent slab form.

At EMSiL we conducted preliminary work to ensure that it is feasible to produce samples of CO₂ ice of appropriate size and quality suitable for measurements of mechanical and thermal properties. We have also characterized the produced samples and conducted preliminary mechanical tests on them.

We have confirmed that it is feasible to create thick CO₂ ice samples with high translucency. This will serve as a starting point for future measurements of mechanical and thermal properties of CO₂ ice of different grain sizes, including but not limited to the slab form.

[1] Hansen, C.J., et al. *Icarus*, 205:283–295 (2010); [2] Hayne, P.O. et al., 6th Mars Polar Science Conference, #6012 (2016); [3] Protopapa, S. et al., DPS meeting #48, id.#306.06 (2016); [4] Hansen, G.B. *Adv. Space Res.*, 20:1613–1616 (1997); [5] Seiferlin, K. et al. *Planetary and Space Science*, 44:691–704 (1996); [6] Durham, W.B. et al., *Space Science Reviews*, 153:273–298 (2010); [7] Holstein-Rathlou, C. et al. *Journal of Atmospheric and Oceanic Technology*, 31:447–457 (2014).

Methane, Ethane, and Nitrogen Stability on Icy Bodies

J. Hanley¹, G. Thompson², L. Pearce^{2,3}, W. Grundy¹, H. Roe¹, G. Lindberg², S. Dustrud², D. Trilling², S. Tegler²

¹Lowell Observatory, Flagstaff, AZ, USA, ²Northern Arizona University, Flagstaff, AZ, USA, ³University of Texas, Austin, TX, USA. Email: jhanley@lowell.edu

Many outer solar system bodies are likely to have a combination of methane, ethane and nitrogen. In particular the lakes of Titan are known to consist of these species. Understanding the past and current stability of these lakes requires characterizing the interactions of methane and ethane, along with nitrogen, as both liquids and ices. Previous studies have shown that the freezing point of methane is depressed when mixed with nitrogen. Our cryogenic laboratory setup allows us to explore ices down to 30 K through imaging and transmission spectroscopy. Our recent work has shown that although methane and ethane have similar freezing points, when mixed they can remain liquid down to 72 K. Concurrently with the freezing point measurements we acquire transmission spectra of these mixtures to understand how the spectral features change with concentration and temperature. Any mixing of these two species together will depress the freezing point of the lake below Titan's surface temperature, preventing them from freezing. Also, when ethane ice forms, it freezes on the bottom of the liquid, while methane ice freezes at the top of the liquid, implying ethane ice is denser than the solution, while methane ice is less dense; this holds for all concentrations. We will present new results exploring the ternary system of methane, ethane and nitrogen. In particular we will explore the effect of nitrogen on the eutectic of the methane-ethane system. At high pressure we find that the ternary creates two separate liquid phases. Through spectroscopy we determined the bottom layer to be nitrogen rich, and the top layer to be ethane rich. Understanding the freezing points of combinations of these species has implications for not only the lakes on the surface of Titan, but also for the evaporation/condensation/cloud cycle in the atmosphere, as well as the stability of these species on other outer solar system bodies. These results will help interpretation of future observational data, and guide current theoretical models.

Karolina A. Haupa¹ and Yuan-Pern Lee^{1,2}

¹*Department of Applied Chemistry and Institute of Molecular Science, National Chiao Tung University, Hsinchu 30010, Taiwan*

²*Institute of Atomic and Molecular Sciences, Academia Sinica, Taipei 10617, Taiwan*

Title: *Spectral studies on the reaction $H + HONO$ in solid *para*-hydrogen: infrared identification of hydroxyl nitroxide $HON(O)H$.*

The N/O chemical network is essential in understanding the mechanism of molecules formation in dark interstellar clouds. We present the results of FTIR studies on the $HONO + H$ reaction in solid *para*-hydrogen (*p*-H₂) at 3.3 K. Hydrogen atoms were produced with two different methods. 1) Irradiation of HONO molecules in *p*-H₂ at 365 nm to produce OH radicals which react immediately with *p*-H₂ to produce mobile H-atoms. 2) Irradiation of Cl₂ molecules (co-deposited with HONO) in *p*-H₂ at 405 nm to produce Cl atoms which react immediately with *p*-H₂ to produce mobile H-atoms. In both experiments, we identified the primary product of hydrogenation of HONO, hydroxyl nitroxide - $HON(O)H$, at 3550, 1465, 1372, 896/899 and 631 cm⁻¹. The assignments of lines were derived on consideration of possible reactions and comparison of observed vibrational wavenumbers and IR intensities with values predicted with the B3LYP/aug-cc-pVTZ method. Agreements between observed and calculated D/H and N¹⁵/N¹⁴ isotopic ratios further support these assignments. The importance of these results in the N/O chemical network in dark interstellar clouds is discussed.

Evolution of Organics in Cometary Ice Analogs

Murthy S. Gudipati

Science Division, Jet Propulsion Laboratory, California Institute of Technology, Pasadena, CA
91109, USA.

gudipati@jpl.nasa.gov

Most recent science results from the Rosetta Mission to the comet Churyumov-Gerasimenko (67P/CG) changed our view of how cometary nucleus is made of and how it functions. While more in-situ data is acquired than ever done before, detecting a wide variety of complex organics [1-3] as well as supervolatiles [4] for the first time in a comet's outgassing, Rosetta Mission has opened as many new questions as the old ones answered.

A comet's nucleus is expected to be "frozen in time" since protoplanetary disk has evolved to a solar system with planets like ours, which could be about 4.6 Gy ago. However, it is completely unclear what happened before – during the time when interstellar ice grains in dense molecular clouds collapsed for the first time to form a protostar until the accretion disk became stable and cometsimals of microns to centimeter size became meters to kilometers size – the reservoirs of present-day comets in the Kuiper Belt and Oort Cloud. At the center of this question are the amorphous, crystalline, and clathrate ices that differ in their evolution based on what happened when in terms of temperature, pressure, and radiation.

Our laboratory work [5, 6] is focused on understanding how the organic matter evolves within the amorphous and crystalline ices under radiation conditions that prevail during the molecular cloud to evolved solar system transition. This presentation will review how organic matter could form, evolve and become present-day cometary surface/interior organic composition and the role of cometary impacts on Earth in potentially triggering the origin of life on Earth.

Acknowledgments: This work has been carried out at the Jet Propulsion Laboratory, California Institute of Technology under a contract with the National Aeronautics and Space Administration and partly funded by Rosetta US Science Team.

1. Altwegg, K., et al., *Prebiotic Chemicals—Amino Acid and Phosphorus—in the Coma of Comet 67p/Churyumov-Gerasimenko*. *Science Advances*, 2016. **2**(5).
2. Capaccioni, F., et al., *The Organic-Rich Surface of Comet 67p/Churyumov-Gerasimenko as Seen by Virtis/Rosetta*. *Science*, 2015. **347**(6220).
3. Quirico, E., et al., *Refractory and Semi-Volatile Organics at the Surface of Comet 67p/Churyumov-Gerasimenko: Insights from the Virtis/Rosetta Imaging Spectrometer*. *Icarus*, 2016. **272**: p. 32-47.
4. Rubin, M., et al., *Molecular Nitrogen in Comet 67p/Churyumov-Gerasimenko Indicates a Low Formation Temperature*. *Science*, 2015. **348**(6231): p. 232-235.
5. Lignell, A. and M.S. Gudipati, *Mixing of the Immiscible: Hydrocarbons in Water-Ice near the Ice Crystallization Temperature*. *J Phys Chem A*, 2015. **119**(11): p. 2607-13.
6. Henderson, B.L. and M.S. Gudipati, *Direct Detection of Complex Organic Products in Ultraviolet (Ly Alpha) and Electron-Irradiated Astrophysical and Cometary Ice Analogs Using Two-Step Laser Ablation and Ionization Mass Spectrometry*. *Astrophysical Journal*, 2015. **800**(1): p. 66.

Pathways for characterizing the physical properties of icy regoliths using optical properties

Vishaal Singh¹, Alyssa Rhoden¹, Hiroyuki Sato²

1. School of Earth and Space Exploration, Arizona State University, Tempe 85287 AZ, USA
2. Lunar Reconnaissance Orbiter Camera, Science Operations Center, Arizona State University, Tempe 85287 AZ, USA

Email addresses of the authors for correspondence:

vishaal.singh@asu.edu; alyssa.rhoden@asu.edu; hsato@ser.asu.edu

Abstract

Europa displays unusual photometric properties that are likely related to the detailed structure of its regolith, but our ability to interpret these observations is limited by the lack of “ground-truth” and a dearth of models linking optical and physical properties. Our current understanding of the bulk physical properties of ices on the surfaces of outer solar system satellites is primarily confined to [1] photometric model predictions for bidirectional reflection [a, b, c, d] and [2] experimental studies of terrestrial ices over a range of phase angles, including opposition geometry [e, f, g]. Laboratory studies for characterization of different icy planetary analog surfaces with independent parameter variation are rare [f, h, i, j, k], and research on subsequent application of photometry to determine physical properties of an icy satellite has yet to be established. Such studies are particularly relevant for future mission preparation to Galilean satellites and Saturn’s rings. The Europa Imaging System (EIS), with a suite of narrow and wide angle cameras will acquire images at resolution of 50m/pixel with near global coverage (>95%) at incidence 20-85°, emission 0-75° and phase angles 0-75° during 42 flybys [1]. This wealth of data can provide great insight into the physical, thermal, and chemical properties of Europa’s ice shell if we are prepared to interpret Europa’s observed optical properties. The detailed characteristics of Europa’s regolith are also critically relevant for development of a Europa lander, which is currently under study. Here, we present a pathway towards detailed simultaneous characterization of the bidirectional reflectance function and physical state for icy satellites, with a focus on Europa and interpreting the EIS measurements, using a combination of [1] photometric modeling, [2] field work and [3] lab experiments.

[1] A key goal of our approach is to refine several key parameter assumptions, within the models of Hapke [d] and radiative transfer [c], for application to icy satellites. We are particularly interested in the treatment

of CBOE in opposition surge [f], neglecting porosity, and the assumption of constant roughness. As a starting point, we are analyzing the abundance of datasets available on the Earth's moon to test model assumptions and correlate photometric properties with physical properties of the regolith. The Lunar Reconnaissance Orbiter Camera (LROC) Wide Angle Camera (WAC) multispectral observations have a comparable range of viewing geometry and illumination angles, lending to its analog photometric model application. 66,00 LROC WAC images were used for the initial analyses [m], to establish near-global Hapke parameter maps of the Moon, with subsequent research targeted at regional NAC photometry for correlation of parameter variations to physical properties. We select regions of immature highland crater ejecta for our analysis owing to the comparable higher albedo and slightly higher values of opposition surge which may be related to a variation in grain size distribution of the regolith.

[2] [Kassalainen et al., 2001, 2003](#); [Jost et al., 2013](#) [e, f, n] established terrestrial ice sheets as planetary regolith analogs (without considerations for radiation, atmosphere and temperature conditions) by replicating opposition surge in measured phase curves from field and lab experiments. We intend to extend the measurements of an analog surface's bidirectional reflectance over a large range of incidence, emission and phase angles to ground test our modified photometric model. Multiple field measurements in stable ice sheets of Antarctica (instrumentation listed in f) and concurrent lab experiments on acquired samples, with a radio-goniometer (PHIRE-2) operating in the VIS–NIR spectral range [o], will enable us to interpret the optical properties in terms of composition and physical state of the surface.

[3] A comprehensive study of Hapke parameters using various samples in laboratory experiments, with the application of near-infrared reflectance spectroscopy and imaging with cold-compliant instrumentation, will help identify well-characterized and stable analog materials. We intend to create a 3D analog surface for Europa, using pure ice as the initial material, prior to weathering and chemical analog studies undertaken by [p]. After establishing a correlation using backscattering peaks observed in phase curves, the reflectance data can be fit with our modified Hapke model to reproduce data and compare them to field measurements and Galileo imagery in our regions of interest.

Collectively, this research will: [1] enable development of refined photometry models for determining the global and regional-scale physical properties of outer solar system icy satellites; [2] inform approaches to overcoming the limitations in phase angle observations; [3] improve terrestrial analog sample selection by utilizing field and lab experimental studies, and [4] enable assessment of the temporal evolution of photometric properties of ice samples. [5] It will also offer a unique opportunity for predictive analysis by application to EIS datasets, and [6] can inform regolith particle studies and landing site assessment for a future lander, in conjugation with E-THEMIS. We will discuss results of our lunar analog study as well as

the details of the laboratory and field approaches we are developing for analysis of icy satellite regolith properties.

Keywords: Europa, Lunar photometry, Hapke model, terrestrial analogs, physical properties

References: [a] Minnaert, M. 1941 *Astrophysical Journal*, vol. 93, p. 403-410. [b] Shkuratov, Y. et al. 1999 *Icarus*, Volume 141, Issue 1, p. 132-155. [c] Buratti, B. et al. 1985 *Icarus*, vol. 61, Feb. 1985, p. 208-217. [d] Hapke, B. et al. 1981 *JGR*, vol. 86, Apr. 10, 1981, p. 3055-3060. [e] Kaasalainen, S. et al. 2001 *JQSRT*, v. 70, iss. 4-6, p. 529-543. [f] Kaasalainen, S. et al. 2003 *Astronomy and Astrophysics*, v.409, p.765-769; [g] Jost, B. et al. 2016 *Icarus*, Volume 264, p. 109-131. [h] Shepard, M. and Helfenstein, P. 2007 *JGR*, Volume 112, Issue E3. [i] Shkuratov, Y. et al. 2007 *JQSRT*, Volume 106, Issue 1-3, p. 487-508. [j] Pommerol, A. and Schmitt, B. 2008 *JGR*, Volume 113, Issue E10. [k] Pommerol, A. and Schmitt, B. 2008 *JGR*, Volume 113, Issue E12. [l] Turtle, Z. et al. 2016 *LPI Contribution No. 1903*, p.1626. [m] Sato, H. et al. 2014 *JGR- Planets*, 119, 1775–1805. [n] Jost, B. et al. 2013 *Icarus*, Volume 225, Issue 1, p. 352-366. [o] Pommerol, A. et al. 2011 *PSS*, Volume 59, Issue 13, p. 1601-1612. [p] Hand, K. et al. 2016 *The Astronomical Journal*, 145:110.

Introduction: Coagulation of solids is a crucial process during the first phase of planet formation [1]. Especially water ice particles are important as water is one of the most abundant materials in protoplanetary disks. While the inner parts are dominated by silicates, water ice dominates the growth processes beyond the snowline [2]. For silicates numerous theoretical and experimental studies exist, so that the collision physics for micrometer-sized particles appears well understood [1,3]. For ice particles a comprehensive data base is still missing. Common models as the JKR-theory [4] give a linear dependency between the critical pull-off force between two grains and the reduced radius $R_{red}^{-1} = r_1^{-1} + r_2^{-1}$, with r_1 and r_2 as the radii of the two.

In this context experiments are presented to measure contact forces between ice grains. Additionally, the forces between two spheres are simulated using molecular dynamics. In a first study, the critical torque for rolling and detachment of particles is measured and compared to simulations.

Experiments: The central part of the experiments is a rotating ice cylinder, which is cooled down to temperatures around 200 K. Water is then sprayed into the chamber, so the water droplets freeze out to small ice spheres. The ice cylinder is placed in a vacuum chamber. Fig. 1 shows part of the ice cylinder with ice spheres on top.

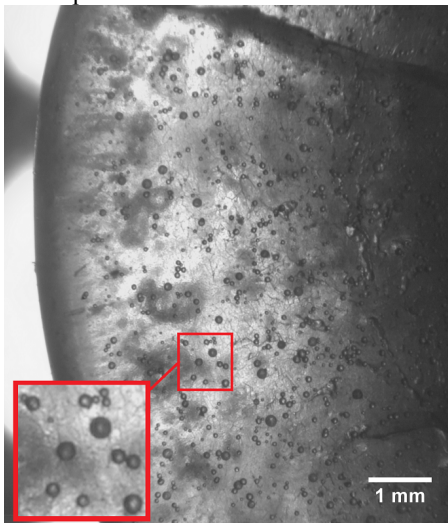


Fig. 1: Ice cylinder with ice spheres on top. The inset shows the particles in more detail. Particles can be single spheres or agglomerates, although the agglomerates were not analyzed within this work.

The ice spheres are deposited on the ice cylinder either as single ice beads or as small agglomerates. Only single ice spheres were analyzed within this study. Once the particles are deposited, the vacuum chamber is evacuated to a pressure of less than 0.05 mbar. The ice cylinder then starts to rotate with increasing frequencies. Due to the centrifugal force the ice spheres on the surface of the ice cylinder start to roll along the surface and are detached, eventually. The particles are observed with a camera.

The rotation frequency of the ice cylinder and the position of the ice sphere at the moment of detachment are derived from the camera images. The radius of the ice sphere is also determined from microscopic camera images. The acting forces at the moment of detachment and therefore also the critical torque for rolling along the surface can then be calculated.

Results: The critical torque for rolling of spherical ice particles on a flat surface has been determined for different particle radii and is presented in Fig. 2. A linear dependency between the critical torque for the onset of rotation and the reduced particle radius has been proposed [3].

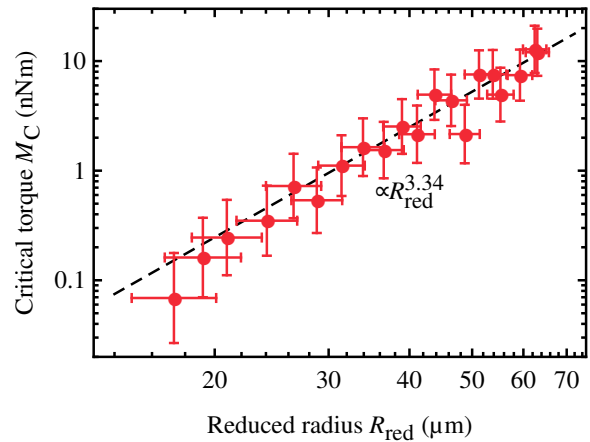


Fig. 2: Critical torque for rolling and its dependency on the particle radius.

Our results show that the critical torque does not scale with the reduced particle radius as predicted, but the increase with the particle radius is stronger. From the first experiments we get a critical torque, which depends on the reduced particle radius by

$M_{crit,exp} \sim R_{red}^{3.34 \pm 0.4}$. As the contact is between a small ice sphere and a flat surface, the reduced radius R_{red} is also the radius of the ice sphere.

Simulations: Numerical simulations for nm-size particles based on molecular dynamics show that a similar size dependence is obtained. The simulations give a dependency between the critical pull-off force F_C and the reduced radius R_{red} of $F_C \sim R_{red}^{2.94 \pm 0.0073}$. Since the critical torque scales linearly with the pull-off force [3], the simulations match experimental data within the standard error.

Conclusion: The first results of our studies indicate that at the given temperature (~ 200 K) the contact forces (critical pull-off torque) between ice grains are stronger than predicted. Experiments as well as numerical simulations show that the critical torque roughly scales with the third order of the reduced radius.

References:

[1] Blum, J. and Wurm, G. (2008) *Ann. Rev. Astronomy and Astrophysics*, 46, 21 [2] Williams, J.P. and Cieza, L.A. (2011) *Ann. Rev. Astronomy and Astrophysics*, 49, 67. [3] Dominik, C. and Tielens, A. (1997) *ApJ*, 480, 647. [4] Johnson, K. et al. (1971), *Proceedings of the Royal Society A*, 324, Iss. 1558, 301-313.

Ices as a source of complex organic molecules in gas and solid phases of interplanetary Solar System objects

N. Abou Mrad¹, A. Fresneau¹, F. Duvernay¹, L. d'Hendecourt^{1,2}, F-R Orthous-Daunay³, V. Vuitton³, P. Poinot⁴, C. Geffroy⁴, T. Chiavassa¹, G. Danger^{1,*}

1. Aix-Marseille Université, PIIM UMR-CNRS 7345, F-13397, Marseille, France

2. Univ. Paris-Sud, Université de Paris-Saclay, Astrochimie et Origines, Institut d'Astrophysique Spatiale, UMR 8617, Orsay 91405, France

3. Université Grenoble Alpes, CNRS, IPAG, Grenoble F-38000, France

4. Université de Poitiers, IC2MP UMR-CNRS 7285, F-86073, Poitiers, France

* Corresponding author

Abstract

Complex organic molecules are detected in gas and solid phases of astrophysical objects. The origin of these molecules is still debated, but a large part is supposed to form at the surface of astrophysical icy grains. These icy grains that can be observed in dense molecular clouds are processed under high energetic processes (VUV photons, ions, electrons) during the star formation. Processing provides the activation of molecules initially present in these ices allowing the development of an important chemical reactivity. In some environments such as the solar nebula, these grains can be warmed releasing in the gas phase a large part of complex organic molecules initially formed at the surface or in the bulk of ice grains. The non-volatile molecules remain on the grains leading to the formation of refractory organic residues. A part of the processed grains can then accrete leading to the formation of interplanetary objects such as comets and asteroids. Therefore, some of the organic matter present in Solar System objects could originate from ices observed in the interstellar medium.

Based on laboratory experiments, we develop a strategy to investigate the potential correspondence between ices of astrophysical objects and organic molecules observed in the gas and refractory organic residues of these objects. We use analytical techniques already developed for space exploration (infrared spectroscopy, gas chromatography coupled to mass spectrometry, mass spectrometry) or under spatialization (orbitrap and liquid chromatography coupled to orbitrap) to probe these different environments and determine the relationships that could exist between ices, gas and organic residue. We demonstrate for the first time the impact of the initial ice composition on the abundances of molecules observed in the gas phase as well as on the molecular composition of residues remaining after the desorption of the most volatile compounds. These information allow us to draw a first chemical link between ices observed in young stellar objects and the organic matter detected inside meteorites, daughters of interplanetary objects such as asteroids. Our strategy allows also to determine complementary analytical techniques required to understand the relations between gas and solid phases of interplanetary objects.

References:

1. Photo and thermochemical evolution of astrophysical ice analogs as a source of soluble and insoluble organic materials in Solar System minor bodies. P. de Marcellus, A. Fresneau, R. Brunetto, G. Danger*, F. Duvernay, C. Meinert, U. J. Meierhenrich, F. Borondics, T. Chiavassa, L. Le Sergeant d'Hendecourt. *Monthly Notices of the Royal Astronomical Society*, 2016, doi : 10.1093/mnras/stw2292.

2. Radical-induced chemistry from VUV photolysis of interstellar ice analogues containing formaldehyde. T. Butscher, F. Duvernay, G. Danger, T. *Astronomy and Astrophysics*, 2016, 593, A60.

3. Insight into the molecular composition of laboratory organic residues produced from interstellar/pre-cometary ice analogues using very high resolution mass spectrometry. G. Danger, A. Fresneau, N. Abou Mrad, P. de Marcellus, F.-R. Orthous-Daunay, F. Duvernay, V. Vuitton, L. Le Sergeant d'Hendecourt, R. Thissen, T. Chiavassa. *Geochimica & Cosmochimica Acta*, 2016, 189, 184-196.
4. Methanol ice VUV photo-processing: GC-MS analysis of volatile organic compounds. N. Abou Mrad, F. Duvernay, T. Chiavassa and G. Danger. *Monthly Notices of the Royal Astronomical Society*, 2016, 458, 1234-1241.
5. Characterization of interstellar/cometary organic residue analogs using very high resolution mass spectrometry, G. Danger, F.-R. Orthous-Daunay, P. de Marcellus, P. Modica, V. Vuitton, F. Duvernay, L. Le Sergeant d'Hendecourt, R. Thissen, and T. Chiavassa, *Geochimica & Cosmochimica Acta*, 2013, 118, 184-201.

Acknowledgments

This work has been funded by the French national programs « Physique Chimie du Milieu Interstellaire » (P.C.M.I, Institut National des Sciences de l'Univers, Centre National de la Recherche Scientifique), the « Programme National de Planétologie » (P.N.P, INSU-CNRS), « Environnements Planétaires et Origines de la Vie » (E.P.O.V, CNRS), the CNES (Centre National d'Etudes Spatiales) from its exobiology program and a PhD grant from the Région Provence Alpes Côte d'Azur (PACA). This work was further supported by the ANR project RAHIIA_SSOM (Grant ANR-16-CE29-0015-01), the ANR project VAHIIA (Grant ANR-12-JS08-0001), the ANR project PeptiSystems (Grant ANR-14-CE33-0020-02) of the French Agence Nationale de la Recherche and finally the Fondation of Aix-Marseille University.

X-rays photolysis of outer solar system ices and its implication on astrobiology

Sergio Pilling¹, Will M. Robson¹, and Fredson A. Vasconcelos¹

¹UNIVAP - Universidade do Vale do Paraíba, São Jose dos Campos, Brazil.

Email: sergiopilling@pq.cnpq.br

Introduction

In this work, we investigate the effects produced mainly by broad band soft X-rays (and X-ray-induced secondary electrons) in ice mixtures that simulates the surface of three moons of giant planets: Europa, Titan and Enceladus, as well as, some icy Transneptunian objects. Such environments are constantly exposed to space ionizing agents (UV and soft X-rays photons, electrons and ions) allowing photodissociation processes, surface photochemistry and prebiotic chemistry. The experiments have been performed using a ultra-high vacuum portable chamber from the Laboratório de Astroquímica e Astrobiologia (LASA/UNIVAP) coupled to the SGM beamline in the Brazilian Synchrotron Light Source (LNLS/CNPEM) at Campinas, Brazil. The beamline was operated in off-focus and white beam mode, which produces a wide band spectral range of photons, mainly from 6 eV up to 2000 eV, with the total average flux at the sample of about $1\text{E}14$ photons $\text{cm}^{-2} \text{s}^{-1}$.

Methodology

Briefly, the samples were produced by the adsorption of a gaseous mixture at 12 K and following by slowly heating to the temperatures in which the irradiation occur, simulating this way the frozen surface of an specific moon of a given giant planet: a) $\text{H}_2\text{O}:\text{CO}_2:\text{NH}_3:\text{SO}_2$ (10:1:1:1) at 90 K for Europa, moon of Jupiter; b) $\text{N}_2:\text{CH}_4$ (19:1) at 12 K for Titan, moon of Saturn, and c) $(\text{H}_2\text{O}:\text{CO}_2:\text{CH}_4:\text{NH}_3)$ (10:1:1:1) at 80 K for Enceladus, another moon of Saturn. For experiment b, we simulate the effect of incoming radiation in the aerosols in the upper atmosphere of Titan. *In-situ* sample analyses were performed by Fourier transform infrared (FTIR) spectrometer. Figure 1 shows a diagram of experimental setup employed in the this work [1].

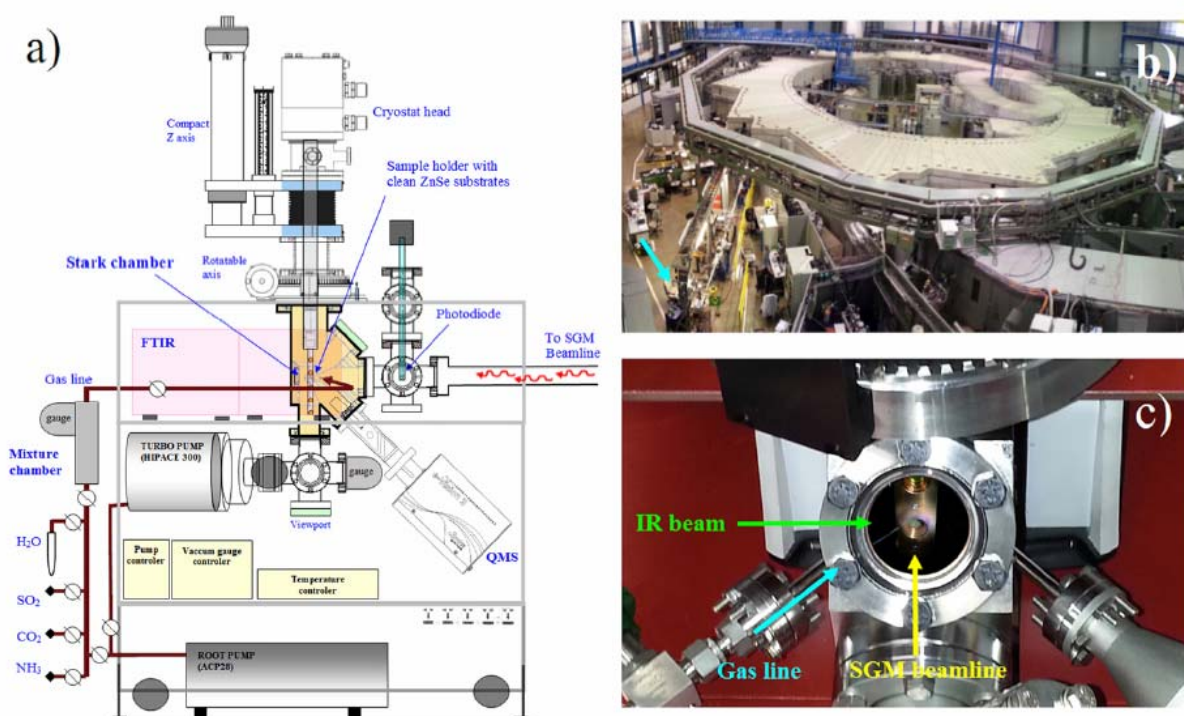


Figure 1. (a) Diagram of the experimental setup (Stark chamber). (b) Illustration of the experimental hall of the Brazilian synchrotron source (LNLS) with the experimental chamber coupled at the SGM beamline (arrow). (c) Illustration showing the frozen sample inside the chamber and ready to be irradiated by synchrotron light.

Results and Discussion

The spectral analysis of the processed samples shows several new bands associated with the formation of organic molecules, including nitriles, hydrocarbons, acids and other organic compounds. The effective dissociation cross sections of parental species were in the order of 10^{-18} - 10^{-19} cm². Half-lives of the parental species extrapolated to the astrophysical scenario was determined.

Conclusion

In case of Europa's experiment, we observe the presence of H₂O₂, H₃O⁺, SO₃, CO, and OCN⁻ among the new species produced [1]. For the experiment simulation aerosols in Titan, we identify the formation of HCN, HNC, CCCN, NH₃ and C₂H₂ [2]. Such molecules possibly will be deposited into the ground and increase the chemical complexity of the surface with time. The irradiation of Enceladus like surface shows as daughter species, OCN⁻, H₂CO and CO among others [3]. Such environments are constantly exposed to space ionizing agents (UV and soft X-rays photons, electrons and ions) allowing photodissociation processes, surface photochemistry and prebiotic chemistry. The processing of such spatial ices have promoted an enhancement in the chemical complexity, similar what may have happened in the early earth triggering the arising of life.

References:

- [1] Pilling S. & Bergantini A., 2015, MNRAS, 811, 151.;
- [2] Vasconcelos F., et al. PSS, submitted;
- [3] Pilling et al., 2016, APJ, in prep.

Electron irradiation of water ice, from thin ice films to dense regolith or ice slabs

A. Galli, A. Vorburger, A. Pommerol, P. Wurz, B. Jost, O. Poch, Y. Brouet, M. Tulej, and N. Thomas
Physics Institute, University of Bern, Switzerland (andre.galli@space.unibe.ch)

The importance of energetic ions impacting the surface of the icy moons of Jupiter for surface weathering and for atmospheric release processes has been studied to some extent in models and in laboratory experiments. The tenuous oxygen atmosphere at Europa, e.g., is believed to be the result of O^+ and S^+ magnetospheric ions sputtering water ice. By comparison, the role of magnetospheric electrons irradiating icy surfaces has attracted little attention.

To better understand the effects of the plasma environment on icy surfaces in the outer solar system, we prepared water ice samples with very different physical properties, ranging from 100 nm ice films to centimeter-thick porous icy regolith (Figure 1) and to dense slabs of ice (Figure 2). We irradiated the different samples with fast electrons, ranging from 100 eV to 10 keV energy, at pressures and temperatures relevant for the large icy moons of Jupiter. One of the known effects is that electron irradiation triggers chemical reactions in the ice (so-called radiolysis), leading to the formation of H_2 , O_2 , and other products. We present new results on the efficiency of radiolysis at energies hitherto not studied in experiments. We also estimate the sputtering yields for electrons ejecting electrons and we study the thermal and electric effects of electron beams in water ice. Finally, we examine the relevance of these experiments for surface processes on the icy moons of Jupiter, considering the few observational constraints on the plasma environment and surface properties.

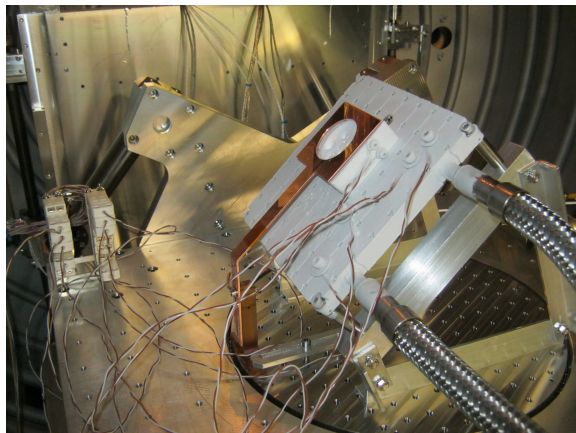


Figure 1: Deep porous ice sample at the end of an experiment. The more energetic electron beams heated up the ice to temperatures where sublimation formed troughs.

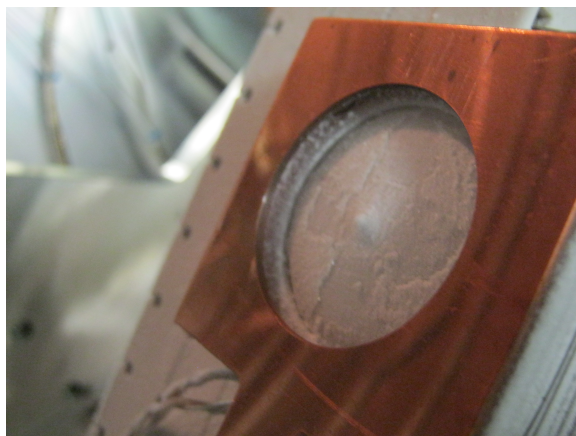


Figure 2: Removing the bright frost layer from a slab of ice with an energetic electron beam.

Evolution of ice/dust mixtures upon sublimation of ice, implications for comets and larger icy objects

O. Poch (1), A. Pommerol (1), B. Jost (1), Z. Yoldi (1), N. Carrasco (2), C. Szopa (2), N. Thomas (1)

(1) Physikalisches Institut und NCCR PlanetS, University of Bern, Switzerland (olivier.poch@csh.unibe.ch),

(2) Université Versailles St-Quentin; Sorbonne Universités, UPMC Univ. Paris 06; LATMOS, CNRS, France

(3) Institut Universitaire de France

The surfaces of many objects in the Solar System comprise substantial quantities of water ice either in pure form or mixed with minerals and/or organic molecules. Sublimation is a process responsible for shaping and changing the reflectance properties of these objects. This peculiar process is not known enough and requires experimental studies.

We present laboratory data on the evolution of the structure and the visible and near-infrared spectral reflectance of icy surfaces made of mixtures of water ice and non-volatile components (complex organic matter and silicates), as they undergo sublimation of the water ice under low temperature and pressure conditions [1,2]. We prepared icy surfaces which are potential analogues of ices found on comets, icy satellites or trans-neptunian objects (TNOs). The experiments were carried out in the SCITEAS simulation setup recently built as part of the Laboratory for Outflow Studies of Sublimating Materials (LOSSy) at the University of Bern [3].

As the water ice sublimated, we observed *in situ* the formation of a sublimation lag deposit, or sublimation mantle, made of the non-volatiles at the top of the samples (Figure 1). The texture (porosity, internal cohesiveness etc.), the activity (outbursts and ejection of mantle fragments) and the spectrophotometric properties of this mantle are found to differ strongly depending on the chemical nature of the non-volatiles, the size of their particles, the way they are mixed with the volatile component and the dust/ice mass ratio. The results also indicate how the band depths of the sub-surface water ice evolve during the build-up of the sublimation mantle.

These data provide useful references for interpreting remote-sensing observations of Rosetta [4], and also New Horizons.



Figure 1: Formation of a dry foam-like porous organic matrix after sublimation of the water ice [1].

[1] Poch, O., *et al.*, (2016a), Sublimation of ice-tholins mixtures: a morphological and spectro-photometric study, *Icarus*, 266, 288-305, <http://dx.doi.org/10.1016/j.icarus.2015.11.006>

[2] Poch, O., *et al.*, (2016b), Sublimation of water ice mixed with silicates and tholins: evolution of surface texture and reflectance spectra, with implications for comets, *Icarus*, 267, 154-173, <http://dx.doi.org/10.1016/j.icarus.2015.12.017>

[3] Pommerol, A., *et al.*, (2015a), The SCITEAS experiment: laboratory studies of the sublimation of icy planetary analogues, *Planetary and Space Science*, 109-110, 106-122, <http://dx.doi.org/10.1016/j.pss.2015.02.004>

[4] Pommerol, A., *et al.*, (2015b), OSIRIS observations of meter-size exposures of H₂O ice at the surface of 67P/Churyumov-Gerasimenko and interpretation using laboratory experiments, *Astronomy & Astrophysics*, 583, <http://dx.doi.org/10.1051/0004-6361/201525977>

Analogue mass spectra of astrobiological relevant organic material for in situ space detectors

Fabian Klenner (1), Frank Postberg (1,2), Ferdinand Stolz (3)

(1) Institute of Earth Sciences, University of Heidelberg, Heidelberg, (2) IRS, University of Stuttgart, Stuttgart, (3) WOI, University of Leipzig, Leipzig

Most astrobiologists agree that it is fundamental to consider amino acids and fatty acids in the search for extraterrestrial life. For future space missions to icy moons with a subsurface ocean it is important to study the mass spectrometric appearance of these organic compounds in impact ionization detectors. Since both of these organic materials exist also in comets and other primitive bodies it is crucial that their biotic and abiotic fingerprints can be distinguished.

With our worldwide unique setup in Heidelberg we are able to generate analogue mass spectra of amino acids, peptides and fatty acids in ice grains that might emerge from ocean bearing moons like Enceladus and Europa. It simulates the impact ionization mechanism in space instruments by an IR-Laser. The resulting spectra are highly comparable to those of icy particles e.g. on the Cosmic Dust Analyzer (CDA) on board the Cassini spacecraft or the Surface Dust Analyser (SUDA) onboard the Europa Clipper mission. The experimental setup (FL-MALDI TOF MS) consists of a vacuum chamber (1×10^{-4} mbar) in which a water beam (radius of $7.5 \mu\text{s}$) is inserted. Chemical substances like amino acids and fatty acids are dissolved in the water beam. A pulsed infrared laser hits the water beam. In this way ions, electrons and neutral molecules of the dissolved substances and water are created. The positive and also the negative ions can be detected in a commercial TOF mass spectrometer.

Our laboratory results show a high sensitivity on the tested substances. The detection limits are in the ppm or even ppb range. Different amounts of the organic substances lead to different intensities of the related peaks in the mass spectra. We are able to easily differentiate between abiotic and biotic signatures in the analogue spectra. By comparing the laboratory results with spacecraft data we have the ability to recognize and distinguish such signatures on icy moons with a subsurface ocean. In the future we aim to create a comprehensive spectrum library for in situ mass spectrometers in space from a wide variety of organic analogue materials in icy grains.

BIO-INSPIRED UNDERWATER ROBOTS FOR LIQUID ATMOSPHERES IN PLANETARY APPLICATIONS. Mannam Naga Praveen Babu¹ and Krishnankutty. P², ¹Department of Ocean Engineering, Indian Institute of Technology Madras, Chennai - 600036, India. ¹E-mail: oe13d006@smail.iitm.ac.in, ²Department of Ocean Engineering, Indian Institute of Technology Madras, Chennai - 600036, India. ²E-mail: pkrishnankutty@iitm.ac.in

Introduction: Liquid atmosphere exists in planet earth, jupiter's moon europa, Saturn's biggest moon Titan, and other unknown celestial bodies like neutron stars, Gliese 581d in the universe. The europa consists of liquid hydrocarbon beneath its ice crusts. The titan planet consists of liquid methane and ethane oceans. Sprawling over 100km and with depths estimated at 300m Kraken Mare is comparable in size to the great lakes. It is the only known body in the solar system with stable liquid seas on its surface like planet earth. The other two main lakes in titan are Punga 200 km, Ligea mare 400 km. NASA's Cassini spacecraft released Huygens probe and received information about Titan and its seas depths, pressures and temperatures. It consists of hydrocarbon mixtures of C₂H₆, CH₄, N₂ and does not freeze unless the temperature drops. Therefore no ice sheet will form at the lake surface under the known Titan's condition. In order to study the chemical composition of the liquid, surface and sub surface currents, mixing and layering in the water column, tides, wind and waves, bathymetry, bottom features and composition on Titan's karken mare conventional underwater vehicles are used for exploration.

The physical exploration of space is carried out by both human spaceflight and unmanned robotic probes (rovers). A rover is a planetary exploration vehicle designed to move across the celestial bodies or on surface of the planets. These rovers can be semi-autonomous or fully autonomous bodies. The main function of these rovers is to collect rock samplings, dust and images of the surface. The advantages of planetary rovers compared to stationary landers are they can make observations at a microscopic level and can conduct physical experimentations and they can examine more territory. However, the conventional underwater rovers are subjected to obstacle avoidance, difficult to maneuver in highly rough terrains and unable to withstand in harsh environments. The bubbling of N₂ during thrusters operation and pressure from propellers are main challenges associated with conventional AUV's in cryogenic atmosphere.

In order to overcome the above challenges and explore liquid atmospheres in Titan karken mare or Jupiter's europa (the fourth largest moon on jupiter), the rover should have the ability to propel and manoeuvre effec-

tively within liquid media without creating turbulence in those liquid mediums and its design must reflect these operational requirements.

The current research is to design the planetary rover based on biological species that live in liquid environments on Earth e.g. aquatic mammals and fish. This would involve the development of a robotic system that was able to replicate the swimming aspects of fishes for liquid environments on planets. This proposed research project will address the design and analysis of a biologically inspired or biomimetic rover concept, for example based on fish swimming, particularly carangiform modes (salmonid). Such robotic systems are highly robust and capable of generating thrust with caudal fin and auxiliary (pectoral) fins. These fins increase the powering aspects of the vehicle in liquid environments and eliminate the needs of rudder devices for maneuvering.

Biomimetic Planetary Robot: The first phase of design considerations will include propulsion mechanisms, efficiencies and power requirements. These will be evaluated through numerical simulations that have been validated against previous studies involving biomimetic autonomous underwater vehicles. The bio-inspired planetary rover is shown in fig. 1. The forward (pectoral) fins have the freedom to oscillate in vertical and/or horizontal plane about the transverse axis and the aft (tail) fin has freedom to oscillate in the horizontal plane about the longitudinal axis. The pectoral fins provide instantaneous stopping ability to rover and help in reducing the turning circle maneuvering parameters. The modes of operation of pectoral fins is shown in fig.2. The pectoral fins are operated by two servos for flapping motion and two rotational motors for rotation of fins shown in fig. 3. The caudal fin acts as main propulsor for the rover shown in fig. 4. The rover also consists of main controller box, wireless remote.

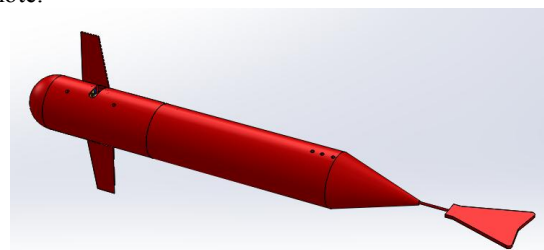


Fig. 1. Bio-inspired Planetary rover

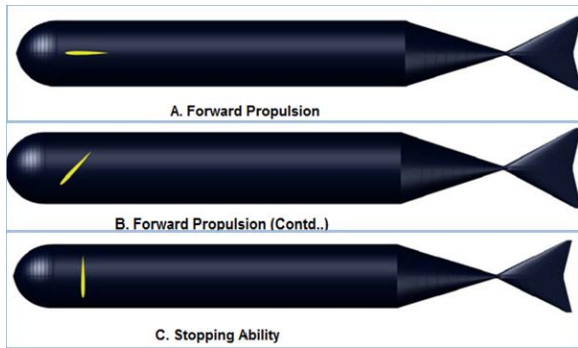


Fig. 2. Pectoral fins in flapping and rotational mode.

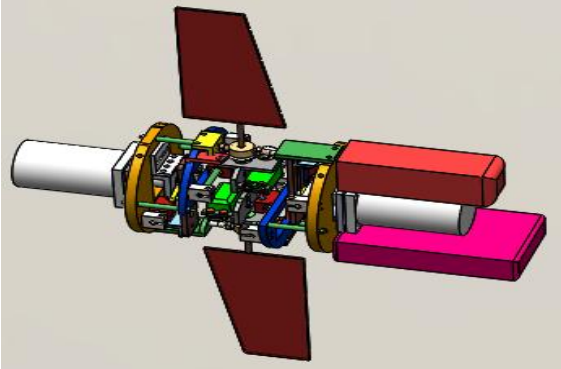


Fig. 3. Pectoral Fins with servo motors and batteries

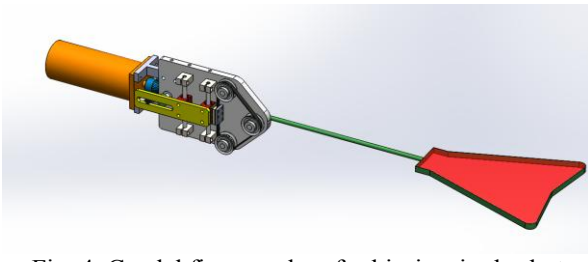


Fig. 4. Caudal fin propulsor for bio-inspired robot

Hydrodynamics of planetary robot: A lift-based propulsion theory is used to estimate the thrust generated by pectoral fins (used as auxiliary thrust device) and an empirical method is used to estimate the torque at the caudal fin. The fish body shape and fin geometrical parameters are also important with regard to the resistance and powering aspects. Numerical studies are conducted with the robotic fish to determine its resistance in bare hull and also for the case fitted with fins. This paper investigates the oscillating motion of caudal fin in yaw mode at different amplitude ratios. The caudal fin generates a reverse von karman vortex street (thrust producing wake) at strouhal number, 0.22. These mechanisms are presented and discussed in the proposed paper. The thrust force on pectoral fins and caudal fin was estimated using strain gauge type force

sensors in self propulsion mode with the help of towing carriage. These results are discussed in the present paper. In the second phase, the numerical simulations of ditching of bio-inspired underwater vehicle hull will be presented here.



Fig. 5. Bio-inspired robot in testing stage.

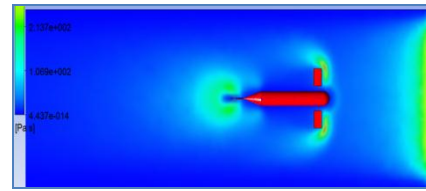


Fig. 6. Flow around the pectoral and caudal fins

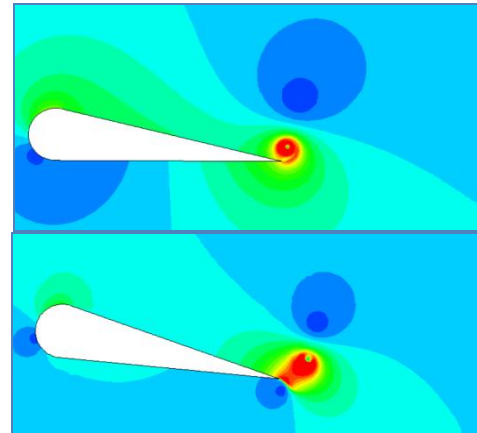


Fig. 7. Reverse von karman vortices around flapping caudal fin

Acknowledgement: The authors would like to thank Dept. of Ocean Engineering, Inidan Institute of technology Madras, Chennai, India for supporting this project.

Bibilography:

- [1] Anderson J, Streitlien K, Barrett D, Triantafyllou M. Oscillating foils of high propulsive efficiency. *Fluid Mechanics* 1998;360:41–72.
- [2] Taylor GK, Nudds RL, Thomas ALR. Flying and swimming animals cruise at a Strouhal number tuned for high power efficiency. *Nature* 2003;425:707.
- [3] Read DA, Hover F, Triantafyllou M. Forces on oscillating foils for propulsion and maneuvering. *Journal of Fluids and Structures* 2003;17:163–83.

Organic compounds from Enceladus in E ring ice grains

Frank Postberg¹

Nozair Khawaja¹, Rene Reviol¹, Lenz Nölle¹, Fabian Klenner¹

(1) Institute for Geosciences, Heidelberg University, Germany (2) IRS, Universität Stuttgart, Germany

Email: (Frank.Postberg@geow.uni-heidelberg.de)

Water ice dominates the composition of the micron and sub-micron sized dust particles in Saturn's E-ring, a ring constantly replenished by active icy jets of the moon Enceladus. Details about the composition of this tenuous, optically thin ring can only be constrained by in situ measurements. The Cosmic Dust Analyzer (CDA) onboard Cassini investigates the composition of these grains by cationic time-of-flight mass spectra of individual ice grains hitting the instruments target surface. From these spectra three compositional types of E ring ice grains have been identified previously: Type-1: Almost pure water, Type-2: Enriched in organics, and Type-3: Enriched in salt.

Unlike Type-1 and 3, organic-enriched Type-2 spectra have not yet been investigated in depth. Here we report a detailed compositional analysis of this type. The spectra analysis is supported by a laboratory ground campaign in Heidelberg. As expected, we find more complex and refractory organic molecules in ice grains compared to the volatile organic material in the gas phase. In contrast to Type 1 and 3, Type-2 spectra display a great compositional diversity, which indicates varying contributions of several organic species. So far we have identified characteristic fragment patterns of at least three classes of organic compounds: aromatic species, amines, and carbonyl group species. The diversity of the identified species requires different generation scenarios for different organic bearing ice grains.

NEW GLOBAL MAP OF LINEAMENTS ON EUROPA

A. Lucchetti¹, E. Simioni², G. Cremonese¹ ¹INAF-Astronomical Observatory of Padova, Vicolo dell'Osservatorio 5, 35131 Padova, Italy (alice.lucchetti@oapd.inaf.it); ²CNR-INFN, Via Trasea 7, 35131, Padova, Italy

Introduction: Physical models have been developed to successfully explain the orientations and locations of many fractures observed on Europa's surface. Between the different fractures located on the surface of the icy satellite global-scale lineaments are present. These features are correlated with tidal stress suggesting that they initiated at tensile cracks in response to non-synchronous rotation [1,2]. In this work we completed a global map of all type of lineaments presented of the surface of Europa, including also cycloidal lineaments that are interpreted to be tensile cracks that form due to diurnal stresses from Europa's orbital eccentricity [3]. We enhanced the mapping of lineaments in comparison to what previously published, tracking about 5500 lineaments located everywhere on the surface of the icy satellite. The aim is to investigate the timing of formation of these lineaments and their orientation, which will be in turn correlated with proposed stress pattern model.

Dataset: We enhanced the mapping of lineaments in comparison to what previously published, tracking about 5500 lineaments with ARCGis software (Fig. 1). We used a mosaic obtained from Galileo SSI images fixing a scale of 500 m/px. We also included in a first analysis about 30 cycloidal lineaments (Fig. 1).

In this dataset we have not considered too short lineaments in order to acquire the 3D lineament information on the hypothesis of the ellipsoidal shape of the satellite. In so doing, we reduce the uncertainty on defining a plane for each lineament and reduce the contribution of features strongly dependent from local geological processes.

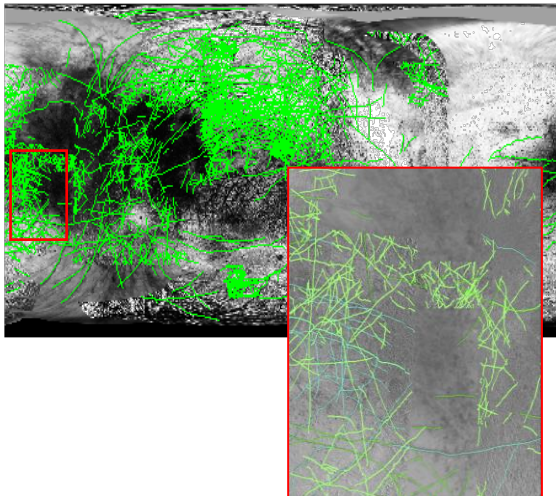


Fig. 1. Mapping of lineaments in 2D (with a close up of a portion of lineaments mapped).

Methods: We analyzed our lineaments mapping using Rose diagrams and Stereo Plots.

Through rose diagrams we found an angle of the principal direction in respect to the leading direction that depends on the lengths' lineaments (Fig. 2), specifically we obtained an angle of 27.4° for long lineaments (N=100), in agreement with [4], and an angle of 36.6° for short lineaments (N=1888), as shown in Fig. 2. However, this is a 2D method that imposes radial symmetry in respect to the polar axis, hence lacking the 3D lineaments information.

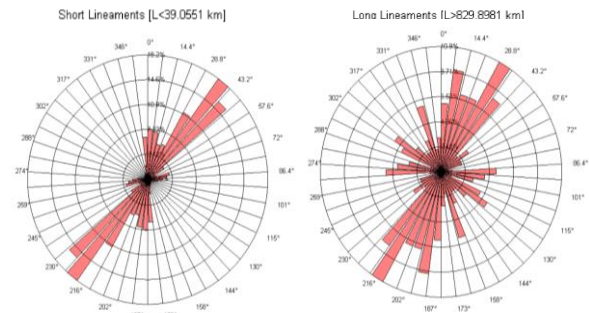


Fig. 2 The Rose Diagrams obtained from the analysis.

For this reason we used the Stereo plot analysis and approach which was already used in [5]. The Stereo Plot shows the orientation of the planes defined by the lineaments with respect to the equatorial plane (the center corresponds to the planes parallel to the equatorial plane) by SVD (Singular Value Decomposition). The point size linearly depends from the lineament length, as shown below (Fig. 3).

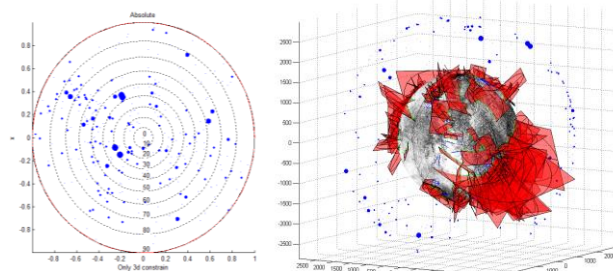


Fig. 3 Stereo Plot in the absolute reference frame.

Looking at the absolute distribution of the versors related to the planes we have realized that there is a

preferred orientation. From this orientation we have identified a new reference system in which the stereo plot does not have a centered distribution. This is in agreement with previous results [4].

Discussion and Conclusions: From the analysis of lineaments presented above, in particular from the 3D density distribution we found the axis of maximal radiality of the lineaments. The radial axis is represented on the map below as green cross and it is 30° tilted in longitude and 10° offset in latitude in respect to the Jupiter direction (Fig. 5).

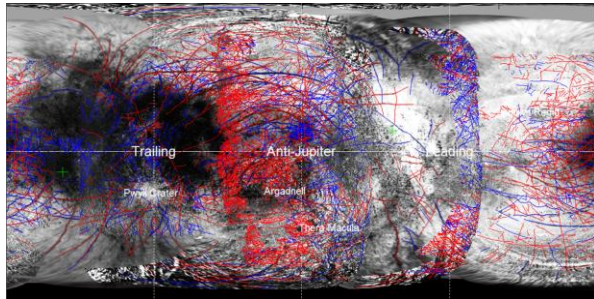


Fig. 4 Map showing the results obtained.

The longitude offset is in agreement with [4], and so partially explained by NSR (Non Synchronous Rotation), while the latitude offset represents a new information which is still under study.

We are still investigating the interpretation of these results considering different processes in order to explain our findings. The offset in latitude would be consistent with true polar wander, as found by [5], but some uncertainties still exist. Indeed, this latter work suggests an episode of 80° true polar wander.

The next step will be (i) the comparison of our results with already proposed stress models and (ii) investigate the timing of formation of these lineaments.

Acknowledgements: This research was supported by the Italian Space Agency (ASI) through the ASI-INAF agreement no.2013-056-RO.

References: [1] Geissler, P. E., et al. "Evidence for non-synchronous rotation of Europa." *Nature* 391.6665 (1998): 368-370. [2] Greenberg, Richard, et al. "Tectonic processes on Europa: Tidal stresses, mechanical response, and visible features." *Icarus* 135.1 (1998): 64-78. [3] Formation of cycloidal features on Europa. *Science*, 285(5435), 1899-1902. [4] McEwen, Alfred S. "Tidal reorientation and the fracturing of Jupiter's moon Europa." (1986): 49-51. [5] Simioni, E., Pajola, M., Massironi, M., & Cremonese, G. (2015). Phobos grooves and impact craters: A stereographic

analysis. *Icarus*, 256, 90-100. [6] Schenk, P., Matsuyama, I., & Nimmo, F. (2008). True polar wander on Europa from global-scale small-circle depressions. *Nature*, 453(7193), 368-371

EVIDENCE OF COMPRESSIONAL TECTONICS ON URUK SULCUS REGION OF GANYMEDE

Costanza Rossi¹; Paola Cianfarra¹; Francesco Salvini¹; Giuseppe Mitri²; Marion Massé²

¹ Science Dept., Università Roma Tre, L.go S.L. Murialdo, 1, 00146 Rome, Italy

² Laboratoire de Planétologie et Géodynamique, Université de Nantes, CNRS, France

ABSTRACT - Ganymede, the largest satellite of Jupiter, shows an icy crust strongly shaped by past and possibly still active tectonics. The surface is subdivided into two terrains, i.e. dark and light terrains, and morphotectonic features are present in both of them. The younger light terrains represent about 65% of the surface and show the presence of deformation features represented by swarms of grooves, i.e. kilometric lineament systems at the regional scale. Several authors proposed extensional tectonic models to explain groove formation, leaving open their possible connection to compressional tectonics. Specific processing of Voyager and Galileo mission images allowed the preparation of a high-resolution mosaic (with maximum resolution up to 50 m/pixel) of the anti-Jovian area framing the Uruk Sulcus light terrain, on which we investigated these lineaments in order to better highlight the tectonic setting which characterizes the area. This area will be investigated by the radar sounder RIME (Radar for Icy Moon Exploration) for ESA's upcoming JUICE (JUperiter ICy moon Explorer) mission. Using methodologies typical of structural geology, we found that these lineaments cluster in the study area around preferential orientation forming lineament domains. The study of the Length/Spacing ratio (i.e. L/S) of these domains allowed to infer the relative deformation intensity and rheology within the crust of the studied region. Computer fit by polymodal gaussian of azimuth-frequency histograms and frequency histograms of the L/S ratio has been performed to identify independent data groups allowing the classification of four lineament domains within Uruk Sulcus. The main domain is oriented N52°W, and the others show average strikes at N68°E, N16°E and N38°E. We propose a new evolutionary tectonic model of the study area. Results demonstrate, for the first time, the presence of significant compressive tectonics within a shear zone on the icy crust of Ganymede. Uruk Sulcus is subjected to regional dextral transpression approximately N-S that in turn is responsible for localized transtension in crustal blocks within the shear zone. A terrestrial analog in the glaciers of Northern Victoria Land, Antarctica, confirms the proposed model.

TITLE:

Erosion rate and seasonality of block falls at the north polar scarps of Mars based on HiRISE images

ABSTRACT:

We estimate the erosion rate of steep scarps at the margin of the north polar ice cap of Mars by identifying active block displacements, their source and their seasonality. This will improve our knowledge of the importance of erosion on the evolution of the north polar ice cap. Thousands of single-block movements or events involving multiple blocks have been captured within 10 years of repeated high resolution imaging by the High Resolution Imaging Science Experiment (HiRISE). These blocks, which are up to a couple of cubic meters in volume, become detached either from the North Polar Layered Deposits (NPLD) or the Basal Unit (BU) [1] and come to rest intact or after breaking up into smaller fragments. We detect the new blocks automatically in co-registered images taken at different times. For the co-registration we use Ames Stereo Pipeline [2] to produce HiRISE Digital Terrain Models (DTMs) and ortho-rectify the images on these DTMs. We focus on retrieving the frequency and seasonality of the events as well as the sizes and shapes of the moved blocks. Our results suggest that block falls are presently an important, regularly recurring seasonal process for certain areas of the north polar scarps of Mars.

The research leading to these results has received funding from the European Union's Seventh Framework Programme (FP7/2007-2013) under iMars grant agreement no 607379.

References:

[1] Russell et al., Landslide erosion rates of north polar layered deposit cliffs and the underlying basal unit, Eighth International Conference on Mars, 2014

[2] Moratto et al., Ames Stereo Pipeline, NASA's Open Source Automated Stereogrammetry Software, LPSC, 2010

AUTHORS:

Lida Fanara^{1,2}, Klaus Gwinner¹, Ernst Hauber¹, Juergen Oberst^{1,2}

INSTITUTIONS:

1. German Aerospace Center, Berlin, Germany.
2. Technical University of Berlin, Berlin, Germany.

In Situ Detection and the Enceladus Plume

B. Southworth, S. Kempf, J. Schmidt, R. Srama, F. Postberg

The Enceladus dust plume offers spacecraft unparalleled access to large (up to several μm in radius), frozen water-ice particles, likely originating from Enceladus' subsurface ocean. In this talk, we discuss potential mechanisms driving a dust plume, and comment on what makes the Enceladus plume unique from the perspective of in situ detection.

One property of the Enceladus plume that has yet to be resolved is mass production. Mass production is essential for estimating the dust-to-gas mass ratio, which is in turn important to resolve the plume source mechanism. However, Schmidt et al. (2008) obtained a total mass production of approximately 5 kg/s based on matching their model to CDA data, while Ingersoll and Ewald (2005) derived a dust production rate of 51 kg/s from the total plume brightness. Here, large-scale simulations of the Enceladus dust plume are run to construct a quasi-steady-state density profile of plume particles about Enceladus. Our model is then constrained to reproduce plume dust density measured during multiple low-altitude Cassini flybys, leading to a bound on plume mass production of < 5 kg/s.

Based on our derived mass production, estimates are made of the total number of particles and total mass of particles collected by a dust detector passing through the Enceladus plume over various trajectories. This also leads to estimates of the necessary flyby altitude to collect particles of a given size.

On the compositional profile of Enceladus' ice plume from the latest Cassini flybys

Nozair Khawaja⁽¹⁾, Frank Postberg⁽¹⁾, Jürgen Schmidt⁽²⁾

(1) Institute of Earth Sciences, Heidelberg University, Germany (2) University of Oulu, Finland

The Chemical Analyzer (CA) subsystem of the Cosmic Dust Analyzer (CDA) on board the Cassini spacecraft generates cationic time-of-flight (tof) mass spectra of impinging ice particles onto the instrument's target. Despite the large number of mass spectra of ice grains (>100000) that have been recorded in the E ring, only less than 100 spectra have been previously acquired directly in the plume. Previously, only a flyby in 2008 (E5) provided sufficient statistics to infer the plume's compositional profile, indicating that the proportions of different compositional populations in the plume vary with altitude (Postberg et al., 2011).

We present here the compositional mapping of the Enceladian plume based on mass spectral data acquired on E17, E18 and E21 that occurred in 2012 and 2015. On these flybys the spacecraft passed horizontally through the dense plume region with moderate speed directly above the tiger stripes. The closest approach on E17/18 and E21 was at 75km and 49km above Enceladus' South Polar Terrain, respectively, whereas the relative speed of the spacecraft was 7.5 km/s on E17/18 and 8.5 km/s on E21. Three distinct compositional families of spectra have been previously identified in the plume (Postberg et al., 2011) representing three different ice particle populations emerging from subsurface Enceladus: i) Almost pure water – Type-1, ii) Organic enriched – Type-2 and iii) Salt rich – Type-3. A boxcar analysis (BCA) was conducted to infer the frequency of these three main compositional types in Enceladus' plume along the spacecraft trajectory during each flyby.

The abundances of different compositional types of the Enceladian ice grains differ from the E ring background confirming the compositional differentiation inside the plume. We compared our results with the E5 flyby, which yielded the best compositional profile but was executed as much higher velocity (~17.6 km/s) and a very different, highly inclined, flyby geometry. The data shows a less pronounced increase in salt rich Type 3 grains as predicted by the model inferred from E5 (Postberg et al., 2011). However, the recent flybys indicate a more drastic increase of organic enriched Type 2 grains in the plume compared to E5.

Rotation-Driven Exospheres of the Icy Galilean Satellites Apurva V. Oza¹ Francois Leblanc¹, Robert E. Johnson^{2,3}, Carl Schmidt¹, Ludivine Leclercq^{1,2}, Timothy A. Cassidy⁴, Jean-Yves Chaufray¹, and Ronan Modolo¹. ¹LATMOS/IPSL, UPMC Univ. Paris 06 Sorbonne Universites, UVSQ, CNRS, Paris, France (apurva.oza@latmos.ipsl.fr), ²Engineering Physics, University of Virginia, Charlottesville, Virginia, USA. ³Physics, New York University, New York, NY, USA. ⁴Laboratory for Atmospheric and Space Physics, University of Colorado Boulder, Colorado, USA.

Introduction: Voyager first observed the infrared reflectance spectra of the icy Galilean satellites, deducing the presence of abundant water ice [1] leading to the prediction of sublimated and sputtered H₂O [2] and O₂ [3] exospheres due to the bombardment of Jovian magnetosphere particles, most pronounced at Europa and Ganymede. Today, due to FUV oxygen aurorae images by the Hubble Space Telescope (HST) we have been able to infer the orbital evolution of the O₂ at Europa [4] and Ganymede [5], highlighting asymmetries between the sunlit trailing (plasma ram) and the sunlit leading (plasma wake) hemispheres. Furthermore, when comparing to exosphere general model (EGM) simulations of the near-surface O₂ exosphere, it was found that most of the O₂ column builds near dusk, generating a permanently asymmetric exosphere [6], [7]. This dusk-over-dawn asymmetry is fundamentally due to the satellite’s rotation, resulting in an exospheric oxygen cycle peaking at dusk in the satellite’s reference frame. The cycle is driven by the changing directions of the incident plasma, responsible for O₂ production with respect to the sub-solar and sub-jovian points throughout the Jovian orbit.

Model: We employ a parallelized 3-D Monte Carlo routine, the core of the EGM, to simulate Europa and Ganymede’s exospheres. Our simulation box extends to ~ 1.5 satellite radii, in which we track ejected molecules in the satellite’s rotating reference frame. Molecules are ejected based on the function distributions for sputtering or sublimation and are sensitive to the changing albedo and temperature of the surfaces (Table 1), all of which are described in detail in [6] & [7]. We calculate the standard thermodynamic quantities: number density $\langle n \rangle$, temperature $\langle T \rangle$ and velocity $\langle v \rangle$. These quantities are then used to reconstruct the LOS column densities as calculated in Table 2 along with estimates of timescales relevant for the exospheres.

Rotation-Driven O₂ Exosphere: The O₂ peaks towards dusk due to the interplay between rapid production and slow migration of the O₂ occurring throughout the orbit. It turns out the O₂ column at a given point in the Jovian orbit is due to the accumulated O₂ flux ejected previously in the orbit. As an example, Fig. 1 illustrates this phenomena for Europa’s exosphere from ejection at

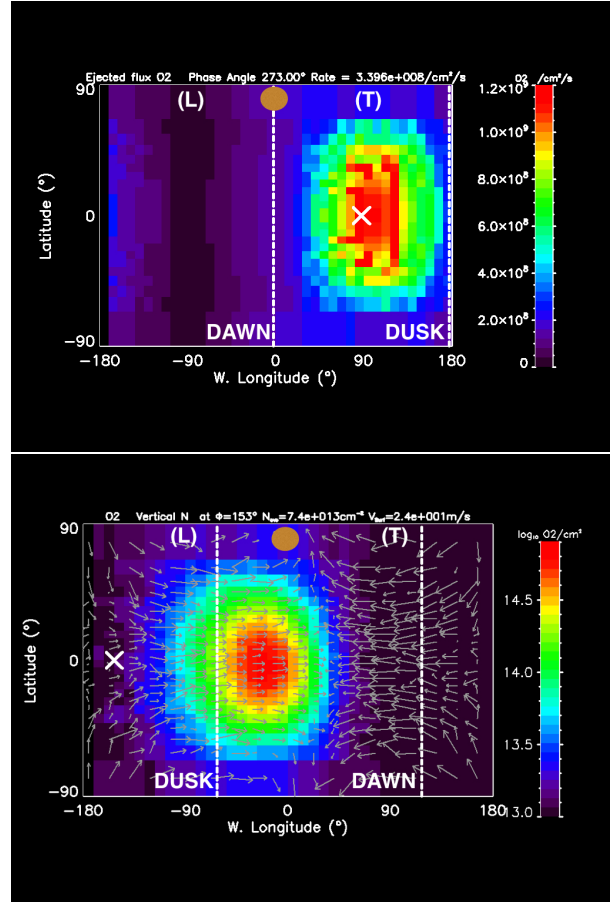


Figure 1: Latitude vs West Longitude maps of Europa where X marks the subsolar point, (L) and (T) are the location of the longitudinal centers of the leading and trailing hemispheres, and the orange sphere marks the direction to Jupiter. **Top panel:** Ejected sputtering flux in O₂ s⁻¹ cm⁻² at a phase angle of 90°. **Bottom panel:** Radial column density in O₂ cm⁻² at 150°. From top-to-bottom: O₂ ejecta at Europa’s sunlit trailing hemisphere builds a column continuously throughout the orbit and arrives near Europa’s sunlit leading hemisphere. White vectors represent the day-night migration of O₂ under rotation.

the sunlit trailing hemisphere which subsequently builds a large column of O₂ at dusk near the leading hemisphere.

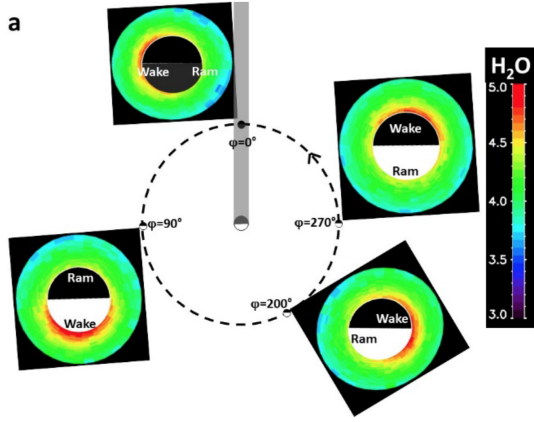


Figure 2: Orbital Evolution of H_2O at Ganymede where ψ designates the phase angle: 270 = sunlit trailing hemisphere, and 90 = sunlit leading hemisphere.

Rotation-Driven H_2O Exosphere: Ganymede's intrinsic magnetic field coupled with the varying subsolar and ambient plasma flow axes described above, results in a noticeable orbital evolution of the largely static H_2O exosphere. In Figure 2 it can be seen that the sunlit leading hemisphere, phase angle 90, is roughly an order of magnitude more dense than the sunlit trailing hemisphere, phase angle 270. This is due to the difference in the access of open field lines to Ganymede's surface allowing more incident ions to bombard and thus sputter H_2O into the atmosphere on the wake side.

This work describes the important effect of rotation on Europa and Ganymede's exosphere which could have further implications on the dynamics of neighboring satellites Io and Callisto.

References

- [1] C. B. Pilcher, et al. Galilean Satellites: Identification of Water Frost. *Science*, 178:1087–1089, 1972. doi:10.1126/science.178.4065.1087.
- [2] R. E. Johnson, et al. Erosion of Galilean satellite surfaces by Jovian magnetosphere particles. *Science*, 213:1027–1030, 1981.
- [3] R. E. Johnson, et al. Planetary applications of ion induced erosion of condensed-gas frosts. *Nuclear Instruments and Methods*, 198:147–157, 1982. doi:10.1016/0167-5087(82)90066-7.
- [4] L. Roth, et al. Europas far ultraviolet oxygen aurora from a comprehensive set of HST observations. *J. Geophys.*, 261:1–13, 2015. doi:10.1016/j.icarus.2015.07.036.

	T_d [K]	A_T -	T_n [K]	A_L -	a_s [R_J]	g_s [$cm\ s^{-2}$]	v_e [km/s]
E	136	0.45	80	0.65	9.6 R_J	131	2.02
G	146	0.37	70	0.43	15.3 R_J	143	2.74

Table 1: **Physical Parameters for Europa (E) and Ganymede (G).** Maximum and minimum surface temperatures, T , as calculated by our thermal model using the trailing and leading albedo values, A , tabulated. a_s is the satellite's semimajor axis in Jovian radii. g_s is the satellite's gravitational acceleration at the surface, and v_e is the escape velocity pertinent for escaping water products such as H_2 .

	$\langle N \rangle_{H_2O}$ cm^{-2}	$\langle N \rangle_{O_2}$ cm^{-2}	τ_s hrs	t_b [τ_s]	t_m [τ_s]	t_x [τ_s]
E	$1.0 * 10^{13}$	$7.9 * 10^{14}$	85	8E-4	4.2	0.98
G	$1.5 * 10^{13}$	$2.3 * 10^{14}$	172	3.9E-4	7.1	1.1

Table 2: **Exospheric parameters for Europa(E) and Ganymede(G).** $\langle N \rangle$ is the orbit-averaged radial column density as calculated from the number densities and temperatures from our simulations. τ_s is the satellite's orbital period. The last three timescales are in units of τ and are estimated solely for O_2 . t_m is the day-night migration time should the exosphere be migrating from one hemisphere to another in random-walks λ : $t_d \sim \lambda^2 t_b$ where t_b is the bounce time for the O_2 molecule given no adsorption to the regolith. t_x is the exospheric production time, estimated roughly as $\sim \langle N \rangle / f_{O_2}$ where f_{O_2} is the sputtering flux.

- [5] M. A. McGrath, et al. Aurora on Ganymede. *Journal of Geophysical Research (Space Physics)*, 118:2043–2054, 2013. doi:10.1002/jgra.50122.
- [6] A.V Oza, et al.
- [7] F. Leblanc, et al.

Acknowledgments: This work is part of HELIOSARES Project supported by the ANR (ANR-09-BLAN-0223) and ANR MARMITE-CNRS (ANR-13-BS05-0012-02). Authors are also indebted to the "Systeme Solaire" program of the French Space Agency CNES for its support. Authors also acknowledge the support of the IPSL data center CICLAD for providing us access to their computing resources and data.

FUTURE MISSIONS TO THE ICY WORLDS OF THE SOLAR SYSTEM

Michel Blanc(*) and the Horizon 2061 team

*Institut de Recherche en Astrophysique et Planétologie (IRAP/OMP), Toulouse, France ;
International Space Science institute (ISSI), Bern, Switzerland ; International Space
Science Institute-Beijing (ISSI-BJ), Beijing, China.

Water is one of the three keys to the access of planetary objects and environments to the prestigious status of « Habitable Worlds ». But where is water in the solar system ? Except for the surfaces or interiors of a few of the differentiated bodies, solar system water reservoirs are found essentially in the ice phase. Hence the importance of building a comprehensive inventory of icy bodies. Space missions as the most powerful tool to visit this family of objects, characterize their ice contents, and try to understand what they tell us both about the early days of our Solar System (the remnants of the Solar Nebula) and about its potential for favoring the emergence of Habitable worlds.

In this talk we will review the different categories of solar system objects that harbour water ice reservoirs : small bodies like comet nuclei, Kuiper Belt Objects, small bodies gravitationally bound to the giant planets, and giant planet's satellites. Recent discoveries invite us to even extend this inventory to objects belonging to the family of main belt asteroids.

We will then attempt to provide a brief summary of the different space missions which are currently in planning or already returning results, and of those about which we are just starting to think for a more distant future. This tentative summary of the stimulating landscape of future missions to the icy worlds of the solar system will be based on the results of the forum « Planetary Exploration, Horizon 2061 » organised in Bern on sept. 13-15 by the International Space Science Institute and the Europlanet RI project.

Future missions to explore ice in the main asteroid belt

Colin Snodgrass

Recent results indicate that there is ice in the asteroid belt, inside the water 'snow line', placing strong constraints on Solar System formation and evolution models. Two proposals to the ESA M5 call seek to improve our knowledge of ice in the main belt: CASTAway, which performs a large spectroscopic survey and multiple flybys to map the diversity of asteroids, and Castalia, which will visit a main belt comet to sample escaping water directly. These complementary approaches will, respectively, help us understand the distribution of ice (and minerals) on a large scale, and measure detailed properties such as isotopic ratios at one location. Both are based on high TRL components and fit within the M5 constraints.

The Castalia mission will rendezvous with the archetypal main belt comet, 133P/Elst-Pizarro, and perform both remote sensing and in situ sampling experiments. The mission continues ESA's scientific legacy from Rosetta, by following up on one of its big surprises (that 67P's D/H ratio doesn't match Earth's water) and making similar measurements at a very different sort of comet. It does this in a medium class mission by having a much simpler spacecraft and operations (no lander, dedicated remote sensing/in situ/communications modes, significant onboard autonomy for navigation), and by the fact that MBCs are many orders of magnitude lower in their total activity than 67P – visiting an ice rich 'active asteroid' is much easier than orbiting a more typical comet.

CASTAway, on the other hand, provides a broad survey that samples the full diversity of asteroids in the main belt, mapping distributions of ice, organics and minerals. It is a 50 cm diameter space telescope equipped with a near-infrared spectrograph and a visible wavelength imager that will perform a very large survey of more than 10,000 asteroids of all sizes and types. By placing this telescope on a trajectory that loops through the asteroid belt, it can target very small asteroids at wavelengths that are impossible from Earth, especially the 3 micron region that is sensitive to water ice and hydrated minerals. It will also perform close flybys of 10-20 asteroids to ~double the number visited by spacecraft, returning resolved imaging and spectroscopy for a carefully selected sample of bodies that covers the diversity of asteroid types.

ICY COLLISIONS: THE ORIGIN OF PLANETS AND COMETS. Grzegorz Musiolik¹, Jens Teiser¹, Gerhard Wurm¹, ¹Fakultät für Physik, Universität Duisburg-Essen, Lotharstr. 1, D-47048 Duisburg, Germany (gregor.musiolik@uni-due.de)

Introduction: The importance to distinguish between different ice species like H₂O and CO₂ in the formation of planetary systems has not been taken seriously into account in recent years. Within the context of collisional growth in protoplanetary disks, these different species can behave very differently. If they additionally appear at various distances to the central star due to their specific sublimation pressure, the growth dynamics also becomes location-dependent. Hence, the formation of planetesimals and larger bodies might be possible only in regions between some of these snowlines.

We analysed collisions between ~100µm large H₂O- and CO₂-ice aggregates and mixtures between both with a mass ratio of 1:1 and a wall covered with the same ice species at a temperature of 80K and a pressure of 1mbar. The collision velocities varied between 0 and 2.5 m/s. We observed three different collision outcomes in the order of increasing impact velocity: sticking, bouncing and fragmentation.

Results: For the CO₂-ice aggregates, we observe a threshold between sticking and bouncing at 0.04 m/s. Comparing these results with other collision experiments for silica spheres [3] and water ice spheres [4] we find out, that this threshold rather matches the behavior of silica spheres. Further experiments with CO₂-H₂O-mixtures and H₂O-aggregates confirm an increasing threshold between sticking and bouncing with increasing amount of H₂O within the aggregates (s. Fig. 1). For pure H₂O samples, we estimate the threshold to be an order of magnitude higher.

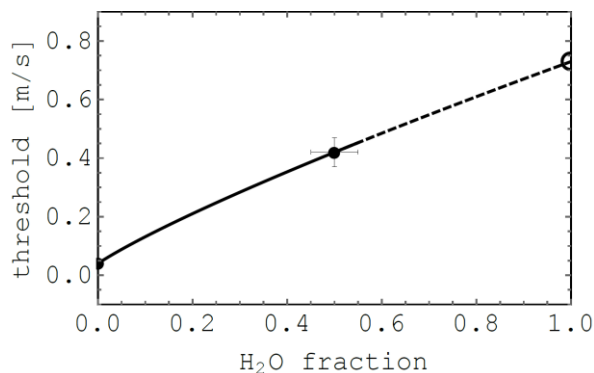


Figure1: The threshold between sticking and bouncing for different ice-aggregates [2].

For the CO₂-aggregates, we observe the onset of fragmentation at 0.75m/s. For the other species, this

threshold increases and is observed only infrequently below impact velocities of 2.5m/s.

Consequences for planet and comet formation:

The outcomes of the experiments suggest, that planet formation should be preferred in the region between the H₂O- and the CO₂-snowline in a protoplanetary disk (s. Fig. 2). Near the center of the star, where silicates prevail, the sticking and therefore also the growth potential is limited due to the bouncing barrier [5]. Beyond the H₂O-snowline at 2 AU, where these silicates are additionally covered by a H₂O ice layer, the growth potential increases due to the higher stickiness of these ice species. Farther away from the central star at the CO₂-snowline at 9.3 AU, the aggregates are mantled by a CO₂-layer and the growth potential decreases again.

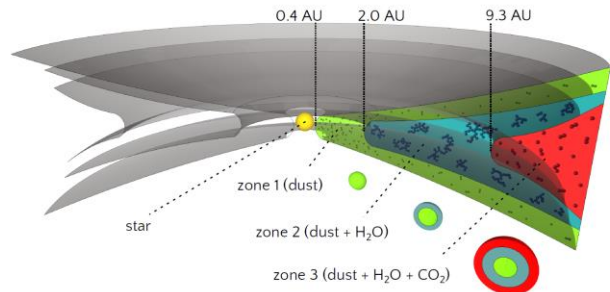


Figure2: A protoplanetary disk divided into zones between the H₂O- and the CO₂-snowline. Growth of larger bodies is preferred in the second zone after the H₂O-snowline [1].

References: [1] Musiolik, G., Teiser, J., Jankowski, T., & Wurm, G. 2016, ApJ, 818, 16 [2] Musiolik, G., Teiser, J., Jankowski, T., & Wurm, G. 2016, ApJ, 827, 63 [3] Poppe, T., Blum, J., & Henning, T. 2000, ApJ, 533, 454 [4] Gundlach, B., & Blum, J. 2015, ApJ, 798, 34 [5] Zsom, A., Ormel, C. W., Güttler, C., Blum, J., & Dullemond, C. P. 2010, A&A, 513, A57

Additional Information: This work is supported by the DFG under the grant number WU321/12-1 and TE890/1-1.

The memories of interstellar ices: deuterium as witness of star formation

Observations have revealed that the abundances of some deuterated interstellar molecules are markedly larger than the cosmic D/H ratio of 10^{-5} . This high degree of deuteration is the result of the high atomic D/H ratio in the gas phase when ices formed. The HDO/H₂O fraction can vary from a few times 10^{-4} in our solar system as well as some high and low mass hot cores to 0.01 in a few low-mass hot cores. This discrepancy seems to be reflecting the chemistry that took place during the formation of the ices in the earliest stages of star formation, before the star was born. The HDO/H₂O ratios indicate that our parent cloud, before the birth of our Sun, was warmer and denser than other star forming environments. While the initial condition during the formation of ices could be responsible for the deuterium fractionation of water in our solar system, experiments showed that isotope-exchanges between water and methanol could also change the deuterium fraction of water during warm-up and evaporation of the ices. Therefore, while the D/H ratio in water and other icy species such as methanol and formaldehyde could detain information (such as the initial conditions) on the earliest stages of the formation of our Sun, the evolution and evaporation of the ices could alter this D/H ratio.

Impact disruption of icy bodies of the Solar System

Range of the size of the targets: ~ (10 cm – 100 km)

J. Leliwa-Kopystynski, University of Warsaw, Poland

jkopyst@mimuw.edu.pl

Laboratory background: Huge amount of experiments related to impact cratering and to impact disruption of the icy and the icy-rocky targets have been performed. Typical target sizes in the experiments is of the order of 10 cm. Impact velocity ranges from a few dozen m/s to a few km/s. Crucial experimental output is the specific energy of disruption Q^* [J/kg] expressed in joules provided by impactor divided per kilogram of the target mass. By definition of disruption the energy Q^* corresponds to situation when after an impact the half of the target mass survives in one piece and another half is dispersed.

Solar System background: The data concerning the largest craters observed on small bodies of the Solar System. In particular the ratio of the crater diameter D of the largest crater observed on the target body to the radius R of that body (Leliwa-Kopystynski et al., 2016). For 21 target bodies (icy and rocky consider together) with radii from ~0.7 km (Dactyl, the Ida's satellite) to ~210 km (Proteus, Neptunian satellite) there is

$$D = (0.90 \pm 0.05)R. \quad (1)$$

The craters with diameters larger than D are not observed. It was estimated that the critical diameter that is the diameter corresponding to specific energy Q^* of impactor are

$$D_{c,icy} \approx 1.2R, \quad D_{c,rocky} \approx 1.6R. \quad (2)$$

Analytical model of impact disruption: It is assumed that the kinetic energy of an impact is used for the breaking of the molecular bonds on the breakthrough (fracture) surfaces, dispersing of ejecta, and changing of the gravitational energy of the system. To these corresponds the energy of cohesion E_s , the kinetic energy of escaping fragments E_{kin} , and the change of gravitational energy ΔE_{grav} related to fragmentation of the target. These energies (when divided by the target mass M) are the specific energies supplied to the target and used for three different processes. The specific energies are Q_s , Q_{kin} , and ΔQ_{grav} , respectively. Their sum is the total specific energy Q :

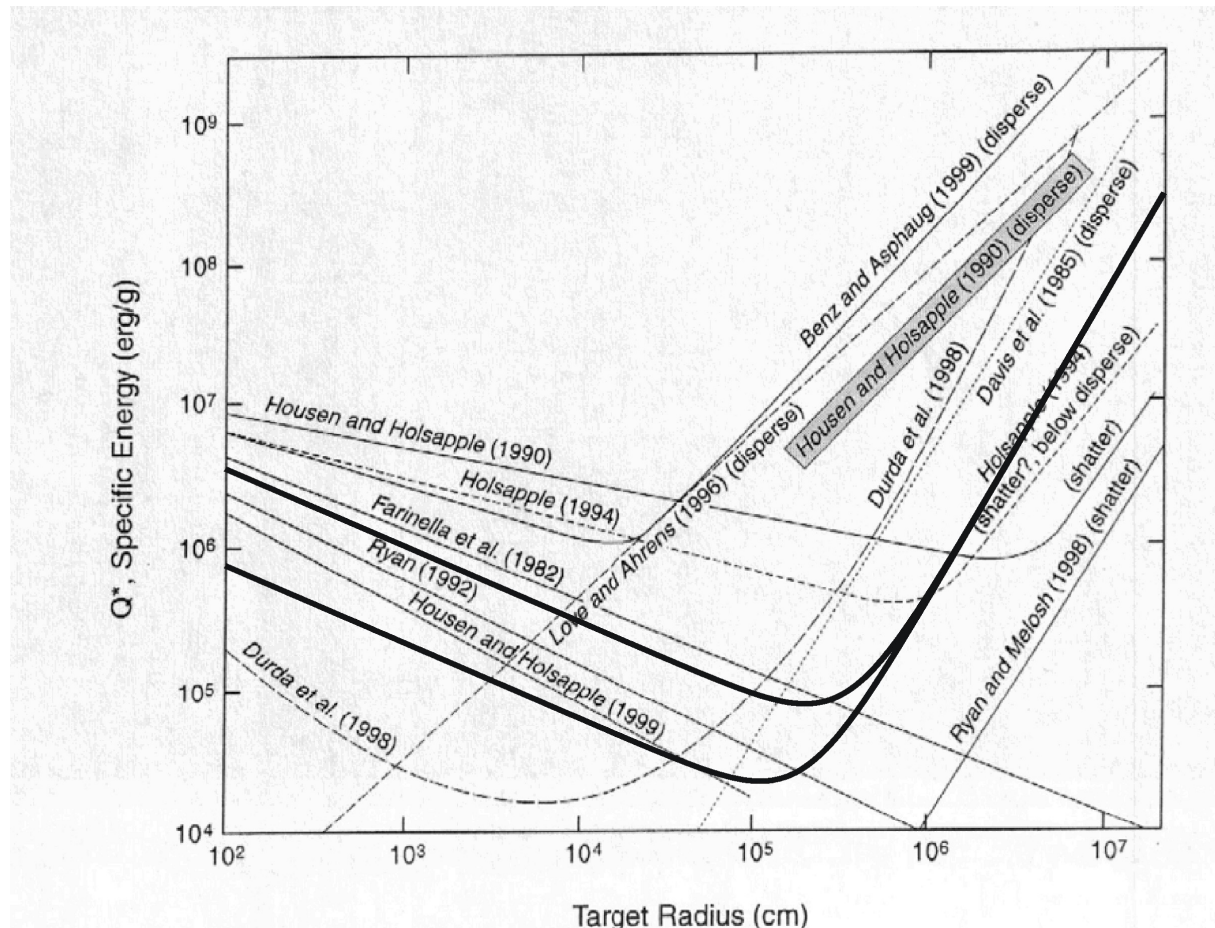
$$Q = Q_s + Q_{kin} + \Delta Q_{grav}. \quad (3)$$

Formula for Q is related to the mass fraction f that escapes the primordial target. Critical impact corresponds to $f=0.5$ and thus $Q(f=0.5) = Q^*$. To use Eq. (3) it is necessary to adopt a model that takes into account a size distribution and velocity distribution of the post-impact fragments. A set of material constants, rather poorly known, are involved in the model. Impact velocity in the different regions of the Solar system is known with better precision (Zahnle et al., 2003).

Some results are given by Leliwa-Kopystynski et al., (2016). They concern the impactor to target size ratio that leads to target damage f . Particular calculations have been

done for the impacts of comets on Saturnian icy satellite Mimas as well as for these impacts that formed families of asteroids (4) Vesta, (15) Eunomia, and (24) Themis.

Fig. 1. Specific disruption energy versus target size presented on the background of the figure compiled by Holsapple et al., (2002). The area in between the heavy lines, Leliwa-Kopystynski et al., (2016) corresponds to the middles of the ranges of the parameters considered in this work. This figure is for the rocky targets. Calculations for other targets (icy and icy-rocky) are in progress.



References:

Holsapple, K., Giblin, I., Housen, K., Nakamura, A., Ryan, E. 2002. Asteroid Impacts: Laboratory Experiments and Scaling Laws, In: *Asteroids III*, eds. by W. F. Bottke Jr, A. Cellino, P. Paolicchi, and R. P. Binzel. Univ. of Arizona Press, Tucson. pp. 443-462, 2002.

Leliwa-Kopystynski, J., Burchell, M. J., Lowen, D. Impact cratering and break up of the small bodies of the Solar System. *Icarus*. **195**, 817-826, 2008.

Leliwa-Kopystynski, J., Włodarczyk, I., Burchell, M. J. Analytical model of impact disruption of satellites and asteroids. *Icarus*, **268**, 266-280, 2016.

Zahnle, K., Schenk, P., Levison, H., Dones, L. Cratering rates in the outer Solar System. *Icarus* **163**, 263 – 289, 2003.

2 HYDROCARBON COMBUSTION. HYPOTHESIS ON THE ORIGIN OF WATER ON EARTH. ISOTOPIC ANALYSIS.

[José Carlos Gómez Cazorla. \(Independent scholar\)](#)
jccazorla39@gmail.com

ABSTRACT.

The detection of hydrocarbons in the interstellar medium and young circumstellar disks by large infrared telescopes, opens up a new range of unexplored possibilities. In this presentation, the combustion of hydrocarbons is proposed as contributing to the origin of terrestrial water, as a byproduct of accretion. Water produced by combusting current hydrocarbons has $\delta^{18}\text{O} = +13.4\text{‰}$ and $\delta\text{D} = -82.8\text{‰}$ SMOW. It can be assumed that the original water δD should have a similar negative value. Another argument is that on Earth, the oxide minerals, as well as seawater and atmospheric oxygen follow the mass dependent terrestrial fractionation line on oxygen $\delta^{17}\text{O} = 0.52 \cdot \delta^{18}\text{O}$. This indicates a single original oxygen reservoir, pointing to an endogenous and homogeneous formation process. The isotopic difference could be accounted for by the Dole effect $\delta^{18}\text{O} = +23.88\text{‰}$ SMOW, caused by the isotopic fractionation of biological respiration. In the first part of the presentation I will explain the process that could have occurred if the Earth had been surrounded by hydrocarbons during primary accretion. In the second part I will analyze the different hydrogen and oxygen isotopes to test the feasibility of the hypothesis. I also note that Titan, one of Saturn's moons, has abundant hydrocarbons. Titan could be the only planetary body that did not suffer major impacts during the formation of the Solar System, thereby preserving the original hydrocarbon composition of the protoplanetary disc.

Two new experimental facilities to study irradiated ices in reflectance

Rosario Brunetto

*Institut d'Astrophysique Spatiale, CNRS, Univ. Paris-Sud, Université Paris-Saclay,
Bât. 121, 91405 Orsay (France), rosario.brunetto@ias.u-psud.fr*

Space weathering processes affect atmosphere-less bodies in the Solar System. They include irradiation by solar wind, galactic cosmic ions, electrons, UV and X-rays, and bombardment by micrometeorites. These processes cause variations in the optical properties of small Solar System bodies surfaces. In particular, space weathering can be responsible for the red coloration of the small objects in the outer parts of the solar system. Several experiments have been performed to investigate the effects of ion irradiation on carbon-rich materials. The irradiation of frozen methane or methanol shows a strong reddening and darkening of the spectra, due to the formation of an organic (C-rich) refractory residue. The color is preserved after the sublimation of the volatile species, and further irradiation of such a solid polymer-like residue produces a darkening and a flattening of the spectra. This process is considered one of the main “nurture” mechanisms. But because of limitations or inconsistencies in the observations and the limited availability of laboratory data, there are still many questions on the subject.

Here I present two new experimental facilities to study irradiated ices in the laboratory. The first setup is called INGMAR (“Irradiation de Glaces et Météorites Analysées par Réflectance VIS-IR”) and is based on a close collaboration between IAS and CSNSM in Orsay (France). This setup is dedicated to VIS-IR spectroscopic analysis of solids of astrophysical interest to be coupled to different irradiation platforms. In the first phase of the project, meteorites, carbons, and ices that are analogs of carbon-rich surfaces are irradiated using 40 keV ions (as a simulation of solar wind) at the SIDONIE platform (CSNSM, Orsay) and analyzed by reflectance spectroscopy. The second setup is called MIEG-GET (“Microscopie et Irradiation Electronique de Glaces et Grains ExtraTerrestres”) and it will be used to spectroscopically analyse meteorites and interplanetary dust mixed with ice (H₂O, CH₃OH, NH₃, CO₂, etc.) at T = 10-300 K and their evolution after electron irradiation at the microscopic scale. This configuration aims to reproduce the behavior of a surface of an “icy” asteroid, a Centaur or a comet. This new setup is currently implemented in collaboration with the SMIS beamline of the SOLEIL synchrotron.

Title: Methane Mapping of Pluto in the Near-Infrared with the Ralph/MVIC Instrument

Authors: Alissa M. Earle, Richard P. Binzel, Will Grundy, Paul Schenk, Carly Howett, Alex H. Parker, Kimberly Ennico, Catherine B. Olkin, S. Alan Stern, Harold Weaver, Leslie A. Young, and The NASA New Horizons Composition Team

Abstract:

The data returned from NASA's New Horizons spacecraft has given us an unprecedented, detailed look at the Pluto system. New Horizons' Ralph/MVIC (Multi-spectral Visible Imaging Camera) is composed of 7 independent CCD arrays on a single substrate. Among these are a red channel (540-700 nm), near-infrared channel (780-975 nm), and narrow band methane channel (780-975 nm). By comparing the ratios of these channels we are able to produce high-resolution methane equivalent width and slope maps of Pluto's surface. From these maps we can then quantitatively study the relationships between methane distribution, redness, and other parameters like latitude and altitude, which help improve our understanding of volatile transport on Pluto.

Micrometeorite impacts and energetic irradiation on Callisto, Ganymede and Europa - Magnetospheric weathering of ices and ice - dust - mixtures in the Jovian system

^{1,3}K.Fiege, ²N. Altobelli, ³M. Tieloff, ¹T.M. Orlando

¹Georgia Institute of Technology, Atlanta, Ga, USA, ²European Space Agency, Madrid, Spain, ³University of Heidelberg, Heidelberg, Germany

In the next decade, two missions will be launched, ESA's JUICE mission and NASA's Europa Clipper mission, aiming at investigating the icy moons of Jupiter, in particular their development of habitable environments for *life as we know it*. Icy moons, harboring a liquid subsurface ocean, hydrothermal activity and cryo-volcanism present a potential habitat for life.

Cryo-volcanism leads to the transport of matter from the subsurface oceans onto the moon's surface and therefore it should be possible to decipher the composition of the suboceanic compounds via remote sensing techniques. However, the surfaces of the Galilean moons are altered, i.e., magnetospherically weathered by the harsh Jovian environment. Space weathering in general affects the surfaces of airless bodies in our solar system. Multiple weathering agents, such as solar wind constituents (ions, photons, electrons), various magnetosphere-specific compounds in the giant planetary systems, and impactors of variable sizes and speeds, from big impactors to micrometeorites, alter the chemical composition, the structure and therefore the optical properties of the surface constituents. Space weathering effects conceal the true composition of a celestial body's surface. Without a quantitative understanding of the effects of each weathering agent on an icy moon's surface, deciphering the intrinsic composition of the moon's surface, and hence, ocean composition, is impossible.

We therefore propose a complementary approach to reveal the effects of individual space weathering agents in the Jovian magnetosphere: combining modeling with space weathering experiments and utilizing data from remote sensing efforts for comparison.

We will fabricate ices and ice-dust mixtures to match the surfaces of the Galilean moons Callisto, Ganymede and Europa. Further, we will irradiate the various ices with energetic particles and analyze the effects of irradiation with IR, UV-Vis and Raman to compare the results with remote sensing data. Moreover, we will conduct micrometeorite impact experiments to investigate the formation of tenuous atmospheres by analyzing the ejecta yield from ices and ice-dust mixtures upon bombardment and its composition via time-of-flight-mass spectrometry. These experiments will improve the qualitative and quantitative understanding of the effect of bombardment of ion/protons/electrons/dust on 'typical' Jovian moon ices.

Mapping of plume deposits and surface composition on Enceladus

T. A. Nordheim¹, F. Scipioni², D.P Cruikshank², R.N. Clark^{3,4}, K.P. Hand¹

¹Jet Propulsion Laboratory, California Institute of Technology, ²NASA Ames Research Center, ³U.S. Geological Survey, ⁴Planetary Science Institute

A major result of the Cassini mission was the discovery that the small mid-sized moon Enceladus is presently geological active [Dougherty *et al.*, 2006; Porco *et al.*, 2006; Spencer *et al.*, 2006; Hansen *et al.*, 2008]. This activity results in plumes of water vapor and ice emanating from a series of fractures (“Tiger Stripes”) at the moon’s South Pole. Some fraction of plume material escapes the moon’s gravity and populates the E-ring as well as ultimately providing a source of fresh plasma in the Saturnian magnetosphere [Pontius and Hill, 2006; Kempf *et al.*, 2010]. However, a significant portion of plume material is redeposited on Enceladus and thus provides a source of surface contaminants. By studying the near-infrared spectral signatures of these contaminants we may put new constraints on the composition of the plumes and, ultimately, their source, which is currently believed to be Enceladus’s global sub-surface ocean [Iess *et al.*, 2014].

Here we present preliminary results from our analysis of observations from the Visual and Infrared Mapping Spectrometer (VIMS) [Brown *et al.*, 2005] onboard Cassini and mapping of plume deposits across the surface of Enceladus. We have investigated the global variation of the water ice Fresnel peak at 3.1 μm , which may be used as an indicator of ice crystallinity [Hansen & McCord, 2004; Jaumann *et al.*, 2008; Newman *et al.*, 2008]. We have also investigated the slope of the 1.11-2.25 μm spectral region, which serves as an indicator of water ice grain size for small grains (< 100 μm) as well as the presence of contaminants [e.g. Filacchione *et al.*, 2010]. Finally, we have identified and mapped an absorption feature centered at 3.25 μm that may be related to organic contaminants, represented by the band depth of the fundamental C-H stretch [e.g. Cruikshank *et al.*, 2014; Scipioni *et al.*, 2014].

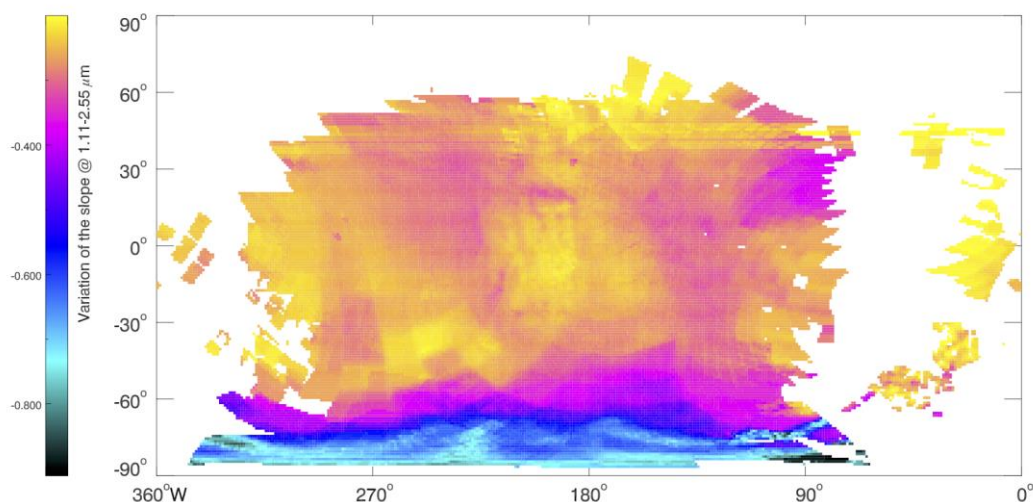


Figure 1 - Variation of the spectral slope in the 1.11 -2.25 μm region due to water ice grain size and the presence of contaminants.

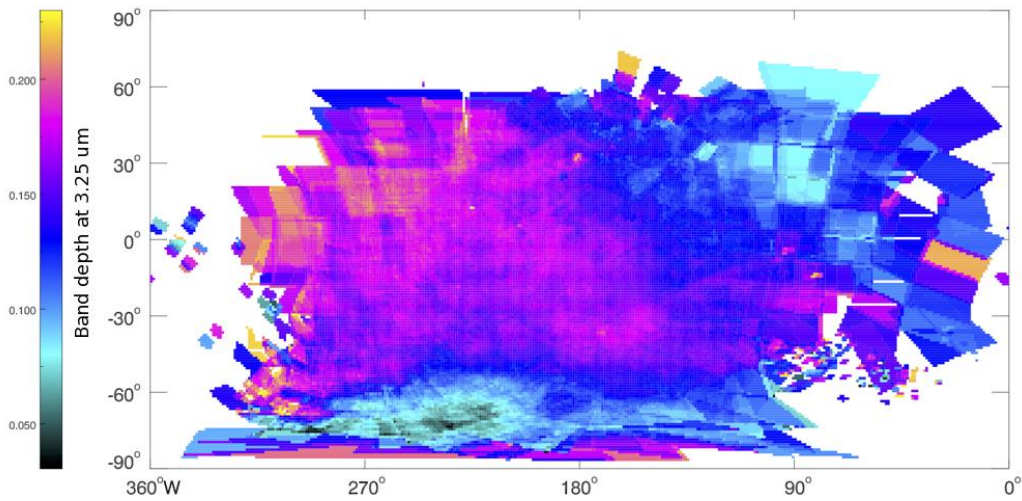


Figure 2 - Variation of the absorption band depth at 3.25 μm possibly due to the presence of organics.

- Brown, R. H. et al. (2005), *Space Sci. Rev.*, 115(1–4), 111–168
 Cruikshank, D. P. et al. (2014), *Icarus*, 233, 306–315
 Dougherty, M. K. et al. (2006), *Science*, 311(5766), 1406–1409
 Filacchione, G. et al. (2010), *Icarus*, 206(2), 507–523
 Hansen, C. J. et al. (2008), *Nature*, 456(7221), 477–9,
 Hansen, G. B. & McCord (2004), *J. Geophys. Res.*, 109(E1), E01012
 Iess, L. et al. (2014), *Science*, 344(6179), 78–80
 Jaumann, R. et al. (2008), *Icarus*, 193(2), 407–419
 Kempf, S. et al. (2010), *Icarus*, 206(2), 446–457
 Newman, S. F. et al. (2008) *Icarus*, 193(2), 397–406
 Pontius, D. H., and T. W. Hill (2006) *J. Geophys. Res. Sp. Phys.*, 111(9), 1–8
 Porco, C. C. et al. (2006), *Science*, 311(5766), 1393–1401
 Sandford, S. A., and L. J. Allamandola (1990), *Astrophys. J.*, 355(1), 357–372
 Scipioni, F. et al. (2014), *Icarus*, 234(2), 1–16
 Spencer, J. R. et al. (2006), *Science*, 311(5766), 1401–1405

Bombardment of Cryogenic Targets with Simulated Hypervelocity Micrometeoroids in the Lab

T. Munsat, R. Dee, M. Gudipati, M. Horanyi, D. James,
S. Kempf, Z. Sternovsky, Z. Ulibarri

*SSERVI-Institute for Modeling Plasma, Atmospheres and Cosmic Dust (IMPACT),
University of Colorado, Boulder, CO 80309
munsat@colorado.edu*

The dust accelerator facility at the SSERVI Institute for Modeling Plasma, Atmospheres, and Cosmic Dust (IMPACT) at the University of Colorado has recently developed a cryogenic ice target which can be exposed to micron and submicron particles accelerated to speeds up to 100 km/s. This capability is motivated by the need for a quantifiable experimental investigation into the hypervelocity micrometeoroid impact phenomena that contribute to the evolution of planetary icy surfaces. Capabilities granted by this facility are crucial to understanding the interesting complex chemistry and surface weathering effects that result from hypervelocity dust impacts and to calibrate instruments for space missions.

The ice target consists of a LN₂ cryogenic system connected to both a vapor deposition system and a movable freezer/holder for a pre-mixed liquid cartridge, for use in single-component ices or salty/multi-component mixtures, respectively. Impact products and chemistry are assessed with an integrated time-of-flight mass spectrometer. We present the early results from studies of hypervelocity iron particle impacts into frozen H₂O, and methanol, bombarded with Fe particles and other materials. Such studies can be used to predict and interpret possible chemical signatures from impact products at planetary surfaces containing similar component materials.

Transient friction experiments to study shear heating on icy satellite faults
Christine McCarthy, Heather Savage, Michael Nielson, Armando Domingos

Measuring the frictional behavior of ice is an important component of understanding icy satellite dynamics and surface morphology, particularly at faults—both normal and cycloidal—where it is unclear whether they grow by continuous small slip increments, by discontinuous large increments, or some more complex process. Additionally, although the surfaces of icy satellites are dominated by water ice, near-infrared spectrometry has identified non-ice phases on many satellites. Hydrated ammonia has been suggested as a possible component on the surface of Enceladus, Titan, and Triton. Ammonia displays a deep eutectic melting temperature with water ice (176K) so that even at extremely cold surface temperatures, small increases in heat, such as that from frictional heating within tidally loaded faults, could create partial melting within the fault zone. Melt generation may be responsible for producing surface features, but is also expected to have a complex relationship with tidal heating and convection. Our experimental project focuses on the microstructure and frictional behavior of ice mixtures important to icy satellites. In particular we are examining the combined viscoelastic and frictional behavior of cyclically loaded ice at temperatures above and below the solidus. Both the equilibrium and flash frozen microstructures of dilute ice + ammonia will be presented. We will also provide preliminary results from a suite of frictional experiments in a double-direct shear configuration with a central sample sliding between two stationary blocks. The periodically loaded central block exhibits both friction at the contact surfaces and some anelastic response within the interior of the sample. We expect to better understand how runaway heating may occur and how cyclic melting and recrystallization during shear heating affect frictional properties and fault zone morphology. Results from this study can be used to model heating rates in icy satellites over time, which are needed for next generation modeling of satellite thermal history and evolution.

Polarimetry of pure and dusty fine-grained ice samples measured in the laboratory

O. Poch (1), H. M. Schmid (2), A. Pommerol (1), B. Jost (1), N. Thomas (1)

(1) NCCR PlanetS and Physikalisches Institut, University of Bern, Switzerland (olivier.poch@csh.unibe.ch),

(2) NCCR PlanetS, Institute for Astronomy, ETH Zurich, Switzerland

Polarimetric observations of atmosphere-less Solar System bodies can help to better probe the texture and the physico-chemical composition of their surfaces. Here, we present measurements performed in the laboratory of the University of Bern on carefully characterized ice/dust samples to provide reference data that can be used to interpret remote-sensing polarimetric observations of astrophysical objects.

We use a Stokes polarimeter to measure the Stokes parameters describing the polarization of the visible light scattered by ice/dust samples illuminated with a randomly polarized light simulating the star light. The polarization is retrieved at multiple phase angles (3-30°) and wavelengths (400-900 nm), allowing to study the shape of the polarimetric phase curves and their spectral dependence. We are performing these measurements on surfaces made of water ice particles having different grain sizes and porosities, as well as mineral/organic dusts, pure or mixed together, as analogues of planetary or cometary surfaces.

The results provide interesting inputs to complement the theoretical models and predict or interpret spectro-polarimetric properties of Solar System objects and circumstellar disks.

Seasonal variation of radial brightness contrast of Saturn's rings viewed in mid-infrared by Subaru/COMICS

Hideaki Fujiwara¹, Ryuji Morishima^{2,3}, Takuya Fujiyoshi¹, and Takuya Yamashita⁴

1. Subaru Telescope, National Astronomical Observatory of Japan, 2. University of California, Los Angeles, Institute of Geophysics and Planetary Physics, 3. Jet Propulsion Laboratory, California Institute of Technology, 4. National Astronomical Observatory of Japan

To investigate the mid-infrared (MIR) characteristics of Saturn's rings, we collected and analyzed MIR high spatial resolution images of Saturn's rings obtained in January 2008 and April 2005 with COMICS mounted on Subaru Telescope, and investigated the spatial variation in the surface brightness of the rings in multiple bands in the MIR. We also composed the spectral energy distributions (SEDs) of the C, B, and A rings and the Cassini Division, and estimated the temperatures of the rings from the SEDs assuming the optical depths. We find that the C ring and the Cassini Division were warmer than the B and A rings in 2008, which could be accounted for by their lower albedos, lower optical depths, and smaller self-shadowing effect. We also find that the C ring and the Cassini Division were considerably brighter than the B and A rings in the MIR in 2008 and the radial contrast of the ring brightness is the inverse of that in 2005, which is interpreted as a result of a seasonal effect with changing elevations of the sun and observer above the ring plane.

NANOINDENTATION AND REFLECTANCE SPECTROSCOPY AS TECHNIQUES TO INFER MECHANICAL, STRUCTURAL AND COMPOSITIONAL PROPERTIES OF UNDIFFERENTIATED CHONDRITIC BODIES

C. E. Moyano-Camero¹, J. M. Trigo-Rodríguez¹, E. Pellicer², J. Llorca³, M. Martínez-Jiménez¹, J. Sort⁴, ¹Institute of Space Sciences (IEEC-CSIC), Campus UAB, Carrer de Can Magrans s/n, 08193 Cerdanyola del Vallès, Barcelona, Spain (moyano@ice.csic.es, trigo@ice.csic.es, mmartinez@ice.csic.es); Departament de Física, Universitat Autònoma de Barcelona, 08193 Cerdanyola del Vallès, Barcelona, Spain (eva.pellicer@uab.cat), ³Institut de Ciència de Materials de Barcelona (ICMAB/CSIC), Campus UAB, 08193 Bellaterra, Barcelona, Spain, ⁴Institució Catalana de Recerca i Estudis Avançats (ICREA) and Departament de Física (Universitat Autònoma de Barcelona, 08193 Cerdanyola del Vallès, Barcelona, Spain (jordi.sort@uab.cat).

Introduction: The asteroids from the Near-Earth Asteroid (NEA) population have intense collisional histories, often including disruption of their primitive parent bodies and breccification [1-3]. The Chelyabinsk meteorite is an ordinary chondrite (OC) with a mixture of different lithologies that point towards being a genomic breccia of LL5-6 material, and with a relatively high S4 degree of shock [4,5]. The most abundant lithology is light-colored, usually with abundant shock veins [4-6]. The second is described as dark-colored, or shock-darkened, due to the amount of interstitial spaces filled with opaque material (metals and troilite) as a consequence of shock mobilization [4-6]. A fine-grained impact melt lithology has also been defined, which experienced the consequences of shock to a larger extent than the previous lithology [4-6], but they are almost identical from an spectroscopic point of view [7]. The spectroscopic distinction of light and dark lithologies, relatively common in OCs, has shown that combinations of these materials can explain some spectral variations of asteroids [7,8]. The processes responsible for the formation of the lithologies have strong effects in their physical properties. Therefore, spectroscopic studies showing the amount of shock-darkened material on an asteroid would provide us insight in its mechanical properties. We analyze several UV-NIR spectra of Chelyabinsk, and relate them with the mechanical properties obtained after nanoindentation experiments. Since most NEAs are S- or Q-class asteroids related to LL meteorites [9,10], we use on this study one sample of the abundant fresh Chelyabinsk meteorite specimens (~1000 kg), as a proxy of this kind of objects [11].

Experimental Setup: We studied a thin (~30 μm) section of the Chelyabinsk meteorite (PL13049) kindly provided by Addi Bischoff. A high-resolution mosaic was created from images obtained with a Zeiss petrographic microscope. An UMIS equipment from Fischer-Cripps Laboratories was used for the nanoindentation tests, using a Berkovich pyramidal-shaped diamond tip, to study the mechanical properties of the lithologies found in this meteorite. Several ultraviolet

to near-infrared spectra (~0.2 to 2.0 μm) were obtained from the meteorite, using a Shimadzu UV3600 UV-Vis-NIR spectrometer.

Results: Shock-darkened lithologies and clasts of impact melt breccias occur as (almost) opaque areas with deep influence of reflectance spectra as previously found [6]. The meteorite spectra are darker than expected for ordinary chondrites, but exhibit distinguishable absorption bands.

Shock-driven processes affected the darkened regions of Chelyabinsk and introduced changes in their mechanical properties. While the porosity in the different studied regions is almost identical, we have seen that the shock-darkened materials tend to be harder than the light-colored lithology. For a given porosity, harder materials show worst momentum multiplication. Therefore, the efficiency of an impact is higher in bodies composed of larger amounts of the light-colored lithology. Also, the shock vein tends to show fractures when indented, which is not seen in the two lithologies studied. These kind of veins represent a structural weakness on asteroids, and therefore an asteroid would tend to be fractured along these veins.

These results need to be taken into account for asteroid deflection missions, such as AIDA.

References: [1] Britt D. et al. (2002) In *Asteroids III*, 485-500. [2] Binzel R. P. et al. (2002) In *Asteroids III*, 255-271. [3] Bischoff A. et al. (2010) *Meteoritics & Planet. Sci.*, 45, 1638-1656. [4] Ruzicka A. et al. (2015) *The Meteoritical Bulletin*, 102, 8-9. [5] Bischoff A. et al. (2013) *Meteoritics & Planet. Sci.*, 48, A61. [6] Righter K. et al. (2015) *Meteoritics & Planet. Sci.*, 50, 1790-1819. [7] Reddy V. et al. (2014) *Icarus*, 237, 116-130. [8] Britt D. T. and Pieters C. M. (1994) *Geochim. Cosmochim. Acta*, 58, 3905-3919. [9] Binzel R. P. et al. (2006), *LPS XXXVII*, Abstract #1491. [10] Vernazza P. et al. (2008) *Nature*, 454, 858-860. [11] Moyano-Camero C. et al. (accepted for publication) *ApJ*.

FROM THE ICY SATELLITES TO SMALL MOONS AND RINGS:
SPECTRAL INDICATORS BY CASSINI-VIMS UNVEIL COMPOSITIONAL
TRENDS IN THE SATURNIAN SYSTEM

Gianrico Filacchione¹, Fabrizio Capaccioni¹, Mauro Ciarniello¹, Phil D. Nicholson², Roger N. Clark³,
Jeffrey N. Cuzzi⁴, Bonnie B. Buratti⁵, Dale P. Cruikshank⁴, Robert H. Brown⁶

1. INAF-IAPS, Istituto di Astrofisica e Planetologia Spaziali, Rome, ITALY.
2. Cornell University, Department of Astronomy, Ithaca, NY, USA.
3. PSI Planetary Science Institute, Tucson, AZ.
4. NASA-AMES, Mountain View, CA, USA.
5. NASA-JPL, Pasadena, CA, USA.
6. Lunar and Planetary Lab, University of Arizona, Tucson, AZ, USA.

ABSTRACT: Despite water ice being the most abundant species on Saturn satellites' surfaces and ring particles, remarkable spectral differences in the 0.35-5.0 μm range are observed among these objects. Here we report about the results of a comprehensive analysis of more than 3000 disk-integrated observations of regular satellites and small moons acquired by VIMS aboard Cassini mission between 2004 and 2016. These observations, taken from very different illumination and viewing geometries, allow us to classify satellites' and rings' compositions by means of spectral indicators, *e.g.* 350-550 nm - 550-950 nm spectral slopes and water ice band parameters [1, 2, 3]. Spectral classification is further supported by indirect retrieval of temperature by means of the 3.6 μm I/F peak wavelength [4,5]. The comparison with synthetic spectra modeled by means of Hapke's theory point to different compositional classes where water ice, amorphous carbon, tholins and CO_2 ice in different quantities and mixing modalities are the principal endmembers [3, 6]. When compared to satellites, rings appear much more red at visible wavelengths and show more intense 1.5-2.0 μm band depths [7]. Our analysis shows that spectral classes are detected among the principal satellites with Enceladus and Tethys the ones with stronger water ice band depths and more neutral spectral slopes while Rhea evidences less intense band depths and more red visible spectra. Even more intense reddening in the 0.55-0.95 μm range is observed on Iapetus leading hemisphere [8] and on Hyperion [9]. With an intermediate reddening, the minor moons seem to be the spectral link between the principal satellites and main rings [10]: Prometheus and Pandora appear similar to Cassini Division ring particles. Epimetheus shows more intense water ice bands than Janus. Epimetheus' visible colors are similar to water ice rich moons while Janus is more similar to C ring particles. Finally, Dione and Tethys lagrangian satellites show a very flat reflectance in the visible, making them remarkably different with respect to the other small moons. Moreover, we have observed that the two Tethys' lagrangian moons appear spectrally different, with Calypso characterized by more intense water ice bands than Telesto. Conversely, at visible wavelengths Polydeuces, Telesto and Methone are in absolute the more blue objects in the Saturn's system. The red slopes measured in the visible range on disk-integrated spectral data, showing varying degrees on all of the satellites, could be caused more by exogenic processes than by geologic and endogenic events which are operating on more localized scales. The principal exogenic processes active in the Saturn's system [11] which alter the satellites and rings surfaces are the E ring particles bombardment, the interaction with corotating plasma and energetic particles, the bombardment of exogenic dark material [12] and the water ice photolysis. A discussion about the correlations between these processes and the observed spectral classes is given. With the approaching of the Cassini "Gran Finale" orbits, VIMS will unveil with unprecedented spatial resolution the spectral properties of many small moons and rings. These data will be extremely valuable to improve our classification of the Saturn's satellites and rings.

REFERENCES

- [1] Filacchione, G., et al., 2007. Saturn's icy satellites investigated by Cassini-VIMS I. Full-disk properties: 350-5100 nm reflectance spectra and phase curves. *Icarus*, 186, 259-290.
- [2] Filacchione, G., et al., 2010. Saturn's icy satellites investigated by Cassini-VIMS. II. Results at the end of nominal mission. *Icarus*, 206, 507-523.
- [3] Filacchione, G., et al., 2012. Saturn's icy satellites and rings investigated by Cassini-VIMS. III. Radial compositional variability. *Icarus*, 220 1064-1096.
- [4] Filacchione, G., et al., 2016. Saturn's icy satellites investigated by Cassini-VIMS. IV. Daytime temperature maps. *Icarus*, 271, 292-313.
- [5] Filacchione, G., et al., 2014. Cassini-VIMS observations of Saturn's main rings: I. Spectral properties and temperature radial profiles variability with phase angle and elevation. *Icarus*, 241, 45-65.
- [6] Ciarniello, M. et al., 2011. Hapke modeling of Rhea surface properties through Cassini-VIMS spectra. *Icarus*, 214, 541-555.
- [7] Cuzzi, J., et al., 2009. Ring Particle Composition and Size Distribution; in *1emphSaturn from Cassini-Huygens*. Edited by M. K. Dougherty, L.W. Esposito, and S.M. Krimigis. Springer, Berlin. pp. 459-509.
- [8] Clark, R. N., et al., 2012. The Surface Composition of Iapetus: Mapping Results from Cassini VIMS. *Icarus*, 218, 831-860.
- [9] Cruikshank, D. P. et al., 2007. Surface composition of Hyperion. *Nature*, 448, 54-56.
- [10] Filacchione, G., et al., 2013. The Radial Distribution of Water Ice and Chromophores across Saturn's System, *The Astrophysical Journal*, 766, Issue 2, article id. 76, 5 pp.
- [11] Schenk, P., et al., 2010. Plasma, plumes and rings: Saturn system dynamics as recorded in global color patterns on its midsize icy satellites. *Icarus*, 211, 740-757.
- [12] Clark, R. N. et al. 2008. Compositional mapping of Saturn's satellite Dione with Cassini VIMS and implications of dark material in the Saturn system. *Icarus*, 193, 372-386.

Processing of Cometary surface by swift ions

Marina G Rachid¹, Sergio Pilling¹, Will R.Rocha¹, J.J. Ding², H. Rothard², P. Boduch²

¹ IP&D/UNIVAP, Av. Shishima Hifumi, 2911, São Jose dos Campos, SP, Brazil

² GANIL-CIRIL-CIMAP, Boulevard Henri Becquerel, BP 5133, 14070, Caen, France

In this work we conducted an experimental study on the effects of medium-mass highly charged and energetic ions with astrophysical ice analogs with composition H₂O, CO₂, CH₄ (10:1:1) in physicochemical condition similar to the ones found in comets and other cold surfaces of solar system such as Enceladus and transneptunians objects (TNO). The measurements were performed at the heavy ion accelerator GANIL (Grand Accélérateur National d'Ions Lourds) employing, and the analysis of data sets were performed *in-situ* by employing Fourier transform infrared spectroscopy (FTIR) in a transmission mode. The frozen sample at 72 K was bombarded by 15.7 MeV O⁺⁵ ions up to the fluence of 3.10¹² ion cm⁻² simulating the incoming cosmic rays and/or solar energetic particles in the interplanetary ices. Here we investigate the stability and chemical changes of astrophysical ice analogs, from the evolution of molecular absorption profiles in the infrared spectra and determine the effective dissociation (destruction) cross section of parents species molecules and the effective formation cross sections of newly produced species (e.g. CO, CO₃, CH₄, H₂O₂, H₂CO₃) in the sample from the radiolysis. Segregation processes of CO₂ of frozen molecules during ice radiolysis were also observed and characterized. These treatment allow us to estimate the half-life of parental species in the frozen surfaces in the presence of incoming ionizing field, as well as, to improve our understanding of chemical evolution and physical-chemical parameters of observed interplanetary ices interacting with cosmic rays.

The enigmatic Comet 29P/Schwassmann-Wachmann 1 (SW1) has been of interest since its discovery almost 100 years ago. A nearly circular orbit around 6 AU, continuous activity outside of the water sublimation line, and frequent outbursts in activity make SW1 a useful observational target for a better understanding of distant cometary activity drivers. Since sublimation of water ice is likely not the primary driver of activity, is the sublimation of supervolatiles and/or the release of gasses trapped in amorphous water ice the driver? Furthermore, why does the comet have frequent major changes in activity despite receiving a nearly constant insolation? These unresolved questions reflect our lack of understanding of the fundamental nature of cometary activity and the ices involved in this activity.

We are working to replicate SW1's complex activity patterns observed in an expansive set of imaging observations (~25 years of SW1 observations) with the synergy of a well-developed 3D Monte Carlo coma model for the determination of SW1's nuclear spin state [1, 2, 3], a quasi-3D thermophysical/chemical nucleus model for simulating activity levels [4, 5], and the incorporation of recent *Rosetta* mission results. This level of detailed thermophysical analysis of an individual comet is usually reserved for spacecraft-flyby targets. Using the most common type of ground-based remote-sensing observations of a comet (dust imaging) to infer physical and dynamical properties of its nucleus, we are undertaking a detailed thermophysical analysis of an unvisited comet nucleus.

We present results from thermal modeling of a homogeneous progenitor nucleus that evolves into a body showing internal material layering, the generation of CO and CO₂ ice pockets, and the production of outbursts, thus bringing us closer to explaining the behavior of this intriguing comet. The progenitor nucleus is thermally evolved in SW1's current orbit using different plausible nucleus interior compositional and layering schemes [4, 6]. The models are constrained by comparing the synthetic dust-mass loss rate and its variability with what has been observed through optical imaging of the comet at various epochs in its orbit.

[1] Samarasinha, N. and Larson, S.: 2014, *Icarus*, **239**, 168-185. [2] Schambeau, C. A., et al.: 2016, *Icarus*, (in revision). [3] Schambeau, C. A., et al.: 2017, *Icarus*, (in prep.). [4] Prialnik, et al. 2004, *Comets II*, 359-387. [5] Sarid, G.: 2009, PhD thesis, Tel Aviv Univ. [6] Meech, K. J. and Svoren, J.: 2004, *Comets II*, 317-335. We thank the NASA Earth and Space Science Fellowship (NNX16AP41H), NASA Outer Planets Research Program (NNX12AK50G), the Space Telescope Science Institute (HST-AR-14294.001-A), and the Center for Lunar and Asteroid Surface Science (CLASS, NASA SSERVI NNA14AB05A) for support of this work.

Bidirectional Reflectance of icy Samples: Application to water ice detection on the Moon and Mercury.

Z. Yoldi (1), A. Pommerol (1), B. Jost (1), O. Poch (1), J. Gouman (1) and N. Thomas (1).

(1) Physikalisches Institut, University of Bern, Switzerland

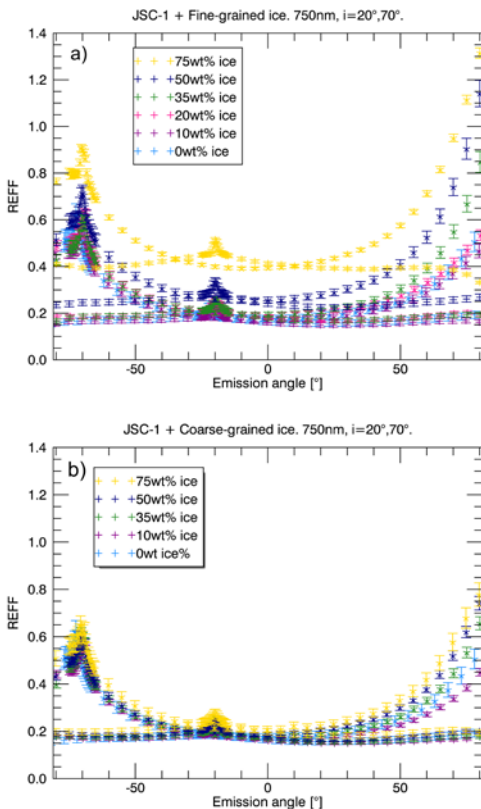
Some permanently shadowed craters at the poles of the Moon and Mercury are thought to host ice in their walls [1, 2, and references therein]. Laser altimeters and cameras can be used to search for potential changes of the surface reflectivity caused by the presence of ice. Laser altimeters currently in orbit around the Moon and Mercury have provided data showing some spatial variability in the reflectance of the polar areas of both bodies. In both cases the possibility of finding the ice mixed within the regolith as in an intimate mixture is explored [3, 4]. Reflectance models applied to the reflectivity measured by the laser altimeters are used for estimating the quantity of ice present in the craters [3].

We have produced intimate binary mixtures of particulate water ice and JSC-1 AF in the LOSSY Ice Laboratory (Laboratory for Outflow Studies of Sublimating materials) at the University of Bern. Two sizes of ice particles (diameters of 6 and 70 microns) and several percentages of ice within the sample are tested. Then, we have measured the Bidirectional Reflectance Distribution Function (BRDF) with the PHIRE-2 instrument; a gonio-radiometer that allows characterizing the BRDF of ice-bearing samples in the VIS-NIR (400-1100nm) spectral range [5].

Phase curves presenting the reflectance as a function of the emission angle are shown in Fig. 1 for fine-grained ice (Fig. 1a) and coarse-grained ice (Fig. 1b). In both cases we observe that, when mixed intimately, relatively high amounts of ice within the sample do not significantly affect its reflectance. In the case of the coarse-grained ice (Fig. 1b), very high amounts of ice are required to produce a photometric signature. In order to expand our experimental findings from a few particular cases to more general trends, we use our data to test existing reflectance models. In particular, we have tested the Hapke [6] and the Hiroi [7] models, to compare their different approaches to compute the reflectance of binary mixtures from the properties of the end members

Figure 1: Reflectance phase curves for binary mixtures of JSC-1 AF and water ice. a) ice diameter: 6 microns
b) ice diameter: 70 microns

and when it is looked at low incidence and phase angles. Looking for ice at high phase angles results in better chances of detection. We will explain how the reflectance models work well in a relative way; they are able to reproduce the shape described by the reflectance, as long as the mixing coefficients



are correctly estimated. Calculating ice concentrations from reflectance data without any knowledge of the mixing coefficients, which strongly depend on the size/shape of the grain, results in very large errors [8].

References

- [1] Feldman et al., 2001. Evidence for water ice near the lunar poles. *Journal of Geophysical Research*, Vol. 106, No E10, Pages 23,231-23,251.
- [2] Lawrence et al., 2013. Evidence for Water Ice Near Mercury's North Pole from MESSENGER Neutron Spectrometer Measurements. *Science* 339, 292.
- [3] Lucey et al., 2014. The global albedo of the Moon at 1064nm from LOLA, *J. Geophys. Res. Planets*, 119, 1665-1679, doi: 10.1002/2013JE004592
- [4] Neumann et al., 2013. Bright and Dark Polar Deposits on Mercury: Evidence for Surface Volatiles. *Science* 339, 296
- [5] Pommerol et al., 2011. Photometry and bulk physical properties of Solar System surfaces icy analogs: The Planetary Ice Laboratory at University of Bern. *Planetary and Space Science* 59, 1601-1612.
- [6] Hapke, 1981. Bidirectional reflectance spectroscopy: 1. Theory (1981). *J. Geophys. Res*, Vol 86, Issue B4 10 April 1981 Pages 3039–3054
- [7] Hiroi and Pieters, 1992. Effects of Grain Size and Shape in Modelling Reflectance Spectra of Mineral Mixtures. *Proc. Of Lunar and Planet. Science*, Vol 22, 313-325
- [8] Yoldi et al., 2015. VIS-NIR reflectance of water ice/regolith analogue mixtures and implications for the detectability of ice mixed within planetary regoliths. *Geophysical Research Letters* 42, 6205-6212.

Impact of radiogenic heating on the formation conditions of comet 67P/Churyumov-Gerasimenko

O. Mousis¹, A. Drouard¹, P. Vernazza¹, J. I. Lunine², K. Altwegg^{3,4}, H. Balsiger³, J.-J. Berthelier⁵, A. Bieler^{3,6}, P. Bochslers³, C. Briois⁷, G. Cessateur⁸, M. Combi⁶, J. De Keyser⁸, F. Dhooghe⁸, B. Fiethe⁹, S. A. Fuselier¹⁰, S. Gasc³, T. I. Gombosi⁶, K. C. Hansen⁶, M. Hässig^{3,10}, E. Kopp³, A. Korth¹¹, L. Le Roy³, R. Maggiolo⁸, U. Mall¹¹, B. Marty¹², H. Rème¹³, M. Rubin³, T. Sémon³, C.-Y. Tzou³, J. H. Waite¹⁰, P. Würz³

⁽¹⁾ Aix Marseille Université, CNRS, LAM (Laboratoire d'Astrophysique de Marseille)
UMR 7326, 13388, Marseille, France

⁽²⁾ Department of Astronomy and Carl Sagan Institute, Space Sciences Building Cornell University, Ithaca, NY 14853, USA

⁽³⁾ Physikalisches Institut, University of Bern
Sidlerstr. 5, CH-3012 Bern, Switzerland

⁽⁴⁾ Center for Space and Habitability, University of Bern
Sidlerstr. 5, CH-3012 Bern, Switzerland

⁽⁵⁾ LATMOS/IPSL-CNRS-UPMC-UVSQ
4 Avenue de Neptune F-94100, Saint-Maur, France

⁽⁶⁾ Department of Climate and Space Sciences and Engineering, University of Michigan
2455 Hayward, Ann Arbor, MI 48109, USA

⁽⁷⁾ Laboratoire de Physique et Chimie de l'Environnement et de l'Espace (LPC2E)
UMR CNRS 7328 – Université d'Orléans, France

⁽⁸⁾ Royal Belgian Institute for Space Aeronomy, BIRA-IASB
Ringlaan 3, B-1180 Brussels, Belgium

⁽⁹⁾ Institute of Computer and Network Engineering (IDA), TU Braunschweig
Hans-Sommer-Straße 66, D-38106 Braunschweig, Germany

⁽¹⁰⁾ Department of Space Science, Southwest Research Institute
6220 Culebra Rd., San Antonio, TX 78228, USA

⁽¹¹⁾ Max-Planck-Institut für Sonnensystemforschung
Justus-von-Liebig-Weg 3, 37077 Göttingen, Germany

⁽¹²⁾ Centre de Recherches Pétrographiques et Géochimiques, CRPG-CNRS, Université de Lorraine
15 rue Notre Dame des Pauvres, BP 20, 54501 Vandoeuvre lès Nancy, France

⁽¹³⁾ Université de Toulouse; UPS-OMP-CNRS; IRAP,
Toulouse, France.

ABSTRACT

Because of the high fraction of refractory material present in comets, the radiogenic decay of elements can generate enough heat to induce the loss of ultravolatile species such as N₂, Ar or CO if the nuclei accreted early in the protosolar nebula. Here we investigate the influence of this decay heat on the formation conditions of comet 67P/Churyumov-Gerasimenko as a function of its accretion epoch and size of parent body. We consider two possibilities: either, to account its bilobed shape, 67P assembled from two primordial ~1 kilometer-sized planetesimals or it results from the disruption of a bigger parent body. To match the volatile content observed in the coma, we find that 67P/Churyumov-Gerasimenko must have formed several Myr after the protosolar nebula initiation, independent of i) the size of parent body and ii) the composition of the icy material (amorphous ice, clathrates or crystalline ice). This places stringent conditions on the formation timescales of 67P/Churyumov-Gerasimenko and other comets.